KEMIAN LAITOS
JYVÄSKYLÄN YLIOPISTO

# Towards *myo*-inositol based hydrogelators

M.Sc. thesis

University of Jyväskylä

Department of Chemistry

11.05.2024

Sarita Orava

JYVÄSKYLÄN YLIOPISTO

ii

# Abstract

In this master's thesis, the literature part focuses on the structural aspects, properties, and importance of *myo*-inositol in numerous biological functions. In addition, the potential and challenges of functionalizing *myo*-inositol and its ability to act as a gelator in low molecular weight gels are discussed.

The aim of the experimental part was to prepare *myo*-inositol based amphiphilic low molecular weight gelators and investigate their gelling properties in biocompatible gels. The *myo*-inositol based derivatives designed in this work were 2-*O*-benzyl-*myo*-inositol and 2-*O*-Fmoc-*myo*-inositol. The functionalizations were carried out according to a three-step retrosynthesis plan: regio- and stereoselective protection of *myo*-inositol, regioselective functionalization with the selected target molecule, and removal of the protecting groups. Benzylated *myo*-inositol derivative was successfully synthesized, and the reaction conditions of this reaction were optimized. Functionalization with Fmoc-moiety was performed under two different reaction conditions, but the desired Fmoc derivative could not be synthesized.

In gelation experiments for benzylated *myo*-inositol, flake formation and partial gel were observed by increasing the concentration. Based on this result, some amphiphilic *myo*-inositol derivatives may have the potential to act as a gelator in biocompatible gels, but further studies are required to confirm this hypothesis.

# Tiivistelmä

Tämän Pro gradu -tutkielman kirjallisessa osassa keskitytään *myo*-inositolin rakenteeseen, ominaisuuksiin ja siihen, mikä tekee *myo*-inositolista merkityksellisen yhdisteen biologisissa ympäristöissä. Lisäksi tarkastellaan *myo*-inositolin funktionalisoinnin mahdollisuuksia ja haasteita sekä sen kykyä toimia gelaattorina alhaisen molekyylipainon geeleissä.

Tutkielman kokeellisessa osassa tavoitteena oli valmistaa *myo*-inositolipohjaisia amfifiilisiä alhaisen molekyylipainon gelaattoreita ja tutkia niiden geeliytymisominaisuuksia bioyhteensopivissa geeleissä. Työn suunnitellut johdannaiset olivat 2-*O*-bentsyyli-*myo*-inositoli ja 2-*O*-Fmoc-*myo*-inositoli. Funktionalisoinnit toteutettiin kolmivaiheisen retrosynteesisuunnitelman mukaisesti: *myo*-inositolin paikka- ja stereoselektiivinen suojaus, paikkaselektiivinen funktionalisointi valitulla kohdemolekyylillä ja suojausryhmien poisto. Työssä onnistuttiin syntetisoimaan bentsyloitua *myo*-inositolin johdannaista ja optimoimaan kyseisen reaktion reaktio-olosuhteita. Funktionalisointi Fmoc-osan kanssa suoritettiin kahdessa eri reaktio-olosuhteessa, mutta haluttua Fmoc-johdannaista ei onnistuttu syntetisoimaan.

Bentsyloidulle *myo*-inositolille suoritetuissa geeliytymistesteissä havaittiin hiutaleiden muodostumista ja pitoisuutta kasvattamalla osittaista geelin muodostumista. Tämän tuloksen perusteella joillakin *myo*-inositolin amfifiilisillä johdannaisilla voisi olla potentiaalia toimia gelaattorina bioyhteensopivissa geeleissä, mutta hypoteesin vahvistamiseksi lisätutkimukset ovat välttämättömiä.

# Preface

The experimental part of this master's thesis was carried out between February and April 2023 at the Nanoscience Center of the University of Jyväskylä. The literature part was started in August 2023 and finished in March 2024. The topic of the thesis was limited to the possibility of *myo*-inositol derivatives acting as gelators in biocompatible gels. Google Scholar and Scopus databases were used to search for information in the thesis.

The thesis was supervised by Professor Maija Nissinen, and postdoctoral researcher Efstratios Sitsanidis supervised the experimental part. I would like to thank both for their exceptional guidance and invaluable advice during this project. In addition, I would like to thank Docent Elina Sievänen for being the second examiner of the thesis.

# Table of contents

# Abbreviations

| | |
|---|---|
| BDA | Butane-2,3-diacetal |
| BnBr | Benzyl bromide |
| CGC | Critical gelation concentration |
| COSY | Correlated spectroscopy |
| CSA | (±)-Camphor-10-sulfonic acid |
| DCM | Dichloromethane |
| DMA | Dimethylacetamide |
| DMF | Dimethylformamide |
| DMSO | Dimethyl sulfoxide |
| Fmoc-Cl | 9-Fluorenylmethyl chloroformate |
| FTIR | Fourier-transform infrared spectroscopy |
| HAT | Hydrogen atom transfer |
| HK | Hexokinase |
| HMIT | $H^+$/*myo*-inositol transporter |
| HR-MS | High-resolution mass spectrometry |
| IMPase | Inositol monophosphatase |
| IP | Inositol polyphosphate |
| LMW | Low molecular weight |
| MGC | Minimum gelation concentration |
| MIOX | *Myo*-inositol oxygenase |
| MIPS | 1-D-*myo*-inositol-phosphate synthase |
| M.p. | Melting point |
| mRNA | Messenger ribonucleic acid |
| NMR | Nuclear magnetic resonance |

NOESY       Nuclear Overhauser effect spectroscopy

PBS         Phosphate buffered saline

PC          4-CzIPN

PI          Phosphatidylinositol

PIP         Phosphatidylinositol polyphosphate

RT          Room temperature

SET         Single electron transfer

SMIT1/2     Sodium-dependent *myo*-inositol transporter

TFA         Trifluoroacetic acid

$T_{gel}$   Sol-gel transition temperature

TLC         Thin-layer chromatography

## LITERATURE PART

## 1 Introduction

Inositol is a cyclic polyol consisting of six carbons, each substituted with a hydroxyl (OH) group. In 1850, Scherer first separated the inositol from the muscle extract and named it after the tissue with the Greek prefix "*myo*".[1] 1887, Maquenne purified it completely, first from leaves and later from horse urine. The inert chemical nature of inositol compared to glucose, along with its other chemical properties, led him to determine its cyclohexanol structure. Later, the configuration of the major inositol, *myo*-inositol, in eukaryotic tissues was discovered as a result of Posternak's research.[2]

In addition to *myo*-inositol, inositol **1** has eight other isomers because each hydroxyl group can be positioned axially or equatorially (Figure 1). Of the isomers, D-, and L-*chiro*-, *muco*-, *myo*-, *neo*-, and *scyllo*-inositols have been found in nature, while *allo*-, *cis*-, and *epi*-inositols are synthetic isomers.[3] The term inositol covers all nine different isomers, the only difference being the positioning of the six hydroxyl groups. For this reason, the term inositol is sometimes used in the plural when talking about inositols. It is also quite common for inositol to be used to refer to *myo*-inositol.
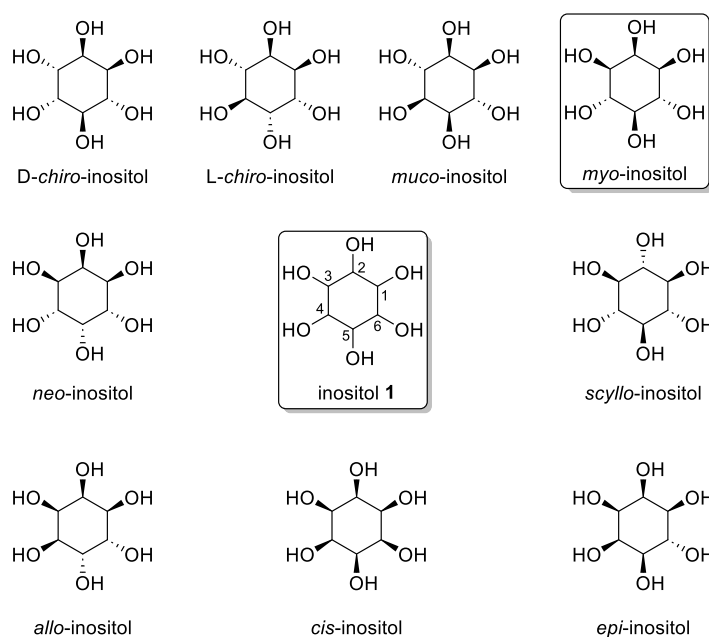


Figure 1. Nine stereoisomers of inositol **1**.

*Myo*-inositol is the best known and most studied isoform due to its abundance and significant biological functions.[4] It is widely found in nature in plant and animal cells in its free form, i.e. not bound to other chemical groups or molecules, as well as in its phosphorylated derivatives. *Myo*-inositol can be synthesized in organisms from glucose, which is its only known biosynthetic pathway. In mammals, it can also be obtained from dietary sources, such as grains and fruits. *Myo*-inositol is transported from the extracellular fluid into the cells by specialized transporters.[4,5]

In mammalian cells, the biological role of *myo*-inositol and its derivatives is essential for cell survival and homeostasis. They are important in many cellular processes, such as signaling, cell wall formation, and phosphate storage.[1,3] In addition, they are involved in stress response, nerve function, and cholesterol and glucose metabolism in the human body.[1] Disturbed inositol levels have been found to be strongly associated with many physiological and pathological disorders.[6] The potential of *myo*-inositol and its derivatives in various medical applications, such as in the treatment of various diseases and other therapeutic methods, has been investigated.[1]

Due to its numerous functions, *myo*-inositol is widely used in industries. In the food industry, it is used as an additive in energy drinks and foods, acting as a nutritive and functional sweetener. In cosmetics, it promotes cell growth and helps prevent aging. In the pharmaceutical industry, it acts as a dispersant for various drugs and is used in the treatment of diseases, such as cancer and diabetes.[7]

Considering the uses of *myo*-inositol in the pharmaceutical industry without forgetting the biological aspect, *myo*-inositol combined with the gels is an interesting target. Gels are used in our daily lives, and they are found in everyday products such as shampoo, hair gel, toothpaste, and contact lenses.[8] Gels consisting of an immobile network, the gelator, and a medium, usually a liquid, can be classified, for example, by the type of bonds formed and the solvent used. Covalently cross-linked networks are polymeric gels, and non-covalently cross-linked gels are supramolecular gels, also known as low molecular weight (LMW) gels. Hydrogels have water as a solvent, organogels have an organic solvent, and ion gel has ionic liquid as a solvent.[9,10]

The possibility of using *myo*-inositol as a gelator has attracted interest in recent decades. *Myo*-inositol derivatives have been reported in a limited number of organogels[11,12] and in hydrogels[13] even less. The literature part of this study focuses on *myo*-inositol and examines its properties and roles in biological environments. In addition, the functionalization of *myo*-inositol is discussed and concluded with examples of *myo*-inositol based gels. The experimental part focuses on the synthesis of amphiphilic *myo*-inositol based gelators and their gelling behavior.

## 2 Inositol

Sugar alcohols, also known as cyclitols or polyols, are monocyclic saturated hydrocarbons. They contain at least three hydroxyl groups, each of which must be attached to a different carbon atom in the ring. Sugar alcohols and their derivatives are small organic molecules with neutral charge and low toxicity. These properties make them osmoprotectants and help organisms cope with extreme osmotic stress. This is one of the many roles sugar alcohols can play in cells.[1]

Inositol ($C_6H_{12}O_6$, 180.16 g/mol) is a cyclic carbohydrate with a cyclohexane ring and six OH groups attached to each carbon atom. The structure of inositol is like the cyclic form of monosaccharides, such as glucose(Figure 2).[14] It belongs to the cyclitols and can be called cyclohexanehexol,[3] 1,2,3,4,5,6-cyclohexanhexol[7], or cyclohexane-1,2,3,4,5,6-hexol[5]. Inositol forms a special class of natural metabolites. It is a crystalline white powder and relatively stable in air. Inositol is highly water soluble, slightly soluble in ethanol, ice acetic acid, glycol, and glycerin and insoluble in organic solvents, such as ether and chloroform.[7]
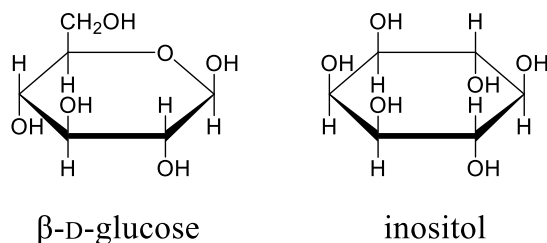


Figure 2. Molecular structure of β-D-glucose and inositol.

The specific structure of inositol, with six chiral centers, is thought to have 64 potential stereoisomers. Due to the symmetry of the molecule, there are nine actual isomers, as shown in Figure 1.[14] Its stereoisomeric forms are determined by the spatial orientation (axial or equatorial) of its six hydroxyl groups attached to the cyclohexane ring.[1] Of the isomers D-*chiro*- and L-*chiro*-inositol are enantiomers.[1] After *myo*-inositol, *chiro*-inositol is the second most common stereoisomer of inositol.[14]

# 3 *Myo*-inositol

## 3.1 The chemical and biological point of view

*Myo*-inositol, also known as *cis*-1,2,3,4-*trans*-4,6-cyclohexanehexol,[7] is a meso isomer of 1,2,3,4,5,6-hexahydroxycyclohexane.[3] It has five equatorial and one axial hydroxyl groups. The axial one is attached to the 2nd carbon of the ring, and the other carbons can be numbered from 1 to 6, starting from the first carbon clockwise or counterclockwise (Figure 3). A symmetrical plane runs through the 2nd and 5th carbons of the molecule. *Myo*-inositol occurs naturally in both free and combined forms as its derivatives. In the derivatives, despite its meso configuration, it is almost always present in the optically active form.[3]
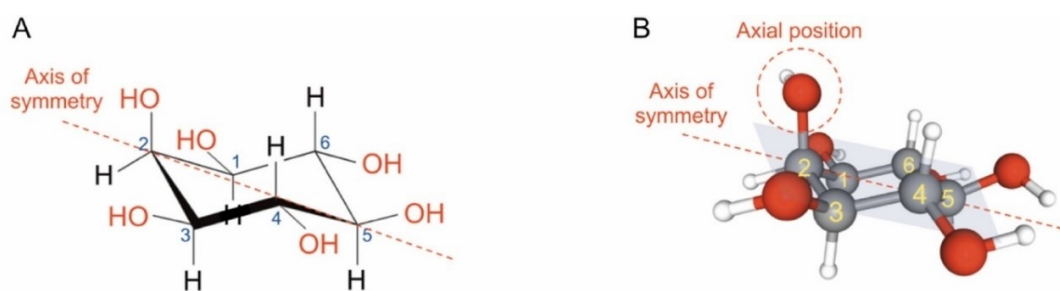


Figure 3. A: The chair conformation of *myo*-inositol emphasizes the role of the axial hydroxyl group at position 2. The alternating equatorial positioning of the other hydroxyl groups minimizes the steric barrier. The symmetry axis of *myo*-inositol passes through carbons 2 and 5, so carbons 1 and 3, and 4 and 6 are enantiomeric. In this thesis, the numbering of the carbon atoms in *myo*-inositol is counterclockwise. B: Relative size of each atom (carbons – grey, oxygen – red, and hydrogens – white) in *myo*-inositol. Reprinted with permission from ref. 4, Copyright 2023, Elsevier, CC BY 4.0.

Inositols are involved in various metabolic and biochemical functions in different organs and tissues. *Myo*-inositol can participate in these biological processes in a free or phosphorylated forms, which are essential components of cells.[15] Functions of *myo*-inositol and its derivatives include metabolic homeostasis, messenger ribonucleic acid (mRNA) export and translation, regulation of ion channel permeability, stress response, cell growth, apoptosis, reproductive

functions, fetal development, neural development and function, and osteogenesis.[1] In its free form, *myo*-inositol serves a critical cellular function as an osmolyte.[4]

*Myo*-inositol can be obtained from dietary sources, for example, and was previously classified as a member of the vitamin B family because of these biological roles.[5,14] Inositol is commonly referred to as vitamin $B_8$, which is not entirely accurate due to the endogenous synthesis of inositol from glucose.[1,15] Inositol is mainly produced in the mammalian kidneys at a rate of about 4 g per day, unlike other known vitamins that cannot be synthesized by mammals.[5,14] Endogenous *myo*-inositol production also involves other organs, such as the brain and liver.[15] Therefore, it is no longer considered an essential dietary nutrient.[5]

## 3.2 Phosphorylated *myo*-inositols

Phosphorylated *myo*-inositols, including inositol polyphosphates (IPs), phosphatidylinositol (PI), and phosphatidylinositol polyphosphates (PIPs), are important compounds with many biological functions.[16] PI and PIPs belong to the phosphoinositides, which are a small fraction of the phospholipids in the cell. However, they play a dominant role in almost every aspect of cellular life and death. For example, they regulate ion channels, transporters, and pumps and control endo- and exocytic processes. Metabolic disorders of these phosphoinositides are associated with cancer, diabetes and obesity.[17]

## 3.2.1 Inositol polyphosphates (IPs)

One class of phosphorylated *myo*-inositols are inositol polyphosphates, also known as inositol phosphates. They consist of a *myo*-inositol core that is phosphorylated at different OH positions.[16] This class of organic compounds can occur in different phosphorylation states, $IP_x$ ($x = 1, 2,…6$). In terrestrial ecosystems, they are synthesized by plants and accumulate in the soil to form the dominant class of organophosphorus. They are also found in aquatic environments where they can contribute to the growth of cyanobacteria, which in turn contributes to eutrophication.[18] The IP structure has 63 possible permutations, but we focus on

three of them because of their major biological role: *myo*-inositol-(1, 2, 3, 4, 5, 6)-hexakisphosphate (IP$_6$), *myo*-inositol-(1, 3, 4, 5, 6)-pentakisphosphate (IP$_5$), and D-*myo*-inositol-(1,4,5)-triphosphate (IP$_3$) (Figure 4).[16]
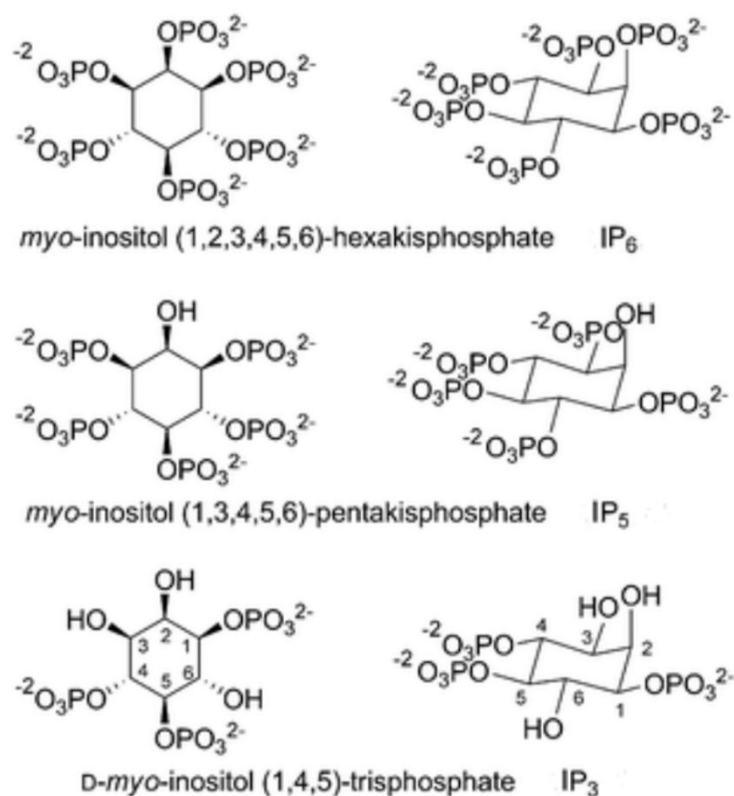


Figure 4. Example structures of inositol phosphates, which play an important biological role.
Used and adapted with permission of Royal Society of Chemistry, from Inositol polyphosphates, diphosphoinositol polyphosphates and phosphatidylinositol polyphosphate lipids: Structure, synthesis, and development of probes for studying biological activity, Best, M. D.; Zhang, H. and Prestwich, G. D., Natural Product Reports, 27, Copyright 2010, permission conveyed through Copyright Clearance Center, Inc.

The most common inositol polyphosphate isomers are the achiral meso structures IP$_6$ and IP$_5$. Their concentrations in the cell are typically 10–100 µM. IP$_6$, also known as phytate[19] or phytic acid[5], is involved in immune response, neurotransmission, calcium channel activation, protein kinase and phosphatase regulation. In addition, due to its antioxidant properties, it acts as an antineoplastic agent in several carcinomas, which is why it is considered a useful dietary component. IP$_5$ has been implicated in virus assembly, cell proliferation, chromatin remodeling and calcium channel regulation.[16]

IP$_3$ is a biologically active inositol polyphosphate that plays an important role as a secondary transmitter of calcium release. It is critical in several calcium-dependent physiological processes, including cell growth, specialization, secretion, muscle movement, embryonic development, and immune function. In addition to these best understood structures, half of the 63 possible permutations of IP have been identified as metabolites of various biological systems. However, only a few have been assigned biological functions. It is possible that only these certain IPs are primarily involved in metabolism or that much more research is needed to elucidate the contribution of others.[16]

## 3.2.2 Phosphatidylinositol (PI)

Phosphatidylinositol, also known as inositol phospholipid, is a membrane lipid found in the cell membranes of all living cells, including plants, animals, fungi, and bacteria.[5] *Myo*-inositol is a major component of this glycerophospholipid with a phosphate group and two acyl chains attached (Figure 5).[20] Of all the phosphorylated *myo*-inositols, PI is the most abundant in mammalian cells due to its role as the precursor of all inositol polyphosphates and phosphatidylinositol polyphosphates.[21,22] PI accounts for approximately 80 % of all *myo*-inositol based phospholipids in eukaryotic cells.[21]
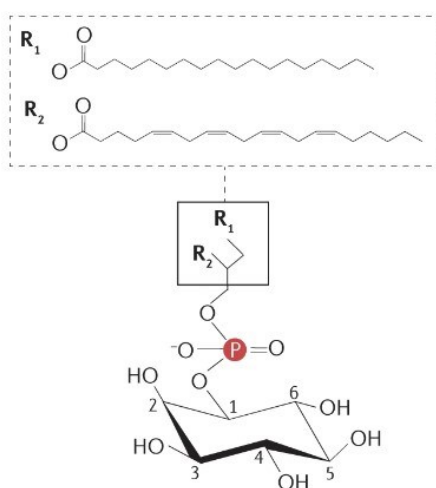


Figure 5. The chemical structure of phosphatidylinositol represented with the 1-stearoyl (R$_1$), 2-arachidonyl (R$_2$) acyl chain configurations most found in phosphoinositides.[20] Reproduced and adapted with permission from Springer Nature.

In addition to being a membrane structure and a precursor of IPs and PIPs, PI and its metabolites are involved in regulating many cellular processes, such as signal transduction, mRNA export from the nucleus, and acting as a store for second messengers.[22] Many diseases, including bipolar disorder, are associated with alterations in PI metabolism. PI can be synthesized in the endoplasmic reticulum from *myo*-inositol and cytidine diphosphate-diacylglycerol, catalyzed by phosphatidylinositol synthase (Figure 6).[5,20]



Figure 6.  Phosphatidylinositol synthesis.[5]

### 3.2.3 Phosphatidylinositol polyphosphates (PIPs)

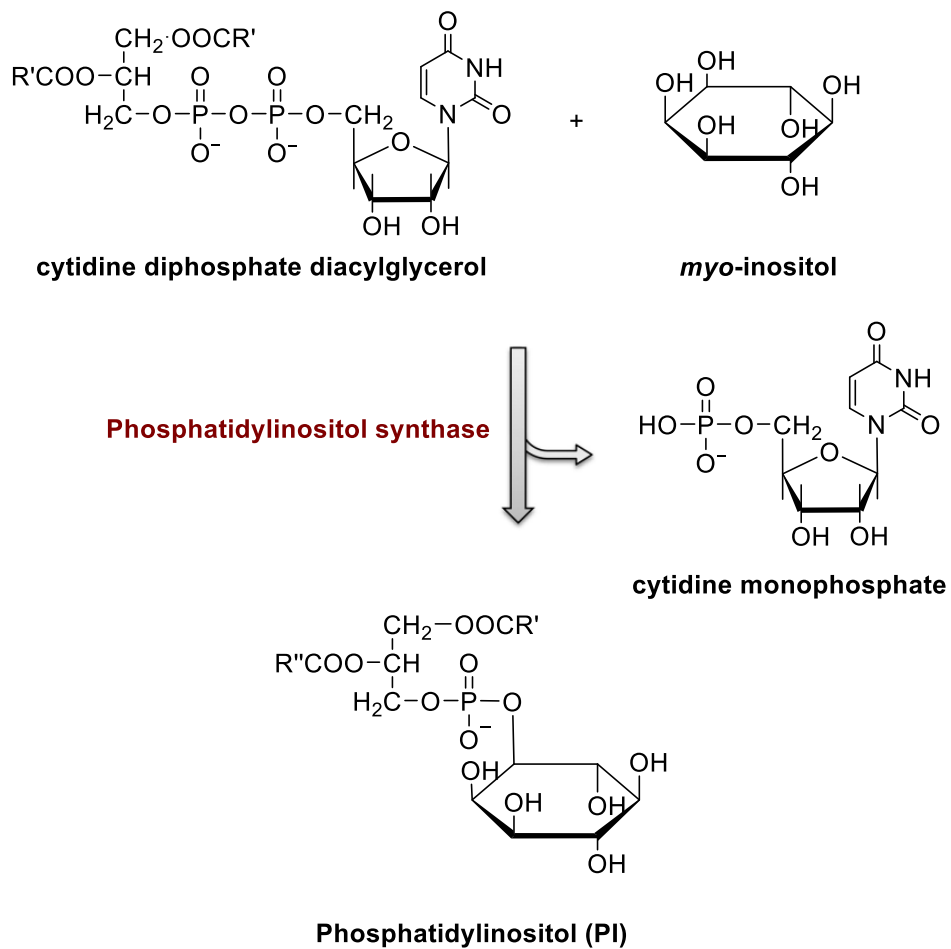Phosphatidylinositol polyphosphates, also known as polyphosphoinositides, are another important structural class of *myo*-inositol based phospholipids.[16] They are phosphorylated derivatives of phosphatidylinositol: the free hydroxyl groups at positions 3-5 of the *myo*-inositol ring of PI are readily phosphorylated by cytoplasmic lipid kinases.[23] Phosphatidylinositol forms the structural backbone, but seven isomers form the PIP family due to phosphorylation at different sites (Figure 7).[19] They make up a much smaller proportion of cell membrane phospholipids than others but are recognized as key integrators of membrane dynamics, affecting all aspects of cell physiology and disease.[20,23]
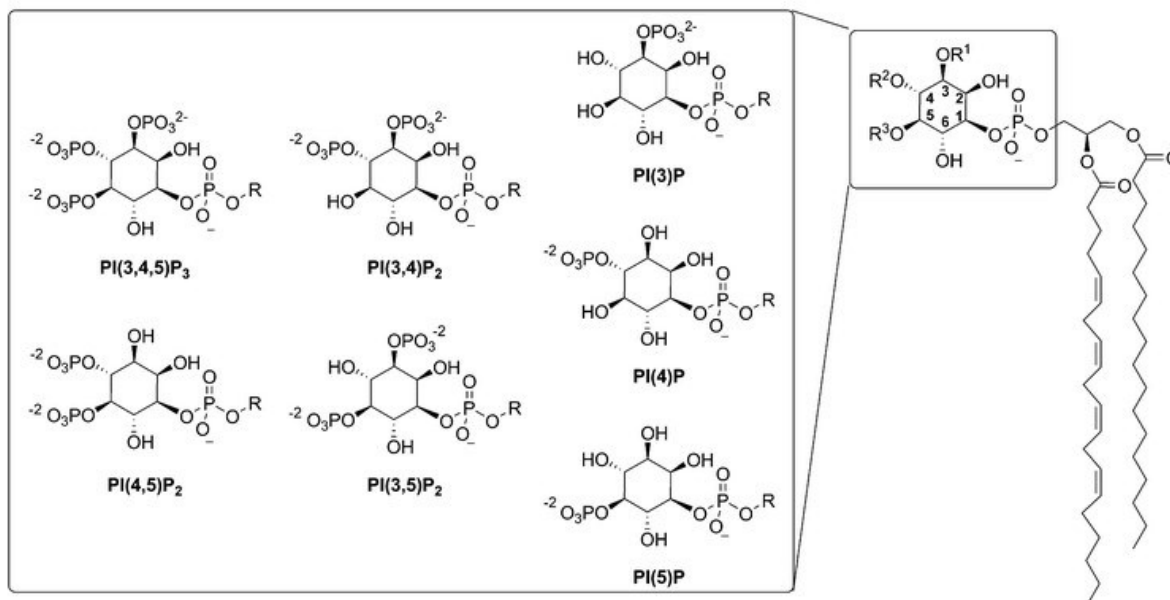


Figure 7. Seven isomers of phosphatidylinositol polyphosphate. Used with permission of Royal Society of Chemistry, from Inositol polyphosphates, diphosphoinositol polyphosphates and phosphatidylinositol polyphosphate lipids: Structure, synthesis, and development of probes for studying biological activity, Best, M. D.; Zhang, H. and Prestwich, G. D., Natural Product Reports, 27, Copyright 2010, permission conveyed through Copyright Clearance Center, Inc.

PIPs are found in various parts of the cell, including the cell membrane, endoplasmic reticulum, Golgi apparatus, nucleus, lysosomes, and endosomes.[21] They are bound to the lipid bilayer component of cell membranes so that the phosphorylated *myo*-inositol group is located on the membrane surface. This is a key feature that distinguishes the activities of PIPs from soluble

IPs.[19] Polyphosphoinositides function mostly as acidic markers that identify different membranes, rather than as important structural components of the lipid bilayer. Their primary role is interaction with proteins, as they instruct specific proteins on how to function within these membranes.[23] Cell signaling involves the activation of membrane-bound proteins and their intracellular transport in soluble form.[16] These protein-lipid binding events control many key physiological pathways by regulating protein function and subcellular location. Defects in binding and lipid composition lead to severe diseases.[16]

## 3.3 Dietary sources of *myo*-inositol

*Myo*-inositol can be ingested with food in addition to being produced endogenously. In the human diet, inositol from plant and animal sources is present as a free molecule, as $IP_6$, or as inositol-containing phospholipids.[5] From animal sources, inositol is mostly present in its free form, or as an inositol-containing phospholipids, whereas in plant foods, inositol is mainly present as $IP_6$.[24]

$IP_6$ is the major form of phosphorus storage in many plant tissues, especially seeds. In fact, phytic acid is abundant in Brazil nuts, walnuts, and almonds. Among common foods, fresh fruits, vegetables, and seed-containing foods, such as grains, beans, and nuts, are the most abundant in *myo*-inositol. Among grains, oats and their bran contain more *myo*-inositol than other grains, and among vegetables, beans and peas have the highest levels. Among fruits, cantaloupe melon and citrus fruits, with the exception of lemon, are exceptionally high in *myo*-inositol.[5]

The dietary intake of *myo*-inositol is 225-1500 mg/day per 1800 kcal, depending on the composition of the diet.[5] The average Western diet is estimated to provide about 1g of total inositol per day. [25] In mammalian cells, 99 % of inositol is in the form of *myo*-inositol and only 1 % in the form of D-*chiro*-inositol.[26] The toxicity of *myo*-inositol has not been studied directly, but its effect in preventing various diseases has been studied. These studies have also provided information on the toxicity of *myo*-inositol. Clinical studies have found that symptoms begin at 12 g/day or higher doses. Adverse reactions include gastrointestinal symptoms such as nausea, flatulence, and diarrhea. The severity of adverse reactions remains the same at a dose of 30 g/day.[27]

# 4 Metabolism and transport of *myo*-inositol

Inositol can be supplied endogenously or exogenously to the cell from three different sources: (1) biosynthesis of *myo*-inositol from glucose, (2) regeneration of phosphorylated *myo*-inositols, and (3) via specialized *myo*-inositol transporters from the extracellular fluid (Figure 8).[5,28] The homeostasis of *myo*-inositol levels in cells and tissues is regulated by the excretion processes involved in its metabolism, such as efflux, renal catabolism, and incorporation into phosphoinositides.[5]
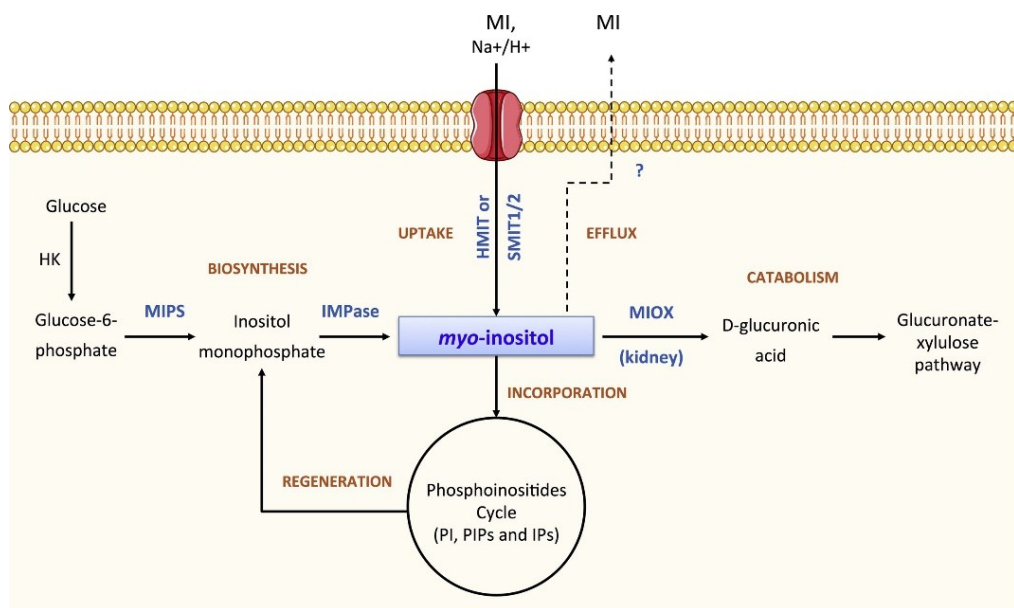


Figure 8. Regulation of intracellular levels of *myo*-inositol by several mechanisms. Abbreviations: HK hexokinase; HMIT $H^+$/*myo*-inositol transporter; SMIT1/2, sodium-dependent *myo*-inositol transporter; IMPase inositol monophosphatase; MIOX myo-inositol oxygenase; MIPS 1-D-*myo*-inositol-phosphate synthase; PI phosphatidylinositol; PIPs phosphatidylinositol polyphosphate and IPs inositol phosphates. Reprinted from Biochimie, Vol 95, Croze, M. L. and Soulage, C. O., Potential role and therapeutic interests of myo-inositol in metabolic diseases, 1811-1827, Copyright 2013, with permission from Elsevier.

## 4.1 Digestion and absorption

Exogenously, i.e. from dietary sources, obtained *myo*-inositol is absorbed through the gastrointestinal tract as inositol phosphate derivatives, including $IP_6$, as PI, or in free form.[24] Phytic acid-derived *myo*-inositol can be released in the intestine of monogastric animals by phytase enzymes in the intestinal mucosa. Phytases are found not only in animals but also in plants and microorganisms. These enzymes can release free inositol and orthophosphates and their intermediates, such as the mono-, di-, tri-, tetra-, and pentaphosphate forms of inositol. A large portion of the ingested phytic acid is hydrolyzed to inositol.[5]

A significant portion of ingested *myo*-inositol is consumed as phosphatidylinositol. It can be hydrolyzed in the intestinal lumen by pancreatic phospholipase A.[5] After hydrolysis, lysophosphatidylinositol enters the intestinal cell. There, it is reacetylated or hydrolyzed again to form glycerylphosphorylinositol.[24] When ingested in its free form, *myo*-inositol is absorbed from the human digestive tract via the active $Na^+/K^+$-ATPase transport system. In healthy individuals, the circulating plasma concentration of *myo*-inositol is approximately 30 µM, and the half-life is 22 minutes.[5] Once in the bloodstream, it is transported by specialized *myo*-inositol transporters to different tissues and cells in the body.[29]

## 4.2 Intracellular syntheses

*Myo*-inositol can be produced intracellularly by two biochemical pathways: *de novo* biosynthesis from glucose and by catabolizing phosphorylated *myo*-inositols.[28,29] On the other hand, formed free *myo*-inositol stimulates incorporation into phospholipids as PI synthesis (Figure 6).[5] Endogenous biosynthesis of *myo*-inositol directly from D-glucose occurs in several mammalian tissues, including kidneys, brain, liver, testis and mammary gland.[30] This *de novo* biosynthesis can be divided into three steps. First, hexokinase (HK) converts D glucose to glucose-6-phosphate via HK-mediated phosphorylation. Following this, glucose-6-phosphate is converted to *myo*-inositol-3-phosphate by 1-D-*myo*-inositol phosphate synthase (MIPS). Finally, *myo*-inositol-3-phosphate is dephosphorylated by inositol monophosphatase (IMPase) to form *myo*-inositol (Figure 9).[15] The second step of this biosynthesis reaction is the rate-limiting step in many organisms.[5]

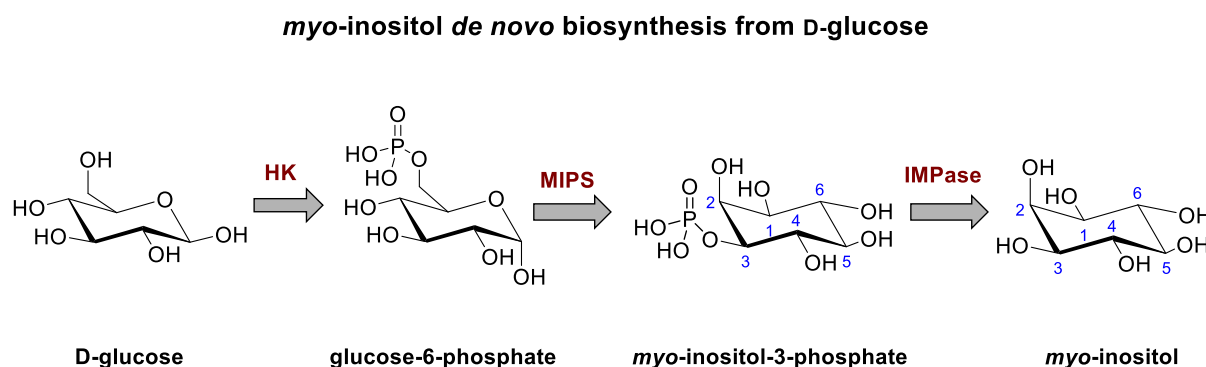**myo-inositol de novo biosynthesis from D-glucose**



Figure 9. *Myo*-inositol *de novo* biosynthesis.[5] Abbreviations: HK hexokinase; MIPS 1-D-*myo*-inositol-phosphate synthase; IMPase, inositol monophosphatase.

This three-step synthesis is the only identified *myo*-inositol biosynthetic pathway found in humans, higher plants, animals, fungi, algae, and cyanobacteria. All known forms of inositol, including stereoisomers and their derivatives, are produced in the metabolic processes of *myo*-inositol.[14] The *myo*-inositol biosynthetic route can be controlled at multiple levels and by a variety of mechanisms, including epigenetic changes in the genes encoding the enzymes involved. Epigenetic regulation consists of inherited genomic phenotypic changes that do not involve nucleotide sequence changes. Specifically, epigenetic factors can affect the expression of the gene responsible for mammalian inositol synthase, resulting in alternatively spliced isoforms, one of which may have a detrimental effect on enzyme activity.[31]

The biosynthetic role of *myo*-inositol is important in the human body, where tissues have different capacities for *myo*-inositol biosynthesis depending on their functional needs. The brain, in addition to the kidneys, produces large amounts of *myo*-inositol. The brain is dependent on its production and recycling because the adsorption of inositol across the blood-brain barrier is not efficient due to the rapid saturation of its transporters.[31]

*Myo*-inositol can also be produced intracellularly by the dephosphorylation of inositol phosphates following the degradation of phospholipids in inositol-containing membranes.[15] In *myo*-inositol formation, the critical intermediates in IP dephosphorylation are isoforms of IP$_3$, I(1,4,5)P$_3$ and I(1,3,4)P$_3$. In the final step, IMPase is responsible for the conversion of intermediate to free inositol, as in the *de novo* biosynthesis of *myo*-inositol.[29] The free *myo*-inositol formed, in turn, stimulates the synthesis of PI. This synthesis occurs in the endoplasmic reticulum, as shown in Figure 6.[15,29]

## 4.3 Specialized transporters

*Myo*-inositol has a significant impact on cell signaling in the cytoplasm and intracellular organelles.[32] Inositol is transported from the extracellular fluid into mammalian cells by three specialized sodium and proton transporters: the sodium-dependent ($Na^+$) *myo*-inositol cotransporters 1 and 2 (SMIT1 and SMIT2) and proton *myo*-inositol symporter (HMIT), which transports *myo*-inositol together with $H^+$ (Figure 10).[4,32] Sodium ion-coupled inositol transporters are found in humans and animals, whereas proton-coupled transporters are found in all classes of eukaryotes.[33]
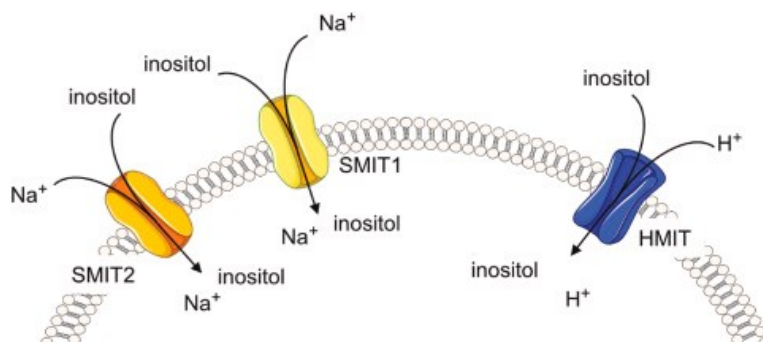


Figure 10. Inositol transporters in mammals. Reprinted with permission from ref. 4, Copyright 2023, Elsevier, CC BY 4.0.

SMIT1 is a high-affinity $Na^+$-dependent active transporter, whereas SMIT2 is relatively similar kinetically but pharmacologically distinct.[32] SMIT1 and SMIT2 both respond to osmotic imbalance. To generate sufficient energy for active *myo*-inositol transport, SMIT1 and SMIT2 cotransport two $Na^+$-ions along the concentration gradient. Remarkably, SMIT2 also transports D-*chiro*-inositol, in contrast to SMIT1.[5] HMIT is a lower affinity $H^+$-dependent active transporter that does not appear to have a co-regulatory function in mammals. HMIT is normally expressed on intracytosolic membranes and, for example, in neurons located in the Golgi apparatus.[32]

The expression of these transporters varies in the human body. HMIT is mainly expressed in the brain and, to a lesser extent, in kidneys, oocytes, and fat cells. SMIT1 is expressed in the kidneys, brain, pancreas, placenta, skeletal muscles, heart, and lungs, and SMIT2 is expressed in the heart, small intestine, kidneys, liver, skeletal muscle, and placenta, and to a lesser extent in the brain.[31]

## 4.4 Catabolism and excretion

Inositol degradation is inactive in many mammalian cell types and has, therefore, been studied less than inositol synthesis.[4] Unlike *myo*-inositol synthesis, its catabolism occurs only in the kidneys. Inositol degradation is initiated by *myo*-inositol oxygenase (MIOX), which is a proximal tubular-specific enzyme. Despite its name, MIOX is also a cleavage substrate for D-*chiro*-inositol.[15] It catalyzes the oxidative cleavage of inositol to D-glucuronic acid. The activity of MIOX was originally detected in rat kidney homogenate, but the gene was subsequently detected in humans and bacteria.[4]

MIOX oxidatively cleaves the cyclic ring of *myo*-inositol in renal proximal tubule cells (Figure 11). This produces D-glucuronic acid followed by conversion to xylitol and further catabolized to D-xylulose-5-phosphate via the glucuronate-xylulose pathway. Finally, D-xylulose-5-phosphate enters the pentose phosphate cycle, one of the most important pathways for producing oxidative energy.[15,34]



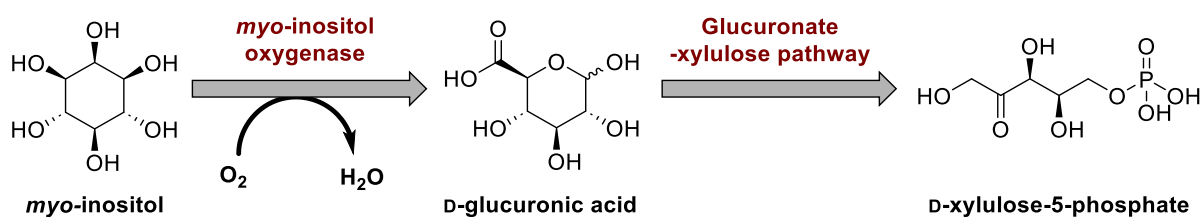Figure 11. *Myo*-inositol catabolic pathway in the kidneys.[5]

In the kidneys, primary urine contains a significant amount of *myo*-inositol. Approximately 98 % of this is reabsorbed into the blood.[34] Only a small fraction of the renal excretion of inositol occurs in the urine, indicating that the kidneys play an important role in regulating plasma inositol levels in both humans and animals.[5,34]

# 5 *Myo*-inositol intracellular depletion and effects

Intracellular *myo*-inositol levels are regulated by several processes, including cellular biosynthesis, the phosphoinositide cycle, intestinal absorption, extracellular uptake, efflux, and degradation (Figure 8). Changes in these processes can lead to intracellular abnormalities in the levels of *myo*-inositol.[5] The main causes of *myo*-inositol depletion are related to decreased activities of synthases such as MIPS and IMPase. This may result in decreased PIPs and diacylglycerol levels, decreased $Na^+/K^+$-ATPase activity, and impaired cell development, differentiation and transformation.[29]

It has also been found that a deficiency of intracellular *myo*-inositol is associated with osmotic stress in the cell. Increased intracellular osmolarity provokes *myo*-inositol release and leads to intracellular *myo*-inositol depletion in chronic conditions. In addition, some substances, such as lithium and valproic acid, have been shown to cause intracellular *myo*-inositol depletion. Lithium is used for mood stabilization by increasing serotonin accumulation in the central nervous system, but it also inhibits *myo*-inositol synthesis by impairing the activity of phosphatases, such as IMPase. The effect of valproic acid on *myo*-inositol synthesis was associated with inhibition of MIPS.[29]

Alterations in *myo*-inositol homeostasis can alter inositol metabolism and lead to decreased inositol levels. As a result, a person may be exposed to several pathological conditions, such as polycystic ovary syndrome, hypothyroidism, and metabolic and hormonal imbalances, such as metabolic syndrome, weight gain, dyslipidemia, and hyperinsulinemia. In addition, diabetes, cancer, especially breast and lung cancer, and neuropathological and psychiatric disorders, including Alzheimer's and Parkinson's disease, have been associated with decreased levels of *myo*-inositol.[31]

Due to the multiple biological roles of *myo*-inositol, its use as a therapeutic agent in the treatment of these various diseases is supported by its low toxicity, good drug tolerance, potential use during pregnancy, wide distribution, and easy availability.[1]

# 6 *Myo*-inositol functionalization

*Myo*-inositol has attracted great synthetic interest due to its diverse structures and important biological functions. Synthetic methods, such as *de novo* synthesis and protecting group-based strategy, have been developed to prepare potential *myo*-inositol derivatives that may contribute to drug discovery for inositol-related diseases (Figure 12). The *de novo* strategy uses non-inositol-derived products as starting materials to produce all nine inositol stereoisomers through multi-step chemical reactions. A readily available commercial *myo*-inositol is used as starting material in a protecting group-based strategy. Different protecting groups are used to separate, mask, and unmask chemically equivalent OH groups, ultimately leading to site-specific modifications of *myo*-inositol. From a synthetic point of view, both methods require many steps to protect and deprotect functional groups, making direct functionalization of *myo*-inositol an interesting option.[6]
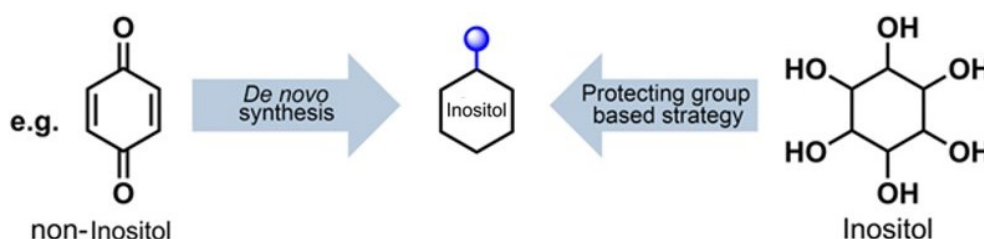


Figure 12. General strategies for the synthesis of inositol derivatives from non-inositol starting materials and inositol. Used and adapted with permission of Royal Society of Chemistry, from Site-selective C–H alkylation of *myo*-inositol via organic photoredox catalysis, Cao, H.; Guo, T.; Deng, X.; Huo, X.; Tang, S.; Liu, J. and Wang, X., Chemical Communications, Vol 58, Copyright 2022, permission conveyed through Copyright Clearance Center, Inc.

The primary steps in the preparation of biologically significant inositol derivatives involve intermediates in which hydroxyl groups are protected, leaving free hydroxyl groups in the desired positions. These protected inositol derivatives, along with their counterparts, are synthesized from various sources, including natural cyclitols and their derivatives, carbohydrates, chiral acids, benzene derivatives, cyclohexene, and p-benzoquinone (Figure 13).[3]
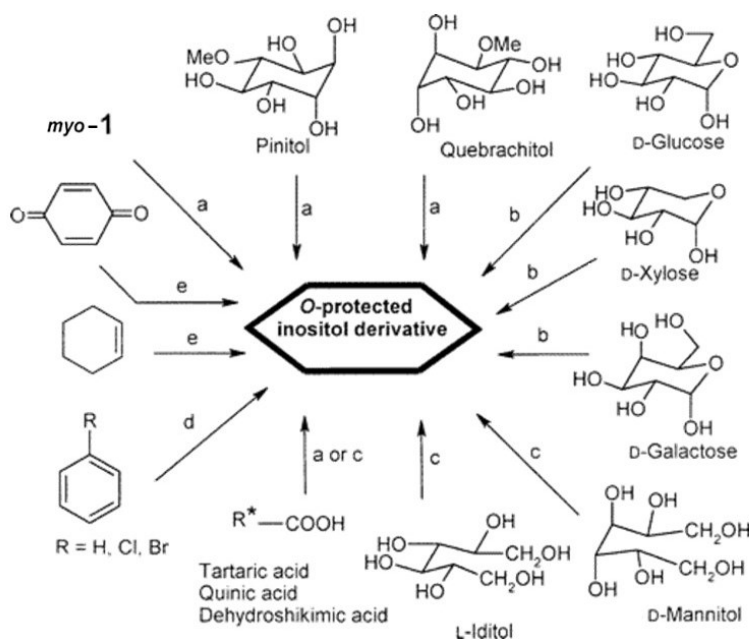
Figure 13. Synthesis pathway of protected inositol derivatives according to starting material: a) hydroxyl group protection and deprotection, b) Ferrier reaction, c) SmI$_2$-mediated cyclization, d) *Pseudomonas putida*-mediated hydroxylation followed by dihydroxylation reactions, and e) hydroxylation. Reprinted and adapted with permission from Regioselective Protection and Deprotection of Inositol Hydroxyl Groups, Sureshan, K. M.; Shashidhar, M. S.; Praveen, T. and Das, T., *Chem. Rev.*, **2003**, *103*, 4477–4504. Copyright 2003 American Chemical Society.

Each of these options presents challenges. The use of *myo*-inositol as a starting material inevitably involves multiple protection and deprotection reactions due to the six secondary hydroxyl groups. To obtain enantiomerically pure protected inositol, it's essential to undergo either chemical or enzymatic resolution of intermediates. Chiral compounds, pinitol and quebrachitol, avoid the resolution problem but require inversion of the axial hydroxyl group to obtain *myo*-inositol derivatives. Carbohydrate starting materials provide optically pure intermediates due to the chirality of the starting materials but require C-C bond formation, usually via the Ferrier cyclization reaction. Benzene and its derivatives undergo microbial oxidation to form cyclohexadiene diols, which are common intermediates in the production of isomeric inositols or their derivatives.[3]

Synthesis routes from commercially available *myo*-inositol to produce protected *myo*-inositol derivatives and their analogs are often the most popular because they are inexpensive and easy to use. Due to the symmetry of *myo*-inositol derivatives, several methods have been developed to obtain enantiomerically pure products, such as desymmetrization of the products and efficient resolution of racemic compounds.[3]

## 6.1 Regioselective protection

For inositols, the direct introduction of the desired functional group at a specific site is synthetically problematic due to the similar reactivity of several hydroxyl groups. In general, the first step is to convert them into acetal derivatives. *Myo*-inositol has been used as a starting material in synthesizing physiologically important inositol derivatives and the total synthesis of natural products and analogues. In addition, *myo*-inositol has been used as a precursor for gelators, liquid crystals, metal complexes, and surfactants. Inositol monoacetals, diketals, or orthoesters were used in almost all cases to produce the desired molecules.[35]

The formation of partially protected *myo*-inositol is subject to several influences. These include the acidity of unbound hydroxyl groups, hydrogen bonding interactions, adjacent functional groups, protecting groups present, carbocyclic ring configuration, reaction conditions, and reagents used. While in some cases, the reasons for selectivity may be obvious, in others, they may be more uncertain or questionable. However, almost any desired protected *myo*-inositol derivative can be synthesized using a suitable method.[3]

The observed reactivity between *myo*-inositol's six hydroxyl groups is C1 ~ C3 > C4 ~ C6 > C5 > C2. The differences in reactivity between the axial and equatorial groups are well explained by conformation and controllable barriers, but there are some exceptions. Modification of the inositol ring at a particular site may also affect the properties of other functional groups, such as charge distribution, hydrogen bonding, conformational changes, chelation, and controllable barrier. This, in turn, can affect the relative reactivity of hydroxyl groups that have traditionally been protected as ketals of acetone, cyclopentanone, or cyclohexanone.[3]

*Myo*-inositol protective reactions are numerous. For example, *myo*-inositol can be treated with acetone in the presence of an acetic acid and a Lewis acid $ZnCl_2$, followed by acetylation (Figure 14, reaction a), resulted in tetra acetate **2**, which was converted to compound **3** by alcoholysis. A similar reaction, where 2,2-dimethoxypropane was used instead of acetone, resulted in compound **3** in good yield (Figure 14, reaction b). Treatment of *myo*-inositol with an excess of 2,2-dimethoxypropane results in a mixture of ketals. From this mixture, the diketal **5** was isolated as its dibenzoate **4**, primarily because of its lower solubility in dimethylformamide (DMF) (Figure 14).[3]

a) acetone, ZnCl$_2$, AcOH ; Ac$_2$O, pyridine
b) 2,2-dimethoxypropane, TsOH, DMSO
c) Et$_3$N
d) pyridine, BzCl
e) NaOH, MeOH

**2** R$^1$ = Ac (47%)
**3** R$^1$ = H  (76%)
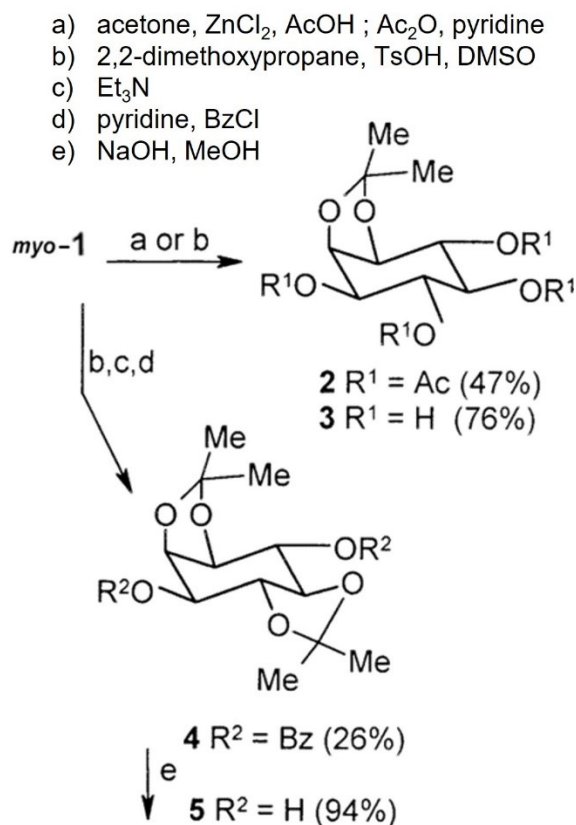
**4** R$^2$ = Bz (26%)

**5** R$^2$ = H (94%)

Figure 14. Different reaction conditions for *myo*-inositol protection reactions. Reprinted and adapted with permission from Regioselective Protection and Deprotection of Inositol Hydroxyl Groups, Sureshan, K. M.; Shashidhar, M. S.; Praveen, T. and Das, T., *Chem. Rev.*, **2003**, *103*, 4477–4504. Copyright 2003 American Chemical Society.

The use of 1,2-diacetals in organic synthesis is on the rise and represents a promising application in inositol synthesis for the selective protection of diequatorial 1,2-diols. This approach has the potential for the synthesis of inositol phosphates and analogues.[36] Butane-2,3-diacetal (BDA) has been used as a protecting group, and its suitability for *myo*-inositol protection was first demonstrated by Monchemp *et al.*[37] In an acid-catalyzed reaction of 2,2,3,3-tetramethoxybutane with *myo*-inositol, a small symmetrical diol **6** was successfully synthesized. Subsequently, the possibility of substituting the butane-2,3-diacetal with a cheap and commercially available butanedione was demonstrated in a screening reaction. Using the butanedione method with 40 h reflux, the *myo*-inositol protection reaction was successfully carried out on a large scale, producing symmetrical diol **6** as the main product and asymmetrical diol **7** as the second main product (Figure 15). Extending the reaction time up to 28 days results in a low-yield asymmetric reaction product **8** in which the inositol ring does not adopt the usual chair conformation.[36]
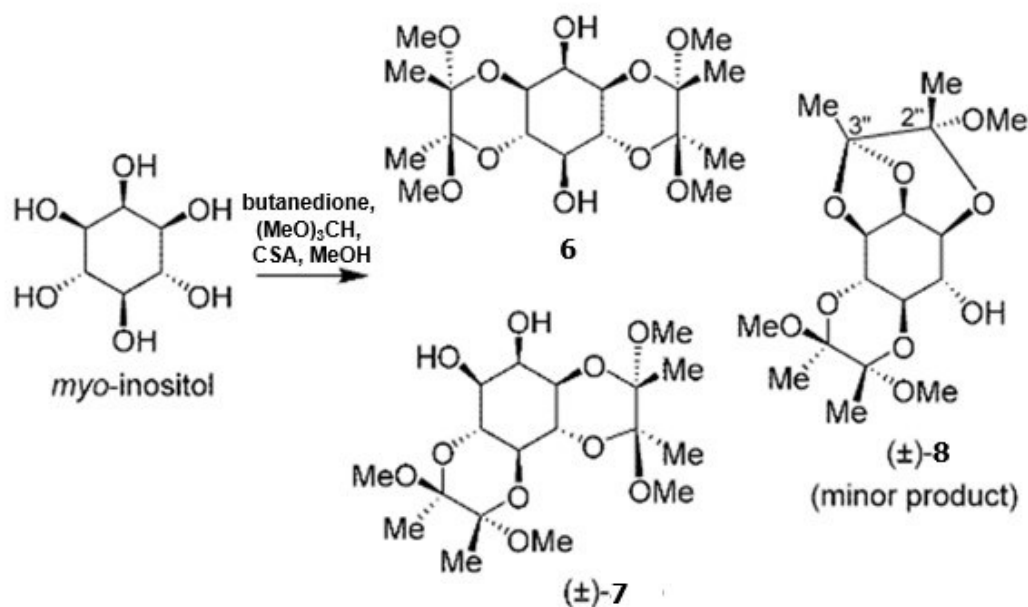
Figure 15. The acid catalyzed reaction of butanedione produces both a symmetric **6** and an asymmetric **7** diol with a 40 h reflux time. Reprinted and adapted with permission from ref. 36, Copyright 2003, John Wiley & Sons, Inc.

In the preparation of *O*-protected derivatives of *myo*-inositol, the ketalization of two or four hydroxyl groups has been the traditional method of protection. However, in addition to ketalization, protection of the C1, C3, and C5 hydroxyl groups of *myo*-inositol as the corresponding orthoesters have emerged. The popularity of orthoesters is because they are readily available in gram quantities as a single product. Conversely, the ketalization of *myo*-inositol results in a mixture of isomers that must be separated by chromatography, and the yields of the individual isomers rarely exceed 30%.[38]

*Myo*-inositol orthoesters **9-12** are prepared between *myo*-inositol and methyl or ethyl orthoesters of selected carboxylic acids (Figure 16). The orthoesters can be isolated in at least 90 % yield by column chromatography or as the corresponding triacetate or tribenzoate without chromatography. Orthoformate **9** is commonly used to synthesize O-protected *myo*-inositol derivatives. *Myo*-inositol orthoesters are not only useful intermediates in synthesizing phosphorylated inositols, but they also have an unusual and interesting chemical structure due to their rigid adamantane-like structure.[38]
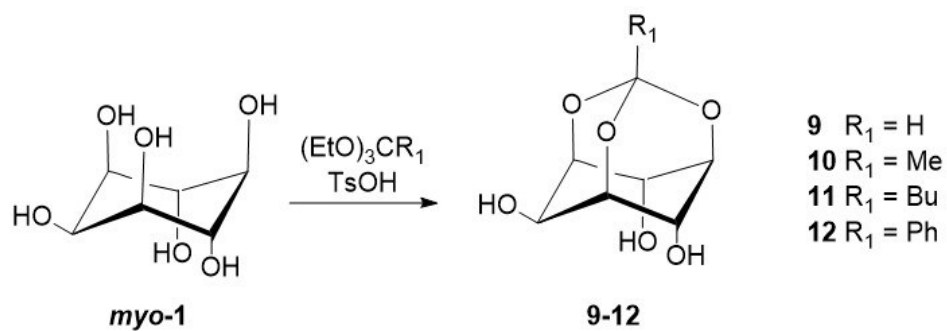
Figure 16. Reaction for orthoesters **9-12** of *myo*-inositol, wherein three free hydroxyl groups are protected.[38]

The use of protecting groups increases the complexity of synthesizing inositol derivatives by increasing the number of intermediates required to generate the final molecule. This, in turn, reduces the overall efficiency of the synthesis. Direct functionalization of inositol would be highly desirable.[35]

## 6.2 Functionalization of unprotected *myo*-inositol

### 6.2.1 Site-selective C-H alkylation

Direct functionalization of *myo*-inositol is the ideal method for synthesizing inositol derivatives. To improve synthetic efficiency, Cao *et al*.[6] reported the possibility of modifying inositol without protecting groups by exploiting photo-redox-mediated hydrogen atom transfer (HAT) chemistry. Selective and direct alkylation of specific sites on *myo*-inositol, achieved under mild conditions, involves a combination of organic photoredox and HAT catalysis (Figure 17).
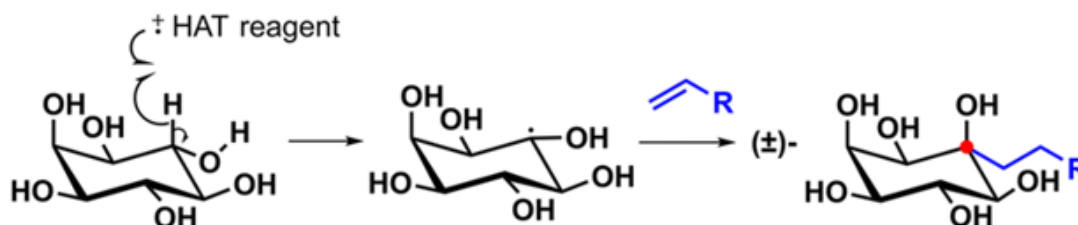


Figure 17. Photoredox-catalyzed HAT for direct C-H alkylation of *myo*-inositol. Used and adapted with permission of Royal Society of Chemistry, from Site-selective C–H alkylation of *myo*-inositol via organic photoredox catalysis, Cao, H.; Guo, T.; Deng, X.; Huo, X.; Tang, S.; Liu, J. and Wang, X., Chemical Communications, Vol 58, Copyright 2022, permission conveyed through Copyright Clearance Center, Inc.

To optimize the reaction conditions, inactivated alkene **13a** (Figure 18, A) was used as a model substrate to increase the scope of the alkylation reagent. In addition, the reaction conditions were optimized by screening the photocatalysts, additives, solvents and their concentrations and substrate ratios used in the reaction. The reaction was tested with different HAT reagents (Figure 18, B). HAT reagents **14a-f** did not give the desired final product. The HAT reagents **14g** and **14 h** gave the CH alkylation product with yields of 26 % and 35 %, respectively. Finally, glycocetacetic quinuclidine **14i** was found to be the best performing catalyst in the reaction, giving 56 % yield, as none of **14j**, **14k**, or **14l**, gave a better yield.[6]
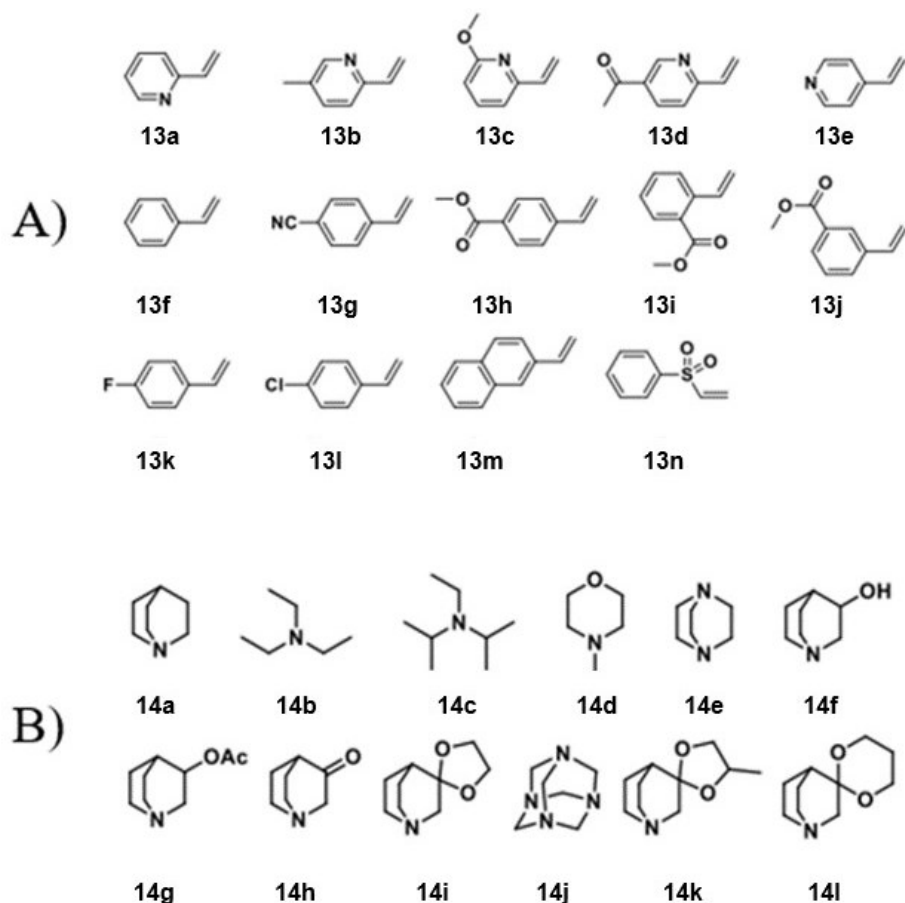
Figure 18. A) Substrates for C-H alkylation of *myo*-inositol; B) HAT catalysts. Used and adapted with permission of Royal Society of Chemistry, from Site-selective C–H alkylation of *myo*-inositol via organic photoredox catalysis, Cao, H.; Guo, T.; Deng, X.; Huo, X.; Tang, S.; Liu, J. and Wang, X., Chemical Communications, Vol 58, Copyright 2022, permission conveyed through Copyright Clearance Center, Inc.

Once the optimum conditions for the reaction were achieved, the extent of the substrate was investigated (Figure 19). The research showed that vinylpyridine derivatives with both electron-donating and electron-withdrawing groups could be attached to the *myo*-inositol C6 position with stereoselectivity. In addition, styrene derivatives with electron-withdrawing groups were found to be good substrates. Several functional groups, such as CN, COOMe, F, and Cl, were compatible with the reaction mixture. On the other hand, styrene derivatives containing electron-donating groups showed a low reactivity.[6]
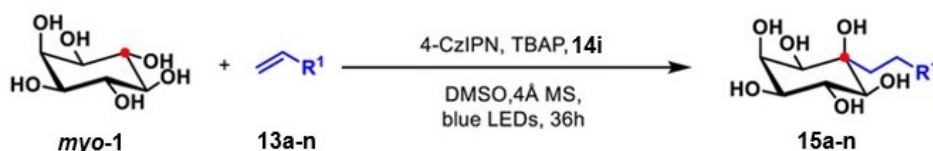
Figure 19. Optimized reaction conditions for site-selective photoredox C-H alkylation. Yields were 21-85 % for various substrates. Used and adapted with permission of Royal Society of Chemistry, from Site-selective C–H alkylation of *myo*-inositol via organic photoredox catalysis, Cao, H.; Guo, T.; Deng, X.; Huo, X.; Tang, S.; Liu, J. and Wang, X., Chemical Communications, Vol 58, Copyright 2022, permission conveyed through Copyright Clearance Center, Inc.

The putative reaction mechanism for the direct functionalization of *myo*-inositol is shown in Figure 20. At the beginning of the reaction, 4-CzIPN (PC) was excited by PC* with blue LED irradiation. This allowed for reductive quenching with HAT reagent, yielding the electrophilic radical I. This radical can remove the hydrogen atom from the C-H bond at the C6 position, forming a stabilized radical III with the concomitant formation of ammonium II. Next, the *myo*-inositol radical was introduced into the alkene, followed by one-electron reduction and proton transfer. This resulted in the formation of the desired product and the return of the PC to its ground state.[6]
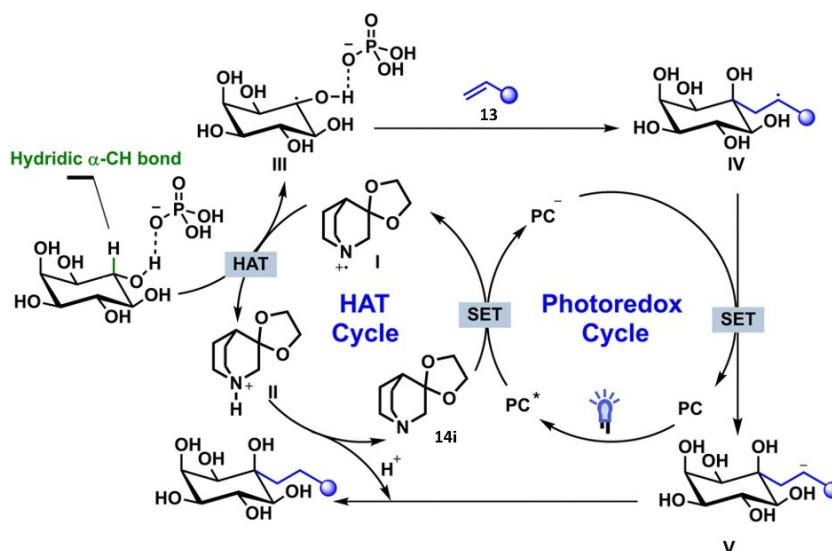


Figure 20. Assumed reaction mechanism. Abbreviations: PC Photocatalyst; SET Single electron transfer; HAT hydrogen atom transfer. Used and adapted with permission of Royal Society of Chemistry, from Site-selective C–H alkylation of *myo*-inositol via organic photoredox catalysis, Cao, H.; Guo, T.; Deng, X.; Huo, X.; Tang, S.; Liu, J. and Wang, X., Chemical Communications, Vol 58, Copyright 2022, permission conveyed through Copyright Clearance Center, Inc.

## 6.2.2 Electrophilic substitution

Yutaka *et al.*[35] reported that unprotected *myo*-inositol could be regioselective functionalized via electrophilic substitution. Unprotected *myo*-inositol reacted with various electrophiles to produce regioselective 1,3-di-*O*-substituted or racemic 1-*O*-substituted derivatives (Figure 21). Tosyl chloride and aroyl chlorides were, for example, used as electrophiles. The outcome of the reaction was influenced by the reaction time and the amount of reagents.
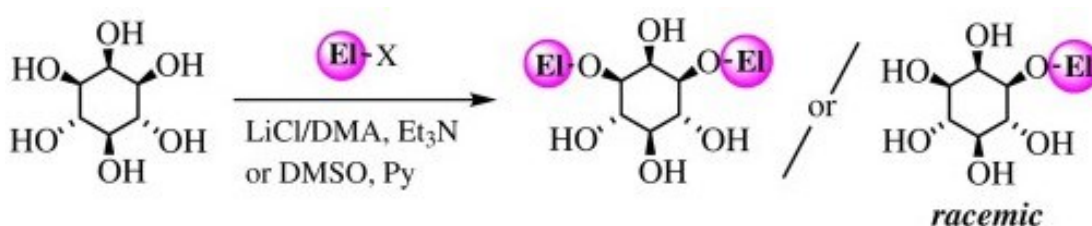


Figure 21. Regioselective functionalization of unprotected *myo*-inositol. Reprinted from Tetrahedron, Vol 69, Watanabe, Y.; Uemura, T.; Yamauchi, S.; Tomita, K.; Saeki, T.; Ishida, R. and Hayashi, M., Regioselective functionalization of unprotected *myo*-inositol by electrophilic substitution, 4657–4664, Copyright 2013, with permission from Elsevier.

Typically, there is a six-step reaction sequence to add the substituent to C1 position of *myo*-inositol, as shown in the synthesis of racemic 1-*O*-acyl-*myo*-inositol (Figure 22, A). The 1,2-cyclohexylidene ketal was derived from *myo*-inositol in two steps, which was then benzylated, hydrolyzed, acylated, and debenzylated to yield the target compound. Similarly, the 1,3-dibenzoate of mesomeric 1,3-di-*O*-substituted *myo*-inositol derivatives was prepared in five steps via orthoesterification (Figure 22, B).[35]
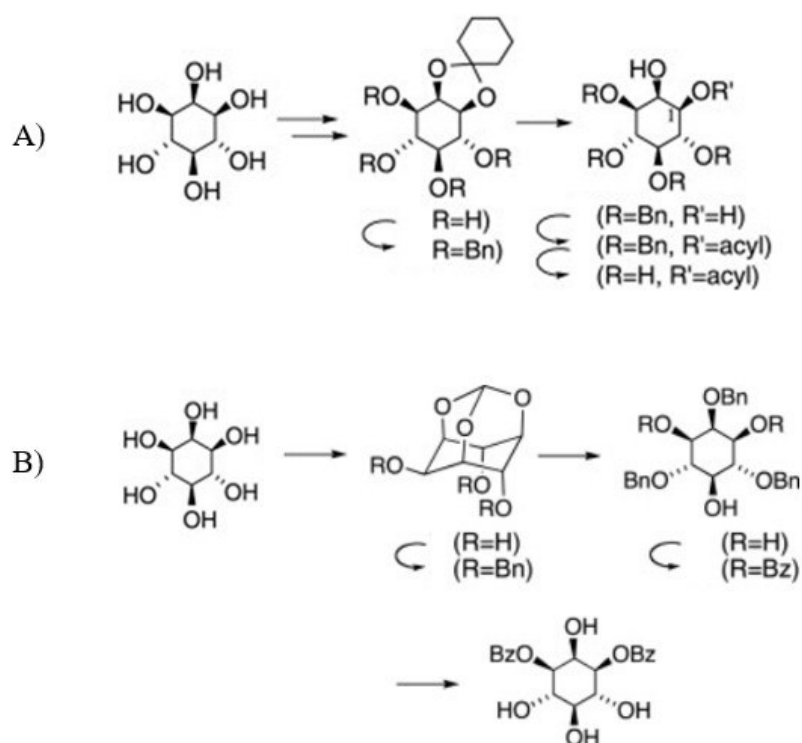
Figure 22. A) A six-step reaction sequence for 1-*O*-acyl-*myo*-inositol; B) A five-step reaction sequence for 1,3-di-*O*-substituted *myo*-inositol. Reprinted from Tetrahedron, Vol 69, Watanabe, Y.; Uemura, T.; Yamauchi, S.; Tomita, K.; Saeki, T.; Ishida, R. and Hayashi, M., Regioselective functionalization of unprotected *myo*-inositol by electrophilic substitution, 4657–4664, Copyright 2013, with permission from Elsevier.

In parallel to the multi-step reaction route, a direct synthesis method based on a dissolution strategy was developed to synthesize the 1,3-di-*O*-substituted target molecule. It was found that in the conventional alcohol acylation method, the low solubility of *myo*-inositol in pyridine slows down the acylation step. On the other hand, increasing the number of inositol substituents accelerates the reaction by increasing the solubility. Dimethyl sulfoxide (DMSO) and dimethylacetamide (DMA) containing LiCl were found to be suitable solvents for inositol. As expected, inositol reacted uniformly in LiCl/DMA solution in the presence of triethylamine to give the desired 1,3-di-*O*-substituted product in excellent yields (Figure 23). For substitution reactions other than silylation, the LiCl/DMA solvent is preferred over DMSO because DMSO is more nucleophilic and tends to react with an electrophile instead of *myo*-inositol.[35]
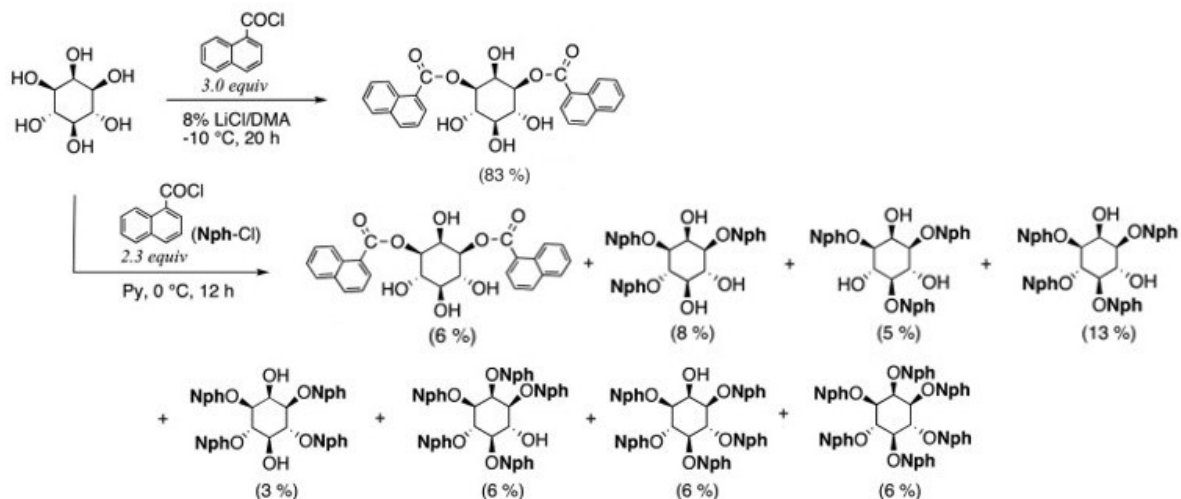
Figure 23. Naphtoylation of *myo*-inositol under different reaction conditions. Reprinted from Tetrahedron, Vol 69, Watanabe, Y.; Uemura, T.; Yamauchi, S.; Tomita, K.; Saeki, T.; Ishida, R. and Hayashi, M., Regioselective functionalization of unprotected *myo*-inositol by electrophilic substitution, 4657–4664, Copyright 2013, with permission from Elsevier.

By adjusting the reaction time and reducing the amount of electrophile, it was possible to selectively monosubstitute one of the two chemically equivalent OH groups (at positions C1 and C3). Several experiments led to the formation of a regioselectively monosubstituted derivative (racemic mixture), which was also accompanied by a small amount of 1,3-disubstitution product (7-21 % yield) (Figure 24). Trimethylsilylation and desilylation methods were used to isolate both products.[35]
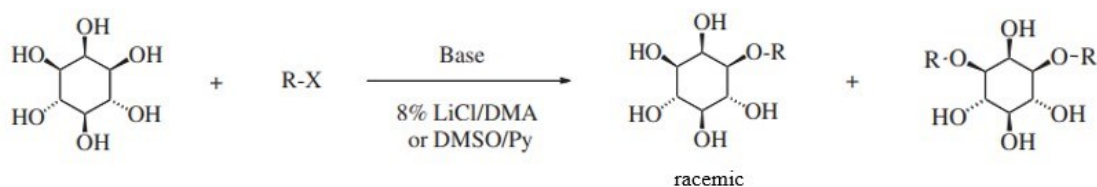


Figure 24. Synthesis of 1-*O*-substituted *myo*-inositol derivatives. Reprinted from Tetrahedron, Vol 69, Watanabe, Y.; Uemura, T.; Yamauchi, S.; Tomita, K.; Saeki, T.; Ishida, R. and Hayashi, M., Regioselective functionalization of unprotected *myo*-inositol by electrophilic substitution, 4657–4664, Copyright 2013, with permission from Elsevier.

Direct functionalization of the hydroxyl groups of *myo*-inositol at positions C1 and C3 with acyl, sulfonyl, phosphinyl and silyl groups was achieved using a DMA solution containing LiCl and DMSO. With a limited number of electrophiles, mainly 1-*O*-mono-substituted derivatives were obtained. The inositol derivatives synthesized in this experiment can be used as surfactant candidates and intermediates for synthesizing various compounds.[35]

## 7 Gels

Gels can be formed from many different chemical systems, so they are often easier to identify than to define. Dorothy Jordan Lloyd[39] proposed that a gel consists of two components: one must be liquid at the temperature of interest and the other solid, the gelator. To meet the definition of a gel, a system should have the mechanical properties of a solid. Although this definition is useful for defining gels, it is imprecise for colloids, which are not all gels. Similarly, not all gels are colloids.[40]

More specifically, gels are semi-solid rigid heterogeneous systems composed of immobile three-dimensional networks and mobile media, usually liquids. Crosslinking of the network fibers provides the rigidity that characterizes a gel.[9] Gels can be classified based on the network type as covalently bonded polymeric gels and physical, non-covalently bonded supramolecular gels (LMW gels).[10] They can also be classified based on the solvent used. Air as a gel medium is called an aerogel, and xerogel is a dried gel.[9]

In polymeric gels, a three-dimensional network is constructed by one-dimensional objects, i.e., chains in which monomer units are covalently linked. In supramolecular gels, the construction of a three-dimensional network consists of zero-dimensional objects, i.e. molecules that must first form one-dimensional objects through self-assembly and non-covalent interactions, which later form a three-dimensional network.[40] In gels, the solvent, which acts as a medium for the three-dimensional network, can account for > 99 % of the total mass, even though the gel behaves as a solid. However, the properties of the gel are mainly due to the gel matrix.[41]

In terms of properties, the gel is classified as a soft material characterized by a jelly-like consistency. The cross-links in covalent and non-covalent gels give them hardness and adhesiveness, making them stable in a liquid in which cross-links are present. Gels are also homogeneous porous materials. The other properties of gels and their applications vary according to the gel type.[9] In this thesis, we focus on LMW supramolecular gels on the way to *myo*-inositol based hydrogels.

## 7.1 Gel formation

The most common method of making gels is to dissolve a gelator in a liquid, often by heating. In the liquid, the gelator exists in small aggregates or as unaggregated molecules. This state is called the sol phase. When the sol is cooled below the transition temperature, it transforms into a gel. In general, a higher concentration of gelator leads to a higher sol-gel transition temperature ($T_{gel}$). The characteristic property of a gel is its elastic rheological behavior: Under low mechanical stress, the gel should not relax over time, or under infinitely long mechanical stress, the gel should not flow.[42]

A simple diagnostic test, the vial inversion method, has been developed to study gel formation. In the vial inversion method, a mixture of solids and liquids is treated as described above and allowed to cool to room temperature (RT) after heating. After 24 hours, the vial is inverted. If no flow is observed, it is classified as a gel with a yield stress.[40,42] Performing and interpreting this simple rheological test requires careful attention, as it is possible to interpret a viscous sol as a gel and a gel with low yield stress as a sol.[42]

The vial inversion method is the most convenient and popular method for studying gel formation, but it is by no means sufficient as the only method for determining gel formation.[10] More detailed studies and measurements of the mechanical properties of gels should be performed using more advanced rheological techniques. These more sophisticated methods are very time-consuming but can distinguish between weak and strong gels.[40]

## 7.2 Low molecular weight gels

Low molecular weight (LMW) gels are supramolecular gels formed by the self-assembly of small molecules, LMW gelators (limited to < 3000 Da)[40], into anisotropic architectures such as long fibers. The gelation process occurs at a sufficient concentration and with a simple trigger, such as heating and cooling or pH trigger. The fibers entangle to form a network capable of immobilizing the solvent by capillary forces and surface tension (Figure 25).[10,41]
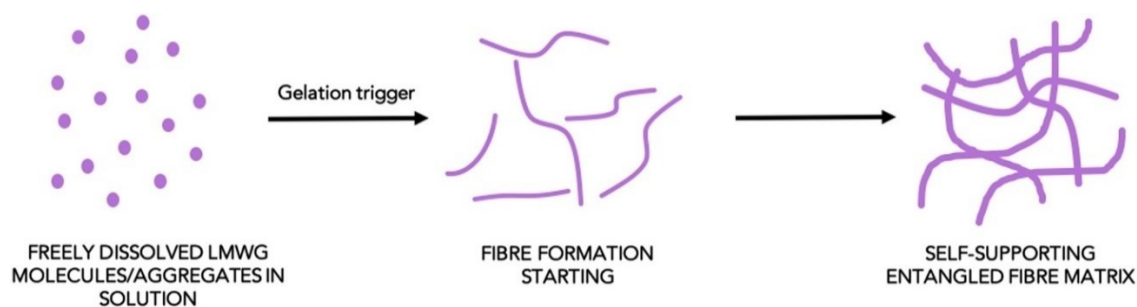
Figure 25. Assumed LMW gelation process. Reprinted with permission from ref. 10, Copyright 2017, Published by Elsevier Inc., CC BY 4.0.

In the gelation process, molecules must interact one-dimensionally to form suitable aggregates at the molecular level.[10] This self-aggregation of LMW gelators is driven by noncovalent interactions between molecules, including hydrogen bonding, halogen bonding, π-stacking, and van der Waals interactions. Due to non-covalent interactions, LMW gel formation is sensitive to changes in the local environment. Physical interactions between the aggregates, such as micelles, ribbons, and fibers, and the solvent cause macroscopic gel properties such as counterflow.[43]

LMW gelators can be divided into two main categories, depending on the polarity of the solvent trapped in the three-dimensional network: organic or water-binding low molecular weight gelators. In addition, ambidextrous LMW gelators that bind both organic and aqueous solvents are also known. Hydrogelators capable of gelling with water in the presence of 1-10 % dimethyl sulfoxide or methanol have been reported. LMW gelators capable of forming gels in water or aqueous solution in the absence of other organic solvents have been reported only in a few cases.[8] Finding biodegradable polymers for biological applications is difficult, which is why LMW hydrogels could find their place in this application area. In hydrogels, aggregation of LMW gelators occurs through hydrophobic interactions and possible π-stacking.[13]

The main difference between polymeric and LMW gels is that the assembly event in LMW gels can be reversed by energy, such as heating. This reversibility of gelation offers many potential applications for LMW gels, such as biosubstrates for the encapsulation, proliferation, and the possible release of cells from the network without cell death, controlled drug release, and many other applications (Figure 26).[10] LMW gels have attracted great interest as they form by a simple trigger, the metastability of gelation (gel-to-sol-to-gel) may be controlled, they are biocompatible materials and structure-function affinity may also be controlled.[10]
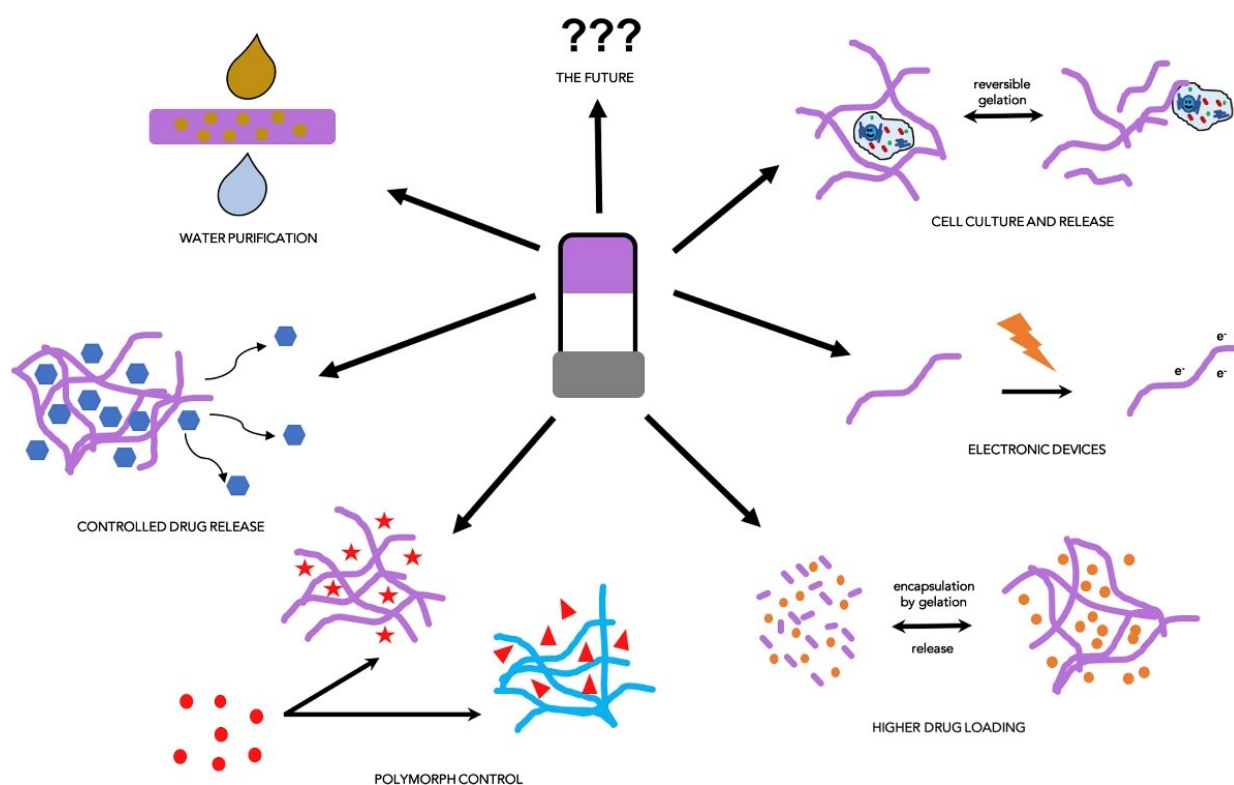
Figure 26. Applications of LMW gels. Reprinted with permission from ref. 10, Copyright 2017, Published by Elsevier Inc., CC BY 4.0.

## 7.3 Challenges of the LMW gelation process

A major challenge in gel research is to decipher the molecules capable of forming gels and the conditions under which they do so, although the process leading to LMW gelation is partially understood. In 1841, the first LMW gelator was discovered as a result of a failed crystallization process.[43] Small molecules with similar structures can have a markedly different tendency to form gels. It has, therefore, been hypothesized that gelation is related to crystallization. However, according to Draper *et al*.[10], there is no reason to assume a link between the two. Vidyasagar *et al*.[12] have confirmed that gelation and crystallization are competing events under certain conditions. Predicting whether a molecule will form a gel is often difficult, so the process of gelation has been characterized as an empirical science.[10]

Libraries and computational approaches have been attempted to predict gelation. The library method involves generating many similar gelator candidates for gelling and testing their gelling

properties. This has allowed the discovery of which molecules form gels without explaining why some molecules gel and others do not. The challenge in testing gelators is that changing one parameter at a time is difficult. For example, a change in the functional group of a molecule to another functional group changes the packing capacity, the molecule's steric bulk, the number of donors or acceptors of potential hydrogen bonds, and the solubility of the compound. The complexity of the gelation process is not revealed by cataloging gelators and their efficacy. Computational methods, such as the graph-based approach, have been used to predict the gelator properties of the gelation process. The reasons why some molecules act as gelators cannot be explained by these methods.[10]

In addition to the gelator, gelation is also influenced by the solvent and concentration.[10] Studies have emphasized interactions between gelator molecules, but the criticality of solvent and gelator molecule interactions should also be considered. It is generally believed that gelator molecules should be sufficiently soluble, but not too soluble, in the solvent used.[43] It is possible for a gelator to form a gel only in the presence of certain solvents or only in the presence of one solvent. The balance between the interactions between the gelator and the solvent is crucial to promote self-assembly into the desired one-dimensional aggregates. Recent studies show that this balance can be predicted based on the properties of the solvent. It has been observed that gelation occurs above the minimum gelation concentration (MGC),[10] also known as critical gelation concentration (CGC),[12] which for LMW gels is generally < 1 wt %. Although the gelator is found to be insoluble in certain solvents, this may be because the required MGC is not reached.[10]

Other factors affecting gelation include temperature, the presence of certain additives, and the role of chirality in gelation.[10,11] Temperature is a key parameter in the gelation process. For most LMW gels, the stable temperature range varies and is again difficult to predict. During the gelation process, various additives can either promote or inhibit gelation.[10] In general, the effect of chirality on gelation is controversial: in some cases, chirality is a prerequisite for gelation, in other cases, it is not. In addition, there are reports of racemic gelators performing better than homochiral gelators.[11]

Despite the extensive interest and research on LMW gels, it is still unclear which molecules can act as gelators and under what conditions to form a gel. Currently, LMW gelators are found by chance more often than by design. In the future, however, it is expected that computational methods will be available to model gel formation.[43]

## 7.4 *Myo*-inositol based gels

### 7.4.1 1D-1,2:4,5-di-*O*-isopropylidene-*myo*-inositol as an organogelator

Sureshan *et al.*[11] conducted a study on the synthesis of various phosphoinositols and noticed that 1D-1,2:4,5-di-*O*-isopropylidene-*myo*-inositol **16a** (Figure 27) gels with benzene. Systematic gelation assay showed that this molecule acts as a gelator in several low polar, often aromatic solvents. Gels were formed at concentrations of 1-2 wt-% (Table 1). The compound was also soluble in common solvents such as dichloromethane, chloroform, methanol, ethanol, and DMSO but insoluble in hexane and diethyl ether. However, very low hexane concentrations resulted in the formation of a partial gel. Because of the simple structure of diol **16a**, the gelation mechanism was investigated at the molecular level.
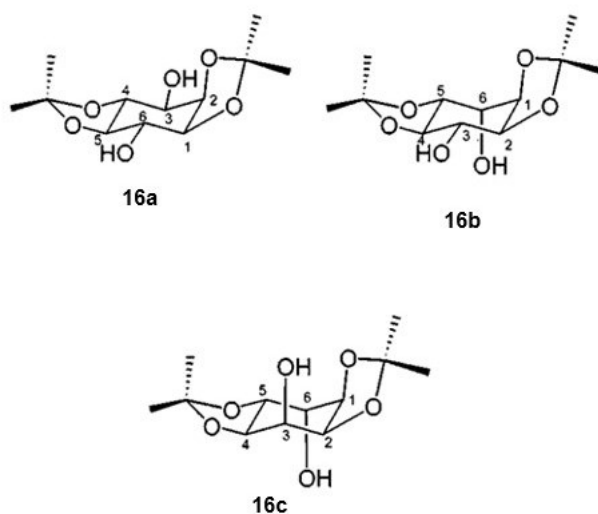


Figure 27. Structures of 1D-1,2:4,5-di-*O*-isopropylidene-*myo*-inositol **16a** and isomeric form *chiro*-diol **16b** and *allo*-diol **16c**. Reprinted and adapted with permission from ref.11, Copyright 2004, John Wiley & Sons, Inc.

Table 1. The data for gels of diol **16a**. Reprinted and adapted with permission from ref.11, Copyright 2004, John Wiley & Sons, Inc.

| Solvent | CGC in wt.-% | $T_{Gel}$ in °C | Appearance |
|---|---|---|---|
| Benzene | 0.7 | 80 | transparent |
| Toluene | 1.0 | 74 | transparent |
| Chlorobenzene | 1.0 | 60 | transparent |
| o-Xylene | 1.3 | 71 | transparent |
| p-Xylene | 1.2 | 74 | transparent |
| m-Xylene | 1.5 | 69 | transparent |
| Ethylbenzene | 2.0 | 57 | transparent |
| CCl$_4$ | 2.0 | 77 | cloudy |

Diol **16a** has two hydroxyl groups, so hydrogen bonds are thought to cause supramolecular polymerization into fibers, followed by entanglement.[11] Shinkai *et al*.[44] discovered that monosaccharide derivatives with two hydroxyl groups capable of forming one-dimensional hydrogen bonding arrays are excellent candidates for effective gelators. This generalization can be extended to inositols because their structure is similar to that of monosaccharides.[11]

The assumption that hydrogen bonding ability causes gelation is also supported by the Fourier-transform infrared spectroscopy (FTIR) spectrum of the benzene gel, which shows a broad peak in the range of 3300-3500 cm$^{-1}$, indicative of hydrogen bonding. Interestingly, a similar peak is also observed in a chloroform solution, although the mixture did not form a gel. No peaks characteristic of free hydroxyl groups were observed in the FTIR spectra, suggesting that both hydroxyl groups of the compound are involved in hydrogen bonding. The positioning of hydroxyl groups in the equatorial positions prevents the formation of an intramolecular hydrogen bond, making intermolecular hydrogen bonding more likely in benzene and chloroform solutions.[11]

In addition to the FTIR spectra, nuclear magnetic resonance (NMR) experiments were used to investigate hydrogen bonding. Due to the similarity of the FTIR spectra, the NMR concentration experiment was performed on the chloroform solution, even though it did not gel, because it is easier to measure compared to the low concentrations of gelator in the benzene gel. In the NMR experiment, both hydroxyl groups shifted downfield with increasing concentration. Relatively speaking, the magnitude of the transfer is greater for OH at the C6 position, making it a more likely donor of hydrogen bonds. This suggests a strong head-to-tail or head-to-head hydrogen bond is observed even in chloroform.[11]

The Nuclear Overhauser effect spectroscopy (NOESY) measurement was used to study the molecular arrangement in more detail. The NOESY spectrum showed cross-peaks between C3-OH and C6-OH, which can only be explained by head-to-tail hydrogen bonding. Furthermore, HH correlated spectroscopy (COSY) NMR showed the same cross-coupling between C3-OH and C6-OH, indicating a strong hydrogen bonding system. HH-COSY NMR also revealed a coupling between C6-OH and C2-H, which is only possible between two adjacent molecules in head-to-tail order. Based on the NMR results, a likely interaction mode between the molecules was determined (Figure 28).[11]
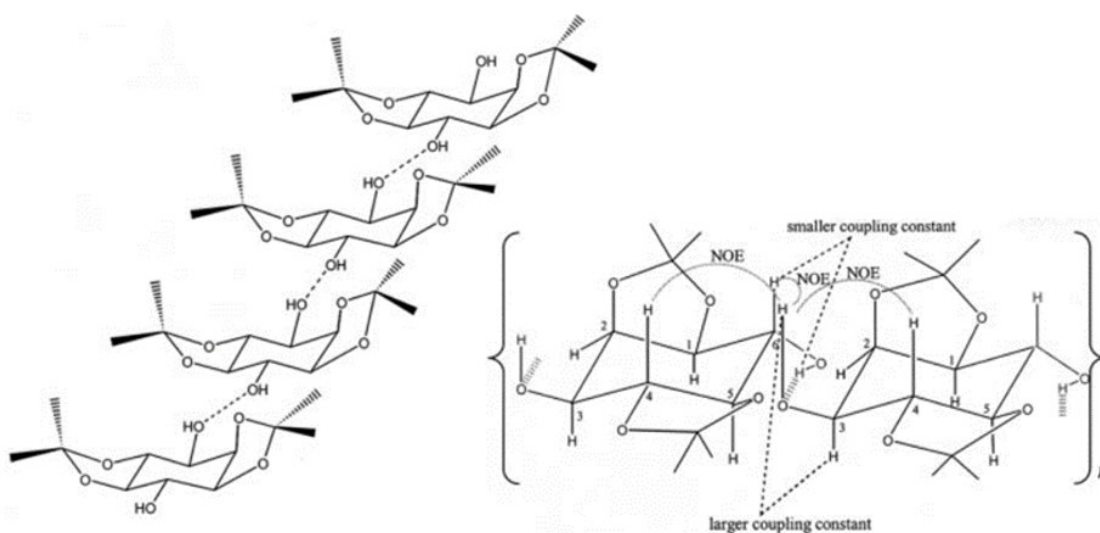


Figure 28. The assumed assembly of **16a** in gel and solution based on NMR spectroscopic studies. Reprinted and adapted with permission from ref.11, Copyright 2004, John Wiley & Sons, Inc.

For inositol derivatives, chirality is one of the key issues. In this study, the effect of chirality on gelation was investigated by performing gelation experiments with racemic ± diol, but no gel was formed in any of the solvents. The role of hydroxyl group orientation in gelation was also investigated by synthesizing isomeric *chiro*-diol **16b** and *allo*-diol **16c** (Figure 27), in which one or both hydroxyl groups are inverted with respect to **16a**. These compounds did not gel with any of the selected solvents. This suggests that the chirality and orientation of the hydroxyl groups play an essential role in this gelation process.[11]

## 7.4.2 Mono-*O*-acyl-*myo*-inositol orthopentanoates as a gelator

In their later research, Sureshan *et al.*[12] developed a new class of gelators using *myo*-inositol as a sugar mimic. Their interest in developing a new class of such gelators stems from carbohydrate-based organogelators, which are one of the most typical hydrogen bond-based organogelators. The general structure of carbohydrate-based amphiphilic gelator **17** is shown in Figure 29 a. The critical structural features of this class of gelators include a 4,6-*O*-arylidene moiety, a vicinal diol motif, and an alkyl group at the anomeric oxygen. During the gel fiber formation, the vicinal diol motif enables the molecules to self-assemble into a one-dimensional zig-zag chain (Figure 29 b) by two parallel hydrogen bonds. In principle, the 1,3-diaxial diols of a six-membered ring can also form such a one-dimensional structure through hydrogen bonds (Figure 29 c and d).[12]
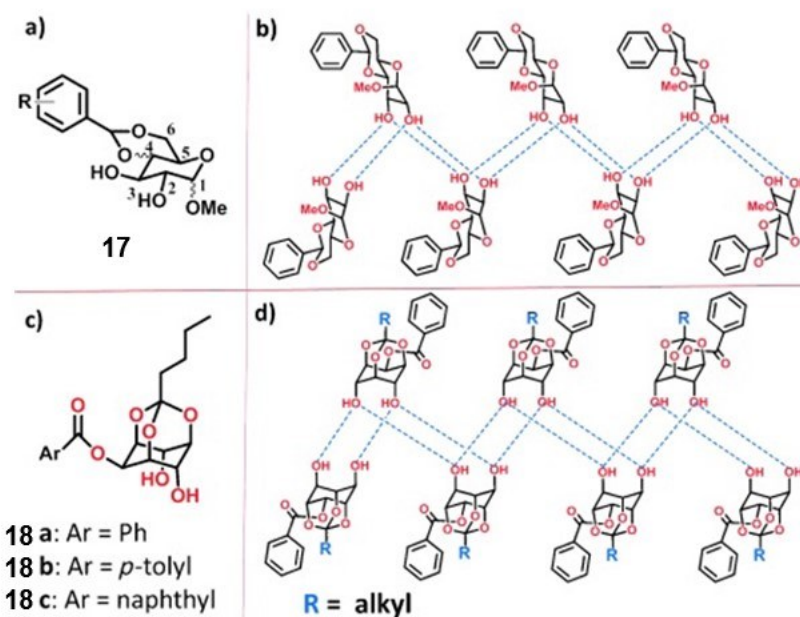


Figure 29. a) General structure of a carbohydrate-based gelator b) 1D zig-zag chain structure in gels and crystals resulting from two parallel hydrogen bonds c) Proposed amphiphiles **18a-c** with cyclohexane-diaxial-1,3-diol motif d) Proposed hydrogen bond formation for **18a-c**. Reprinted and adapted with permission from ref. 12, Copyright 2015, John Wiley & Sons, Inc.

During gelator development, *myo*-inositol orthopentanoate **19** was regioselectively acylated, yielding compounds **18a-c** (Figure 30). As expected, acylated aromatic esters, such as benzoate

**18a**, toluate **18b**, and naphthoate **18c**, were gelled with oils and nonpolar solvents. If the sample remained stable after the inversion of the tube, the sample was classified as a gel. In addition, the CGC and $T_{gel}$ values of the gels were measured (Table 2). Low GCG values and high $T_{gel}$ values indicated that the gels were stable.[8,12]



**19**

**18a**: R = Ph, 76%

**18b**: R = p-tolyl, 64%
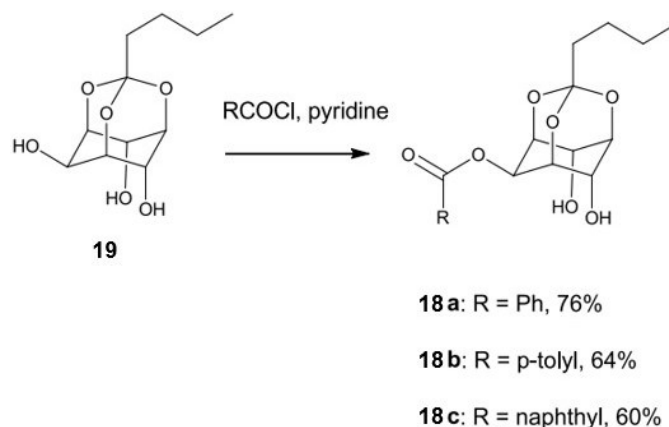
**18c**: R = naphthyl, 60%

Figure 30. Synthesis of mono-*O*-acyl-*myo*-inositol orthopentanoates **18a-c**. Reprinted and adapted with permission from ref. 12, Copyright 2015, John Wiley & Sons, Inc.

Table 2. The data for gels formed by **18a-c**. Reprinted and adapted with permission from ref. [12], Copyright 2015, John Wiley & Sons, Inc.

| S. No. | solvent | 18a | | 18b | | 18c | |
|---|---|---|---|---|---|---|---|
| | | CGC | $T_{gel}$ | CGC | $T_{gel}$ | CGC | $T_{gel}$ |
| 1 | Paraffin oil | 0.16 | 105 | 0.40 | 94 | 0.31 | 98 |
| 2 | Heptane | 0.62 | 53 | 1.25 | 50 | 1.0 | 54 |
| . | Pet ether | 0.71 | 49 | 2.00 | 49 | I | - |
| 4 | Pentane | - | - | - | - | - | - |
| 5 | kerosene | 0.66 | 86 | 1.25 | 64 | 0.59 | 92 |
| 6 | Coconut oil | - | - | - | - | - | - |
| 7 | Xylene | - | - | - | - | - | - |
| 8 | Benzene | - | - | - | - | - | - |
| 9 | Toluene | - | - | - | - | - | - |
| 10 | Pump oil | 0.16 | 125 | 0.50 | 103 | 0.4 | 119 |
| 11 | Petrol | 3.5 | 97 | 4.00 | 88 | 2.10 | 102 |
| 12 | Diesel | 0.47 | 78 | 3.33 | 71 | 0.59 | 76 |
| 13 | Silicon oil | 3.33 | 59[a] | 5.00 | 55[a] | - | - |
| 14 | Sunflower oil | - | - | - | - | - | - |
| 15 | CCl$_4$ | - | - | - | - | - | - |
| 16 | Hexane | - | - | - | - | 1.0 | 48 |
| 17 | Cyclohexane | 0.52- | 53 | 3.33 | 47[a] | 0.77 | 51 |

[a] $T_{gel}$ measured at CGC

In gelation experiments, low concentration solutions formed crystals, and high concentration solutions formed a translucent gel (Figure 31). The results showed that intermolecular hydrogen bonding played an important role in both, and water was involved in the crystallization, through which unidirectional fibrillar layers were formed.[8] When gelators form hydrogen bonds, the water in the solvent competes with the gelators for hydrogen bonds, interfering with the gelation process.[12] In some cases, however, the water is known to promote gelation by acting as an interface between the gelators to form fibrils.[45,46] Sureshan *et al.*[12] believe this is the first case where water in an organic solvent, which is otherwise inducing gelation, induces organogelator crystallization by bridging molecules in a 3D network.
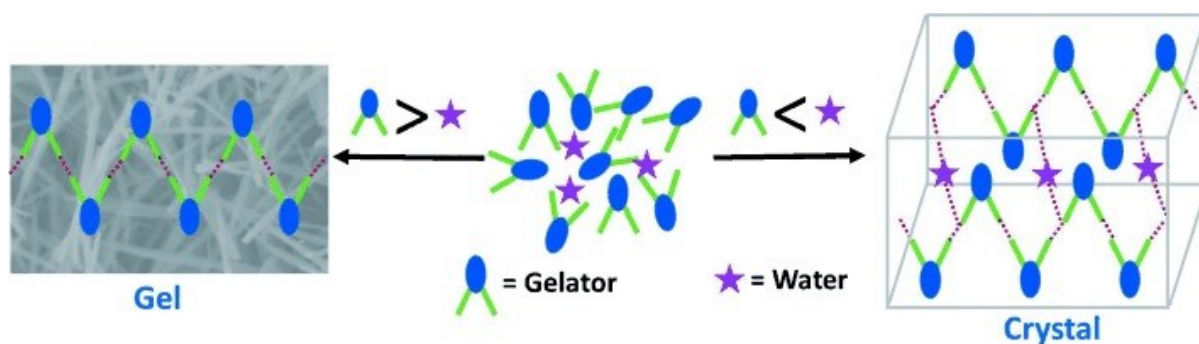


Figure 31. When the gelator concentration is lower than that of water, it tends to crystallize, while higher water concentrations cause the gelator to solidify in the solvent, forming a stable LMW organogel. Reprinted and adapted with permission from ref. 12, Copyright 2015, John Wiley & Sons, Inc.

### 7.4.3 Trinuclear Cu(II) complex of inositol as a hydrogelator

Metallogels, containing either metal complexes, coordination polymers, or single organometallic molecules, form supramolecular aggregates or assemblies through non-covalent interactions such as metal coordination. Metal ions can modify gel formation, affect chirality control, and alter certain physical properties. The interest in LMW gelators stems from their high potential in preparing advanced functional nanomaterials. By adding a second component, the self-assembly of such materials can be tuned.[13]

Complexes of Ag(I) and Cu(II) with bis-urea ligands form soft tunable metallogels, while Au(I) thiolates lead to the formation of pH-responsive supramolecular hydrogel. Polypyridyl ligands contribute significantly to the luminescence properties of metallogels formed by Re(I) and Pt(II) complexes. Sachin *et al.*[13] were interested in a transition metal complex involving *myo*-inositol and a polypyridyl ligand such as 2,2-bipyridyl as a potential molecular hydrogelator. It was the first reported pH-triggered hydrogel formation by a trinuclear copper(II)complex.

The isomers of inositol are expected to have chelating properties as it is a hexahydroxy compound. Small metal ions prefer the tridentate ax-ax-ax mode, while large metal ions prefer the ax-eq-ax mode. In coordination with the Fe(III) center in the *myo*-inositol oxygenase, the *myo*-inositol uses two adjacent oxygen sites, as in separating the D,L-*myo*-inositol derivatives of the copper complex Cu(II). It was found that all *myo*-inositol oxygen atoms can participate in the formation of a coordination bond, albeit two at a time.[13]

While it may seem straightforward to form trinuclear complexes using all six hydroxyl sites of inositol, this isn't necessarily the case. Due to its polyol nature, deprotonation of all six OH groups is challenging under typical pH conditions. Metal coordination can increase the acidity of protons, promoting deprotonation, so coordination becomes easier in cases where all oxygen sites are used at elevated pH. The effect can be enhanced when the metal is attached to a $\pi$-acidic ligand such as 2,2-bipyridyl.[13]

*Myo*-inositol reacted with three equivalents of cupric acetate to form a trinuclear complex $[Cu_3(myo\text{-inositol})(H_2O)_6]$. Due to its small size and ample polarity, it tends to undergo aquation instead of forming a gel across all pH values. The complex serves as a basic structure for constructing trinuclear complexes by substituting water molecules with aromatic ligands, such as 2,2-bipyridine. Ligands that replace water molecules are expected to have hydrophobic interactions or $\pi$-stacking that lead to supramolecular assemblies and provide cavities for trapping water.[13]

In the preparation of the potential LMW gelator, *myo*-inositol was allowed to react with three equivalents of copper and varying amounts of 2,2-bipyridine. No gel formation occurred with 1-2 equivalents of 2,2-bipyridine at any pH or concentration. When a 2.5 % aqueous solution of *myo*-inositol was mixed with three equivalents of $[Cu(2,2\text{-bipyridine})]^{2+}$ complex at pH 12.4, a trinuclear complex formed (Figure 32). When the solution was cooled to RT, a transparent green gel formed. The composition of the gel varied with the concentration: Increasing the concentration resulted in the development of a dense gel, while decreasing the concentration resulted in a dispersed gel that was suspended in the solution.[13]
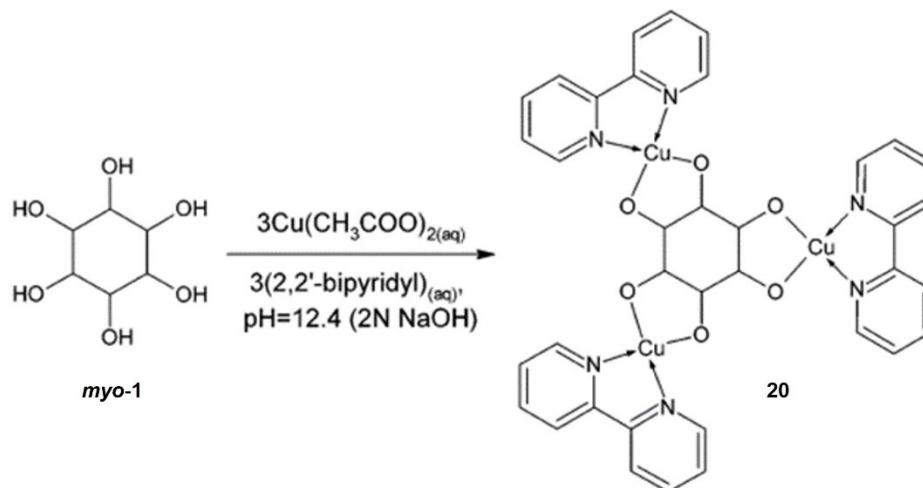
Figure 32. Synthesis of a *myo*-inositol based trinuclear Cu(II)complex **20** hydrogelator. Used and adapted with permission of Royal Society of Chemistry, from A new trinuclear Cu(II) complex of inositol as a hydrogelator, A. Joshi, S. and D. Kulkarni, N., Chemical Communications, 2009, permission conveyed through Copyright Clearance Center, Inc.

Scanning electron microscopic analysis of the xerogel showed a fibrous gel structure with fibrils 2-4 μm in diameter and > 50 μm in length (Figure 33). The xerogel re-gelled when dissolved in water and when the mixture was heated and cooled. When the xerogel was washed with ethanol and dried, a single compound, the complex, was obtained as a residue. Thermogravimetric analysis of this complex revealed the presence of nine water molecules, either in hydrogen bonded or coordinated form. Since the complex, unlike the xerogel, does not form a gel upon addition of water (natural pH), but forms a gel upon addition of water at pH 12.4, both 2,2-bipyridine and hydroxyl ions play important roles in gel formation.[13]
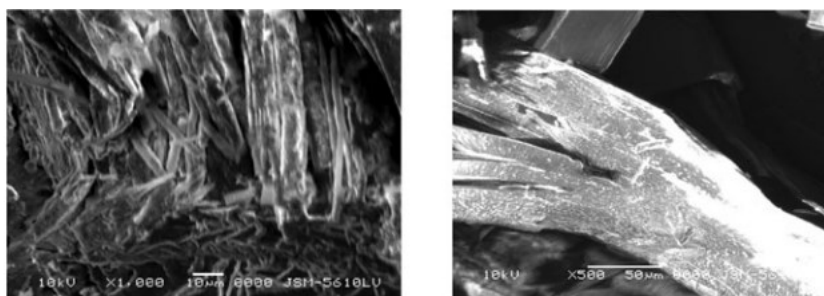


Figure 33. Scanning electron microscopic images of the *myo*-inositol based metallogel. Used with permission of Royal Society of Chemistry, from A new trinuclear Cu(II) complex of inositol as a hydrogelator, A. Joshi, S. and D. Kulkarni, N., Chemical Communications, 2009, permission conveyed through Copyright Clearance Center, Inc.

In the electronic spectra of [Cu(2,2-bipyridine)]$^{2+}$-complex and [Cu$_3$(*myo*-inositol)(2,2-bipyridine)$_3$], changes in absorption maxima were observed. Minor changes in the energy of transitions in coordinated 2,2-bipyridine may result from subtle fluctuations in the intensity of π-interactions between Cu(II) and 2,2-bipyridine. This could be induced by the axial coordination of a hydroxyl ion, thus affecting the energy of the metal orbitals.[13]

The central role of hydroxyl ions in gel formation implies their involvement in the formation of intermolecular OH bridges between trinuclear complex molecules via axial coordination. In addition, this interaction probably extends to hydrogen bonding with *myo*-inositol.[13] Previous studies on sugar-based hydrogelators suggest that sugars with an axial OH group can form a greater number of hydrogen bonds and achieve denser packing through π-stacking interactions between the phenyl substituents, making them more effective as gelators.[47] Considering the similarity of *myo*-inositol, it may have similar H-bonding and orientation effects. The fibrous superstructure of the gel appears to result from axial coordination and hydrogen bonding facilitated by OH groups. The π-stacked 2,2-bipyridine also contributes to forming hydrophobic cavities capable of retaining water molecules and leading to gel formation.[13]

# EXPERIMENTAL PART

## 8 Motivation

Under certain conditions, LMW gelators will form a gel material instead of crystallizing or precipitating, depending on the reaction kinetics and their chemical structure.[41] This work focuses on designing and preparing *myo*-inositol based LMW gelators. The aim of this study was to synthesize in three steps from *myo*-**1** the amphiphilic *myo*-inositol derivatives, 2-*O*-benzyl-*myo*-inositol **21** and 2-*O*-Fmoc-*myo*-inositol **22** (Figure 34), which could act as potential LMW gelators, and to evaluate their gelling behavior. **21** and **22** are amphiphilic in nature, which allows the gelator molecules to solubilize in biocompatible solvent. Amphiphilicity is a basic requirement set in this project to induce gelation.
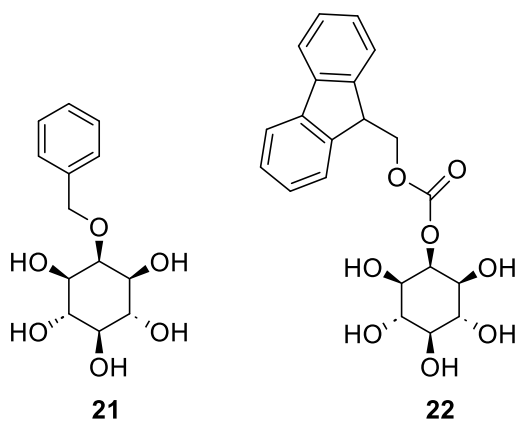


Figure 34. Designed amphiphilic *myo*-inositol derivatives 2-*O*-benzyl-*myo*-inositol **21** and 2-*O*-Fmoc-*myo*-inositol **22**.

The introduction of novel *myo*-inositol derivatives as gelators aims at biocompatible viscoelastic materials with potential applications in drug delivery, targeted therapies, theragnostic and tissue engineering. The addition of the benzyl- and Fmoc-moieties offers the required amphiphilicity, while we hypothesize that π-π stacking and ionic interactions may be the driving forces of self-assembly towards gelation.

# 9 Materials and methods

All chemicals (Table 3) were used without further purification. Saturated brine was prepared by dissolving sodium chloride in deionized water. Phosphate buffered saline (PBS) was prepared by dissolving one PBS tablet in 100 mL of deionized water (Fisher BioReagents, NaCl 137 mM, phosphate buffer 10 mM, KCl 2.7 mM, pH 7.4). 90 % trifluoroacetic acid (TFA) was prepared by diluting 99.5 % TFA. A Mettler Toledo XP205 scale and an Ioniser VWR scale were used to weigh the chemical reagents, glassware, and the total weight of the compounds.

All reactions were monitored using commercially available thin-layer chromatography (TLC) plates (Merck TLC Aluminium sheets Silica gel 60 $F_{254}$, layer thickness 175-225 µm). Compounds were visualized by UV light at 254 nm and stained by Hanessian's stain. Flash column chromatography was performed using Merck Silica gel 60 (0.040-0.063 mm). A Heildolph Laborta 4000 efficient rotary evaporator was used for solvent evaporation.

The NMR spectra were recorded with Bruker Avance III HD 300 MHz, Bruker Avance 400 MHz, or Bruker Avance III 500 MHz NMR spectrometers. NMR spectra were recorded in deuterated solvents, and the transitions in ppm are reported relative to the transition of the deuterated solvent used. The NMR spectra of 400 and 500 MHz instruments were recorded by laboratory engineer Esa Haapaniemi.

The melting points (M.p.) of the products were measured using a Stuart SMP30 instrument. The high-resolution mass spectrometry (HR-MS) spectra were recorded by Dr Anniina Kiesilä using an Agilent 6560 Ion mobility Q-TOF mass spectrometer. The FTIR spectra were recorded on a Bruker Tensor 27 FTIR spectrophotometer. For the gelation tests, a Hielscher UP50H ultrasonic processor was used to sonicate the solution mixtures and a Thermo Scientific block heater was used for heating.

Table 3. Used chemicals

| Chemical reagents | Mw (g/mol) | Manufacturer | Purity (%) |
|---|---|---|---|
| Benzyl bromide (BnBr) | 171.04 | Thermo Scientific | 99 |
| 2,3-Butanedione | 86.09 | Alfa Aesar | 99 |
| (±)-Camphor-10-sulfonic acid (CSA) | 232.30 | Thermo Scientific | 98 |
| Chloroform-d | 119.37 | Euristop | 99.8 |
| Dichloromethane (DCM) | 84.93 | VWR Chemicals | > 99.5 |
| Diethyl ether | 74.12 | VWR Chemicals | > 99.7 |
| Dimethylformamide (DMF) | 73.09 | Thermo Scientific | 99.8 |
| 4-Dimethylaminopyridine | 122.2 | Sigma | - |
| Dimethylsulfoxide-d$_6$ (DMSO) | 84.17 | Euristop | 99.8 |
| Ethyl acetate (EtOAc) | 88.11 | VWR Chemicals | > 99.5 |
| 9-Fluorenylmethyl chloroformate (Fmoc-Cl) | 258.70 | Thermo Scientific | 98 + |
| Hanessian stain (ceric ammonium molybdate solution) | | TCI | |
| Hexane (Hex) | 86.18 | Honeywell | 97 |
| Magnesium sulfate hydrate, anhydrous | 120.37 | Honeywell | > 99.0–101.0 |
| Methanol (MeOH) | 32.04 | VWR Chemicals | ≥ 99.8 |
| myo-inositol | 180.16 | Thermo Scientific | > 98 |
| Petroleum ether | 86.18 | Honeywell | ≥ 90 |
| Phosphate buffered saline (PBS) tablets | | Fisher Chemicals | |
| Sodium carbonate, anhydrous | 105.99 | Riedel-de Haën | > 99.8 |
| Sodium chloride | 58.44 | VWR Chemicals | 99.5–100.5 |
| Sodium hydride | 24.00 | TCI | 60 |
| Sodium hydrogen carbonate | 84.01 | Fisher Chemical | ≥ 99.7 |
| Sodium sulfate, anhydrous | 142.04 | Fisher Scientific | > 99 |
| Toluene | 92.14 | VWR Chemicals | - |
| Triethylamine | 101.19 | Sigma-Aldrich | ≥ 99.5 |
| Trifluoroacetic acid 99.5 % (TFA) | 114.02 | Apollo Scientific | 99.5 |
| Trimethyl orthoformate (HC(OCH$_3$)$_3$) | 106.12 | Alfa Aesar | 99 |

# 10 Results and discussion

## 10.1 Retrosyntheses

A three-step reaction pathway was designed to prepare the desired amphiphilic *myo*-inositol derivatives **21** and **22** (Scheme 1). Functionalization was aimed at the position 2 hydroxyl group due to its axial position. Therefore, a symmetrical diol (meso form) was to be obtained during the selective *myo*-inositol protection reaction, leaving the hydroxyl groups at positions 2 and 5 free. Functionalization can also occur on both free hydroxyl groups, resulting in a diprotected derivative. Functionalization to the hydroxyl group at position 5 alone does not occur, as this is an equatorial positioned hydroxyl group bearing more stearic hindrance than position 2.
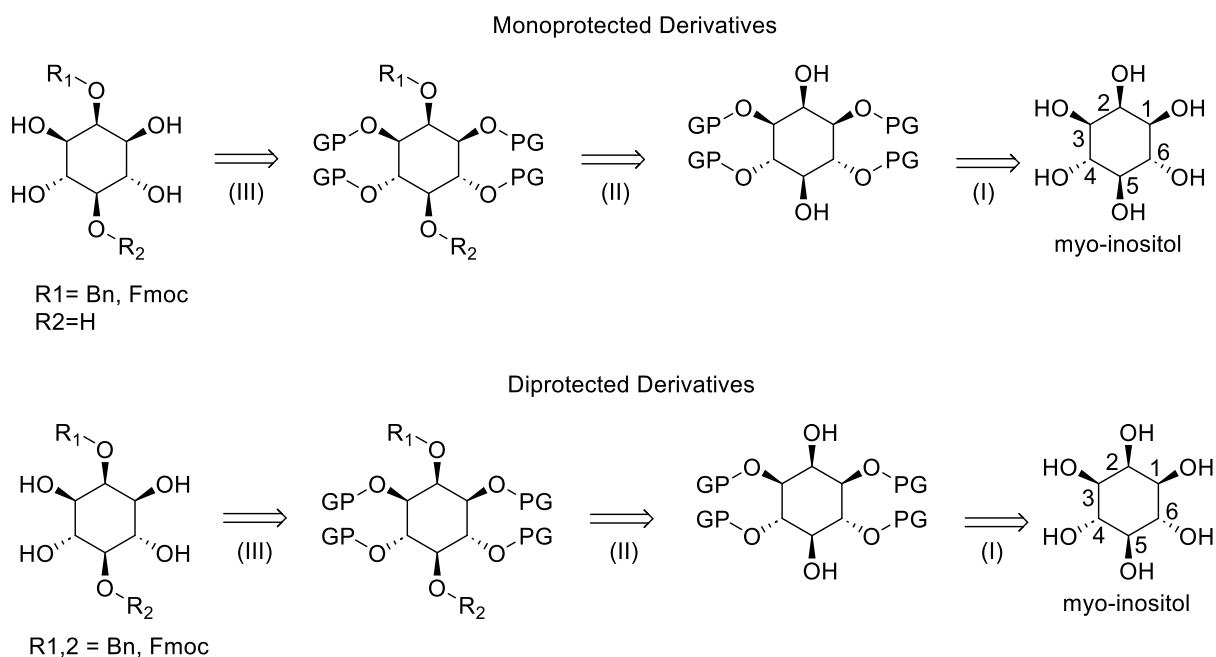


Scheme 1. Retrosynthetic plan for amphiphilic mono- and diprotected *myo*-inositol derivatives.

## 10.2 Implementation of syntheses

Following the retrosynthetic plans (Scheme 1), attempts were made to synthesize amphiphilic *myo*-inositol derivatives by three-step reaction pathways. Only the Bn-*myo*-inositol **21** derivative could be successfully synthesized, whereas the desired Fmoc-*myo*-inositol **22** could not be successfully synthesized. The syntheses and reaction conditions are described in Scheme 2. The reaction mechanisms, observations, optimizations, purification, and characterization of the products are described below for each reaction.
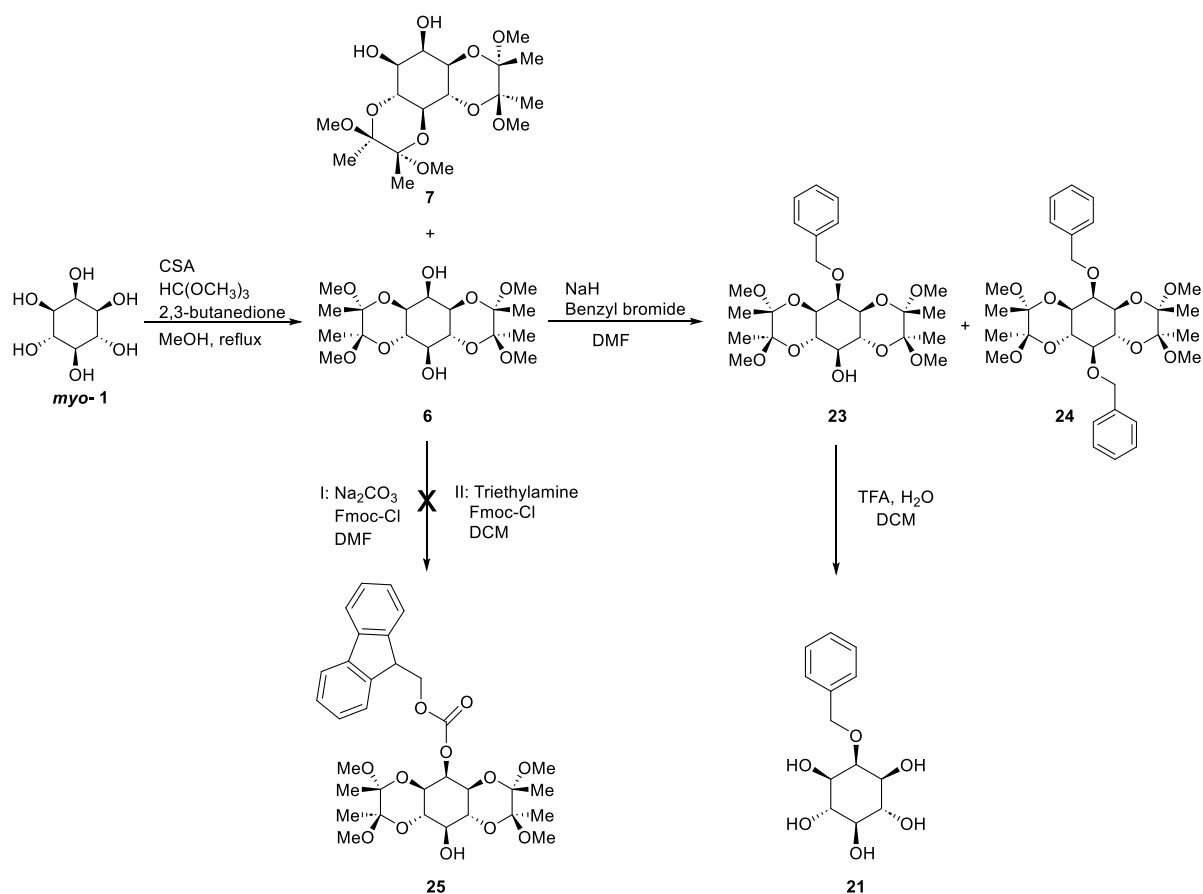


Scheme 2. Performed syntheses and reaction conditions.

## 10.2.1 Selective protection

The synthesis of amphiphilic *myo*-inositol derivatives requires the regioselective protection of the *myo*-inositol hydroxyl groups. The protecting group used is BDA. The acid-catalyzed regioselective and stereoselective protection reaction of *myo*-inositol was performed with camphor sulfonic acid, trimethyl orthoformate and butanedione in methanol and 41 h of reflux time (Figure 15). The reaction mechanism is shown in Scheme 3 below.
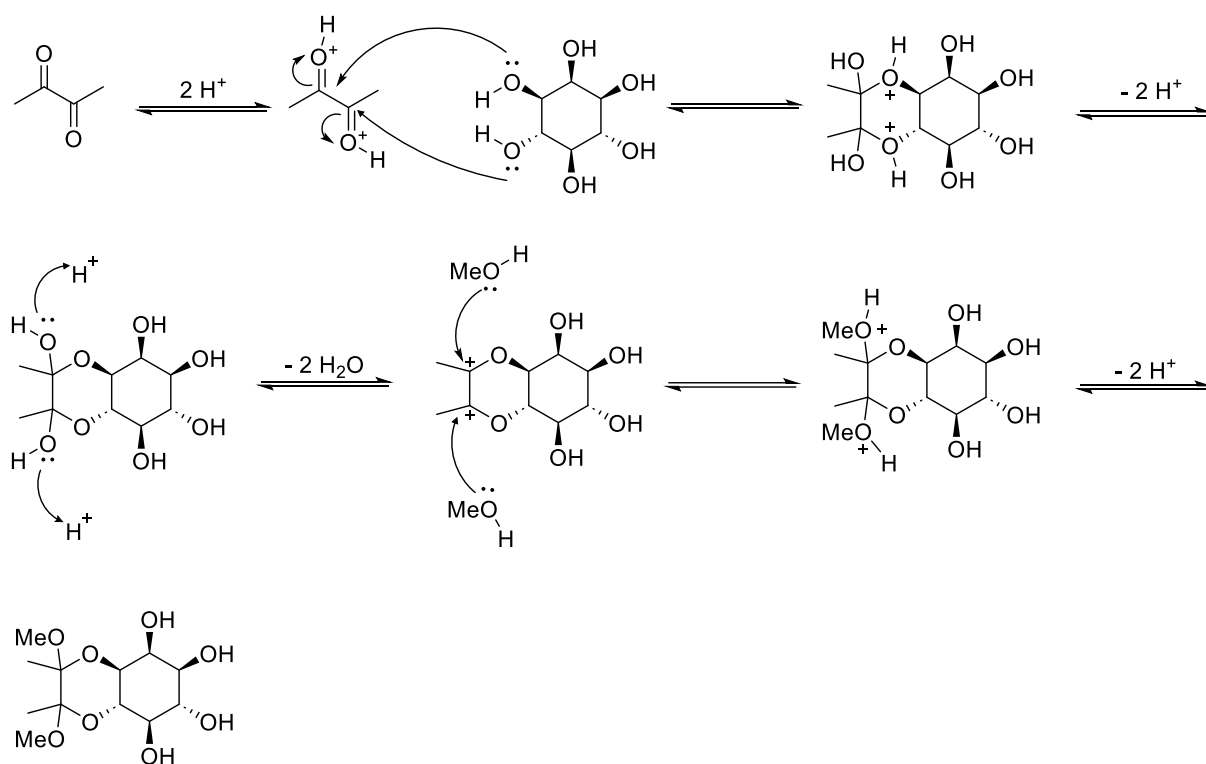


Scheme 3. Stereo- and regioselective protection reaction of *myo*-inositol.

The desired symmetrical diol **6** (Scheme 2) formed during this protection reaction, but also an asymmetrical diol **7** (Scheme 2) formed as a second major product. The asymmetrical diol **7** was not isolated or purified based on our gelation hypothesis (avoid steric hindrance). The yield of symmetrical diol **6** in this reaction was low (24 %). The reaction could be carried out at a large enough scale without trying to optimize the yield of the symmetric product. In their study, Riley *et al.*[48] found that longer reaction times resulted in the gradual formation of a less polar by-product that was more difficult to remove. Low yield is acceptable because the cost of starting materials is low, the reaction is simple to perform, and the product is easy to purify.

The isolation and purification of the symmetrical diol from the red suspension were performed with methanol and diethyl ether washes to dissolve the asymmetrical diol in methanol. The purification worked well because the asymmetrical diol and several minor by-products are much more soluble in methanol than the symmetrical product. The symmetrical diol remained as a white precipitate, and the asymmetrical diol dissolved in the mother liquor and washes.

The synthesis of protected *myo*-inositol was repeated twice, following the identical procedure as above, to obtain adequate material. The corresponding yields are given in Table 4.

Table 4. Yields of different synthetic batches of symmetrical diol **6**

|  | Yield (g) | Yield percentage (%) | Outcome |
|---|---|---|---|
| **Synthesis 1** | 3.34 | 24 | white solid |
| **Synthesis 2** | 3.43 | 24 | white solid |

After purification, the obtained symmetrical compound **6** was characterized by measuring the melting point, NMR, FTIR, and HR-MS spectra (APPENDIX 1). The structure of the symmetrical diol **6** was determined by 2D NMR spectra due to the challenges posed by the symmetry of the product. The melting point, 342-346 °C, with sublimation and decomposition, is in agreement with the literature.[37] No major impurities are observed in the recorded $^1$H and $^{13}$C NMR spectra (Figure 40).

In the $^1$H NMR spectrum (Figure 40), the peak at 1.10 ppm corresponds to methanol and the peak at 1.26 ppm, marked with an asterisk, is an impurity presumably derived by the stabilizers present in the solvents used. The water at 1.56 ppm comes from the NMR solvent. The diol **6** is in meso form because it has a mirror plane in the middle, and the right and left parts are identical. Therefore, although the molecule has four Me and OMe groups, two signals are obtained from each group due to two different orientations of each group. Interestingly, in the $^1$H NMR spectrum, CH (C1, 3, 5) gives only one signal at 4.07-3.99 ppm, even though the OH group is attached to the 5$^{th}$ carbon. This may be due to the equatorial orientation of the OH group on the 5$^{th}$ carbon compared to the axial orientation of the OH group on the 2$^{nd}$ carbon, where C2-H gives its own signal at 3.69 ppm.

## 10.2.2 Functionalization with benzyl bromide

The symmetrical diol **6** was functionalized with benzyl bromide using sodium hydride in DMF, the polar aprotic solvent typically used for these reactions. This Williamson ether synthesis produces 2-*O*-benzyl ether, mono-benzylated product **23**, in this regioselective benzylation of the axial hydroxyl group. The reaction also produces 2,5-*O*-benzyl ether, di-benzylated product **24**, when both axial and equatorial hydroxyl groups are benzylated. Sodium hydride is a common base for deprotonating alcohol groups and promoting nucleophilic substitution. Sodium hydride can act both as a base and a hydride source in these S$_N$2-type reactions.[49] The reaction mechanism of benzylation is shown below in Scheme 4.
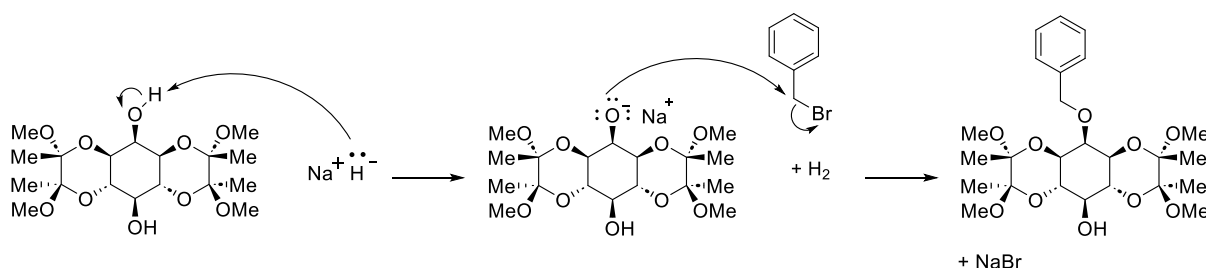


Scheme 4. Benzylation mechanism.

The monoprotected derivative **23** was the desired product based on the hypothesis that it would be a better gelator than its diprotected **24** counterpart. The functionalization was performed twice with BnBr, and the reaction was optimized for the monoprotected derivative. In the first attempt, DMF, NaH and BnBr were added at 0 °C, and the amount of NaH and BnBr were 1.5 and 1.0 equivalent, respectively, compared to the protected *myo*-inositol. In the first reaction, 20 mL of DMF/1.0 g of protected *myo*-inositol was used. In the optimized reaction, 60 mL of DMF/1.0 g of protected *myo*-inositol was used, 2.04 equivalents of NaH and 1.1 equivalents of BnBr. The reaction was carried out at RT, and NaH was added in portions.

In both trials, compounds **23** and **24** were first purified by water and brine washes, followed by flash column chromatography to separate the products. Both products are UV active (at 254 nm), and the diprotected derivative **24** is less polar than the monoprotected derivative **23** due to the two benzyl groups. This explains why it appears higher on the TLC plate and separates first in the flash column chromatography. The difference in their R$_f$ values

(diprotected $R_f$ 0.7; monoprotected $R_f$ 0.4) makes the separation by flash column chromatography quite easy. The corresponding yields for both reactions are given in Table 5.

Table 5. Yields of different synthetic batches towards mono- and di-benzylated protected *myo*-inositol **23** and **24**

|  | Yield (mg) | Yield percentage (%) | Outcome |
| --- | --- | --- | --- |
| **Synthesis 1** | **23:** 610.33 | 57 | white solid |
|  | **24:** 41.50 | 6 | white solid |
| **Synthesis 2** | **23:** 815.00 | 67 | white solid |
|  | **24:** 53.70 | 4 | yellowish solid |

The ability of sodium hydride to act as both a base and a hydride source in the presence of an electrophile, such as benzyl bromide, when DMF is used as a solvent, can lead to the formation of unwanted by-products. Detection of these by-products by conventional visualization methods is challenging and therefore easy to miss.[49] However, despite optimization of this reaction, these unwanted by-products can explain a yield of less than 70 %.

After flash column chromatography, the isolated products were analyzed by measuring the melting points and recording the corresponding $^1$H and $^{13}$C NMR spectra of products **23** (Figure 41) and **24** (Figure 42). In addition, 2D NMR, FTIR, and HR-MS spectra were measured for both products **23** (APPENDIX 2) and **24** (APPENDIX 3). The spectra were used to determine the structure and purity of both products. The melting point of mono-benzylated product **23** was 214 - 216 °C, which corresponds well to the melting point found in the literature[50]. The melting point of di-benzylated product **24** at 164 -166 °C also corresponds well to the literature value[50].

The spectra of the products confirmed the success of the functionalization reaction and purification, as no significant impurities were detected in the $^1$H and $^{13}$C NMR spectra of products **23** and **24**. The $^1$H NMR spectrum of the di-benzylated product **24** is qualitatively similar to the $^1$H NMR spectrum of the symmetrical diol **6**: the CH (C1, C3, and C5) gives only one signal at 3.60-3.50 ppm, probably due to the equatorial orientation of the benzyl group attached to the 5$^{th}$ carbon. The benzyl group attached to carbon 2 is axially oriented, and C2-H gives its own signal at 3.80 ppm. In the NMR measurements, CDCl$_3$ (shift at 7.25 ppm) was used as a solvent, although the molecules have an aromatic region in the same area. This is due

to solubility issues and mainly to avoid potential signal obscuration of the CH or OH groups around 2.5 ppm by using e.g. DMSO (shift at 2.5 ppm) as a solvent.

The FTIR spectra (Figure 35) show differences in the spectrum profiles of compounds **23** (blue) and **24** (orange). In the FTIR spectrum of the di-benzylated product **24**, no O-H stretch is observed in the typical region of about 3500 cm$^{-1}$, compared to the mono-benzylated product **23**. This indicates that there is no free hydroxyl group in product **24**. Otherwise, the FTIR spectra of the compounds are almost identical, as expected.
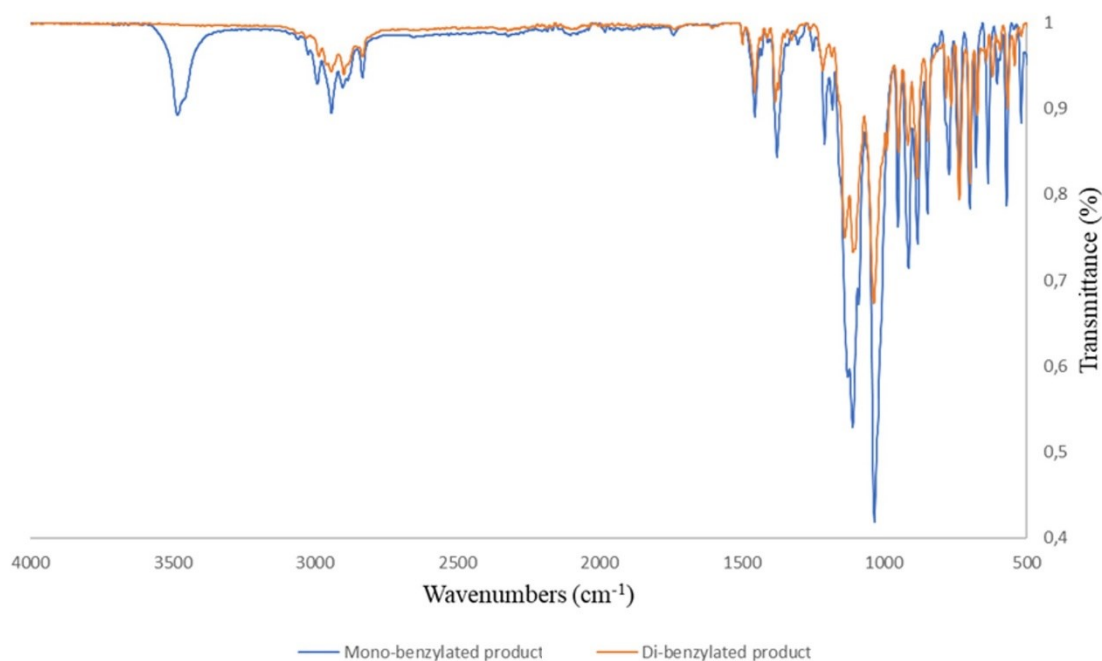


Figure 35. The FTIR spectra of mono-benzylated product **23** (blue) and di-benzylated product **24** (orange).

## 10.2.3 Functionalization with Fmoc-Cl

The functionalization of symmetrical diol **6** with Fmoc-Cl was attempted using a different approach. Fmoc-Cl is an acyl chloride and reacts readily with alcohol with nucleophilic addition-elimination reaction. In our reaction, we hypothesized that it would react with the axial hydroxyl group (C2-OH) of the protected *myo*-inositol **6**. The functionalization was experimented under two different reaction conditions. The reaction mechanism is presented in Scheme 5.
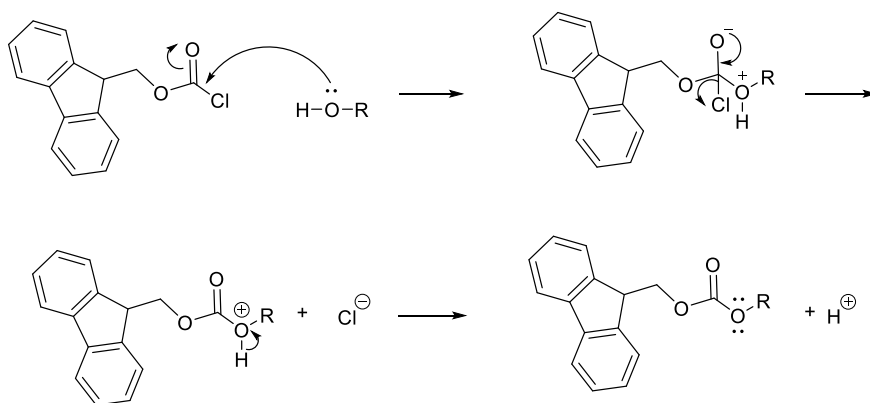
Scheme 5. Reaction mechanism for the Fmoc functionalization of symmetrical diol **6**.

The reaction was performed under basic conditions. The purpose of adding the base is to remove the HCl, as it forms a salt after the base addition. In the first experiment, $Na_2CO_3$ was used as a base and DMF as a solvent. $Na_2CO_3$ was added to the vacuum-dried protected *myo*-inositol **6**, and DMF was added under the $N_2$ atmosphere. Fmoc-Cl was dissolved in DMF and added dropwise to the reaction mixture at 0 °C. The reaction mixture was stirred for 22 h at RT under the $N_2$ atmosphere. After 22 h, the progress of the reaction was monitored by TLC. The TLC plate didn't look very promising, as only the spots of starting materials were clearly interpretable. Despite this, the experiment continued to find out what happened in the reaction. After the workup (washing, drying, and evaporation of the solvents), the crude ^{1}H NMR was measured (Figure 36).
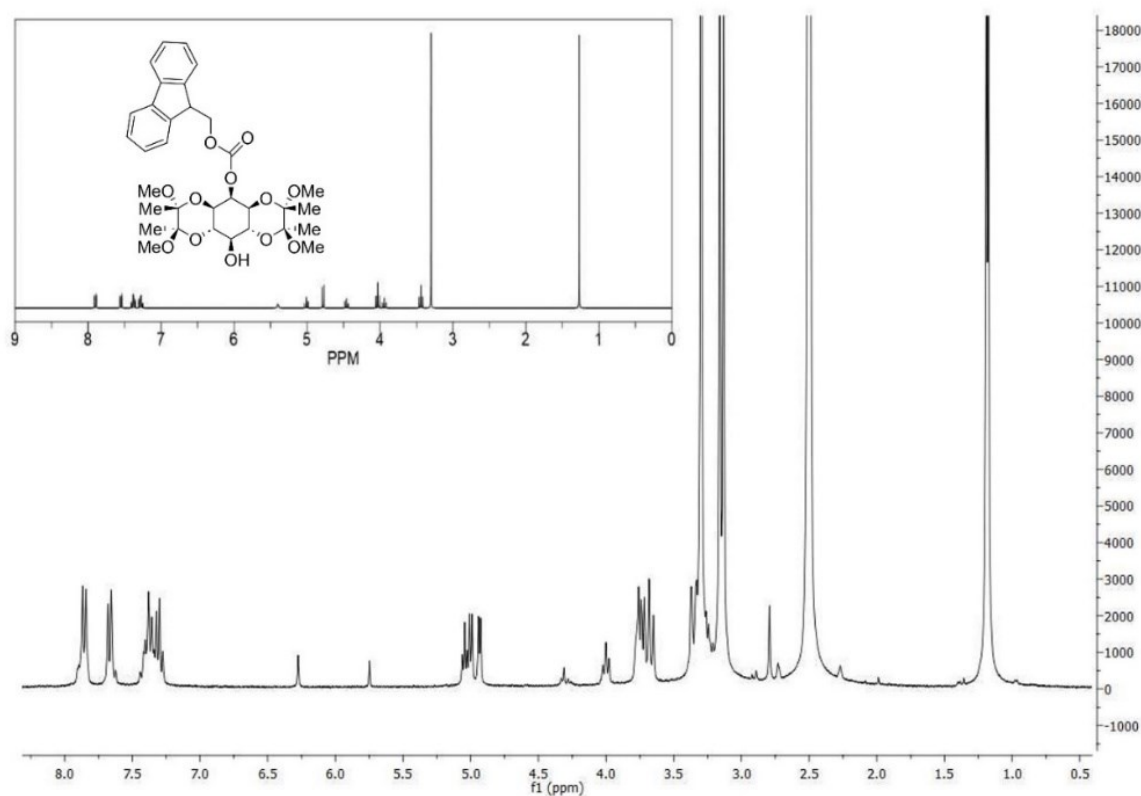
Figure 36. The crude $^1$H NMR (300 MHz, DMSO) spectrum of the first trial to functionalize *myo*-inositol with Fmoc-Cl. At the top of the spectrum is the predicted $^1$H NMR spectrum of Fmoc-functionalized protected *myo*-inositol **25** in DMSO by ChemDraw.

The crude $^1$H NMR showed many similar signals to the predicted $^1$H NMR spectrum by Chemdraw for the desired product. It was decided to separate the resulting product by flash column chromatography to obtain a more accurate $^1$H NMR spectrum (Figure 37). The separated product was a light-yellow solid. The measured $^1$H NMR spectrum showed that no reaction occurred.
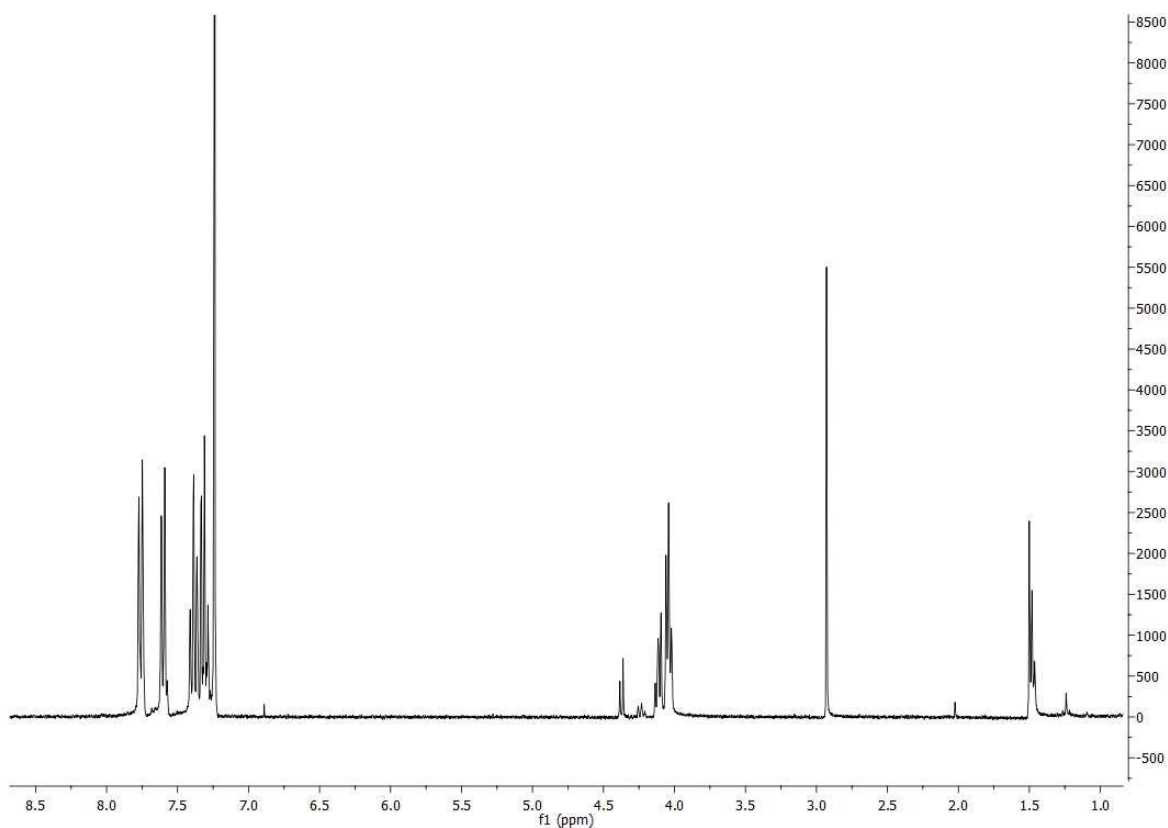
Figure 37. $^1$H NMR (300 MHz, CDCl$_3$) spectrum of the product from the first experiment to functionalize protected *myo*-inositol with Fmoc-Cl separated by flash column chromatography.

The reaction conditions of the first attempt did not produce the desired product, so the reaction conditions were changed. In the second experiment, DCM was used as the solvent, and an organic base, triethylamine, was chosen as the base. Triethylamine was believed to react faster and form the most stable salt. This would also move the reaction kinetics toward the desired product. In the second experiment, 4-dimethylaminopyridine was used as a catalyst, also to facilitate the reaction.

In the second experiment, vacuum-dried protected *myo*-inositol **6** was dissolved in DCM, and triethylamine was added at 0 °C. 4-dimethylaminopyridine was added. Fmoc-Cl was dissolved in DCM and added dropwise to the stirred reaction mixture. The reaction mixture was stirred for 20 h at RT under the N$_2$ atmosphere. The reaction was followed by TLC. The TLC plate showed the same spots as in the first experiment, so the reaction was stopped. The reaction didn't occur with the organic base either.

We hypothesize that the problem with the Fmoc-Cl functionalization is that Fmoc-Cl is too large and can't react with protected *myo*-inositol **6** due to steric hindrance. Potentially, protected

*myo*-inositol **6** could be made reactive by adding NaH to form the alkoxide first, as shown in Scheme 4. Once the alkoxide is formed, Fmoc-Cl could be added. This reaction would require extremely dry conditions, and the addition of Fmoc-Cl should be done in an ice bath due to the extremely reactive species. Due to the large size of the Fmoc group and the steric hindrance, an additional arm could also help the molecule bind to the target molecule.

## 10.2.4 Deprotection

The deprotection was the third step in the retrosynthesis plan (Scheme 1). Since the *myo*-inositol functionalization was optimized for the desired monoprotected derivative **23**, the deprotection was performed only for this product. The amount of the diprotected product **24** was too small for deprotection and following gelation tests.

The deprotection of the mono-benzylated *myo*-inositol **23** was performed twice, under anhydrous conditions, varying the amount of 99.5 % TFA (20 eq and 10 eq) in the reactions. In both reactions, the color of the reaction mixture changed from white to dark brown 10 min after the addition of TFA. After evaporation of the solvents and co-evaporation with methanol, the residues were brown solids, and the $^1$H NMR spectra (Figure 38) showed that impurities, possibly 2,3-dimethoxybutane, were formed instead of 2,3-butanedione in both reactions. Methanol is also seen in the spectrum at 3.16 ppm and 4.01 ppm.
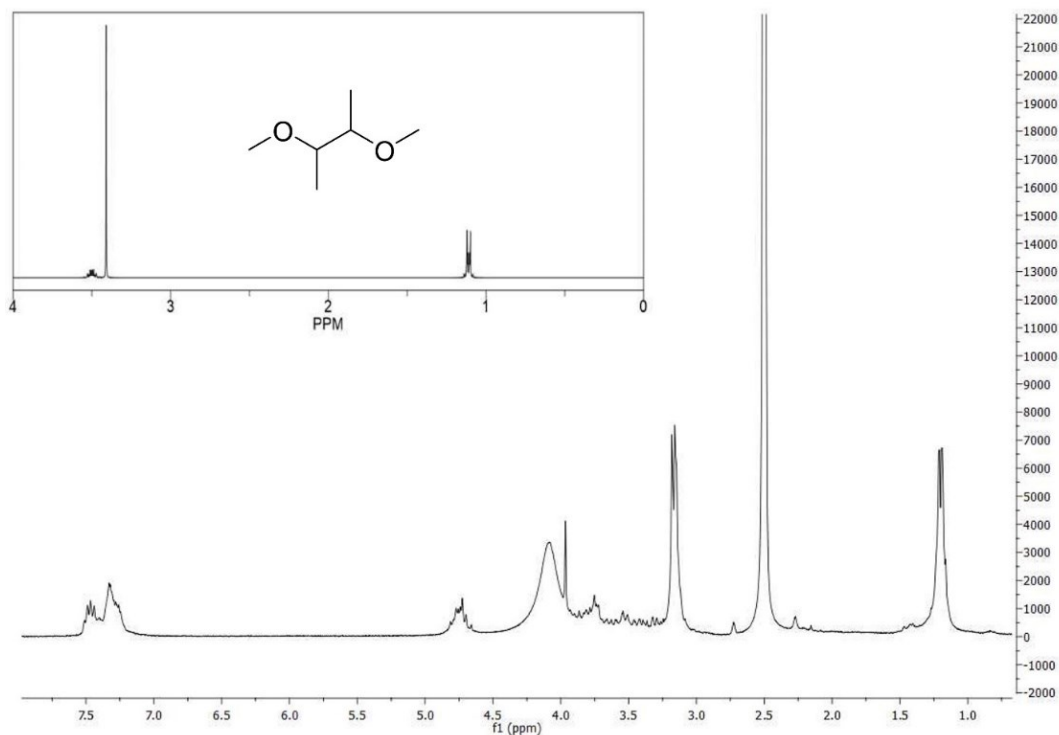
Figure 38. $^1$H NMR (300 MHz, DMSO) spectrum of the deprotection reaction with 99.5 % TFA. At the top of the spectrum is the predicted $^1$H NMR spectrum of 2,3-methoxybutane in DMSO by ChemDraw.

During the optimization attempts, we realized that water should be included in the reaction system for the successful deprotection reaction of the esters (Scheme 3). The addition of 90 % TFA, instead of 99.5 %, formed 2,3-butanedione and instead of a dark brown color, the reaction mixture turned yellow. The solvent was evaporated under vacuum and co-evaporated with methanol until the characteristic buttery odor and yellow color of 2,3-butanedione had disappeared. The deprotection was performed twice (Table 6), first using 100 mg of protected mono-benzylated product **23** and then 695.6 mg, giving 100 % stoichiometric yields. The deprotection worked on a larger scale, but the round bottom flask should be large enough to ease the co-evaporation process.

Table 6. Yields of deprotection reactions for the preparation of 2-*O*-benzyl-*myo*-inositol **21**

|  | Yield (mg) | Yield percentage (%) | Outcome |
|---|---|---|---|
| **Deprotection 1** | 54.21 | 100 | white solid |
| **Deprotection 2** | 377.09 | 100 | white solid |

Product **21** was characterized by measuring the melting point and collecting the $^1$H and $^{13}$C NMR spectra (Figure 43), 2D NMR, FTIR, and HR-MS spectra (APPENDIX 4). The melting point of 241-244 °C agrees with the literature[50]. No impurities are observed in the $^1$H and $^{13}$C NMR spectra. When measuring the $^1$H NMR spectrum, there were issues with shimming, which explains the observed noise of the baseline. Therefore, there is no integration that shows the number of CH (C1, C3, C4, C5, and C6) signals. The $^1$H NMR spectrum shows the peak of the NMR solvent used, DMSO, and its satellite peaks at 2.5 ppm.

## 10.3 Gelation experiments

The synthesized 2-*O*-benzyl-*myo*-inositol **21** was subjected to gelation experiments. **21** was dissolved in a selected biocompatible solvent (1 mL PBS or deionized water) using a 4 mL vial, sonicated, heated to 95 °C, and allowed to cool at RT overnight to allow gelation. The results of the gelation experiments are shown in Table 7.

Table 7. Gelation experiments of gelator 2-*O*-benzyl-*myo*-inositol **21**.

| Solvent (1 mL) | 2-*O*-benzyl-*myo*-inositol (mg) 21 | Outcome |
|---|---|---|
| PBS | 2 | No gel |
| PBS | 5 | No gel |
| PBS | 10 | Flakes |
| PBS | 20 | Partial gel |
| PBS | 30 | Partial gel |
| $H_2O$ | 30 | Partial gel |

The amphiphilic nature of the **21** allowed the dissolution in PBS and water, which was one of the requirements for this project to achieve biocompatible gels. We hypothesized that π-π stacking and ionic interactions are the forces that lead to gelation. 10 mg of **21** in 1 mL of PBS resulted in flakes, so we increased the concentration of the gelator, which resulted in partial

gels (Figure 39). The result was the same when deionized water was used as a solvent instead of PBS.
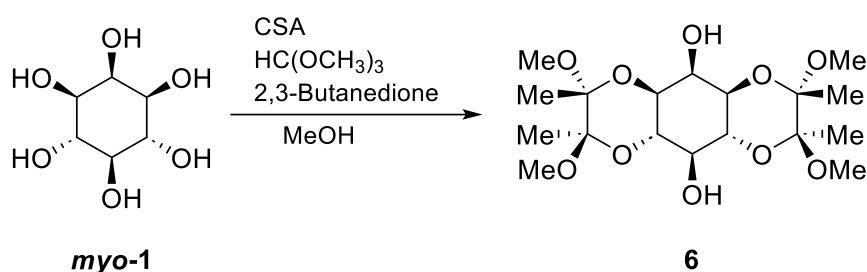


Figure 39. On the left, 10 mg of **21** in PBS formed flakes. On the right, 20 mg of **21** in PBS formed a partial gel.

## 11 Syntheses

The experimental details, data, ^{1}H and ^{13}C NMR spectra for the synthesized compounds are given below. The 2D NMR, FTIR and HR-MS spectra for the compounds are found in the Appendices.

### 11.1 1,6:3,4-bis-[*O*-(2,3-dimethoxybutane-2,3-diyl)]-*myo*-inositol (6)



Scheme 6. Synthesis of 1,6:3,4-bis-[*O*-(2,3-dimethoxybutane-2,3-diyl)]-*myo*-inositol **6**.

Camphor sulfonic acid (CSA; 0.25 g, 1.1 mmol) and trimethyl orthoformate (25 mL, 227.9 mmol) were added to anhydrous methanol (100 mL) under the $N_2$ atmosphere. The mixture was stirred for 15 min at RT. *Myo*-**1** (6.25 g, 34.7 mmol) and 2,3-butanedione (6.37 mL, 72.6 mmol) were added to the stirred solution, and the yellow mixture was refluxed for 41 hours. The red suspension was allowed to cool and filtered under vacuum. The precipitate was washed with methanol (x 5) and diethyl ether (x 5) and dried under vacuum overnight to afford 1,6:3,4-bis-[*O*-(2,3-dimethoxybutane-2,3-diyl)]-*myo*-inositol **6** (3.34 g, 24 %) as a white solid. The ^{1}H and ^{13}C NMR spectra are given in Figure 40.

**M.p.** 342-346 °C

**^{1}H NMR (500 MHz, CDCl₃):** δ 4.07 – 3.99 (m, CH, 3H), 3.69 (td, J = 9.5, 1.9 Hz, CH, 1H), 3.56 (dd, J = 10.2, 2.7 Hz, CH, 2H), 3.29 (s, OMe, 6H), 3.26 (s, OMe, 6H), 2.36 (dd, J = 9.2, 1.6 Hz, OH, 2H), 1.35 (s, Me, 6H), 1.33 (s, Me, 6H) ppm

**¹³C NMR (126 MHz, CDCl₃):** δ 100.11 (C(Me)(OMe)), 99.31 (C(Me)(OMe)), 70.16, 69.05 (CH, C2, C5), 68.86, 68.45 (CH, C1,3; C4, 6), 48.08 (OMe), 47.93 (OMe), 17.73 (Me), 17.66 (Me) ppm

**HRMS (ESI-TOF):** *m/z*: $[M + K]^+$ Calculated for $[C_{18}H_{32}O_{10}K]^+$ 447.1627; Found 447.1637; mass accuracy -1 mDa
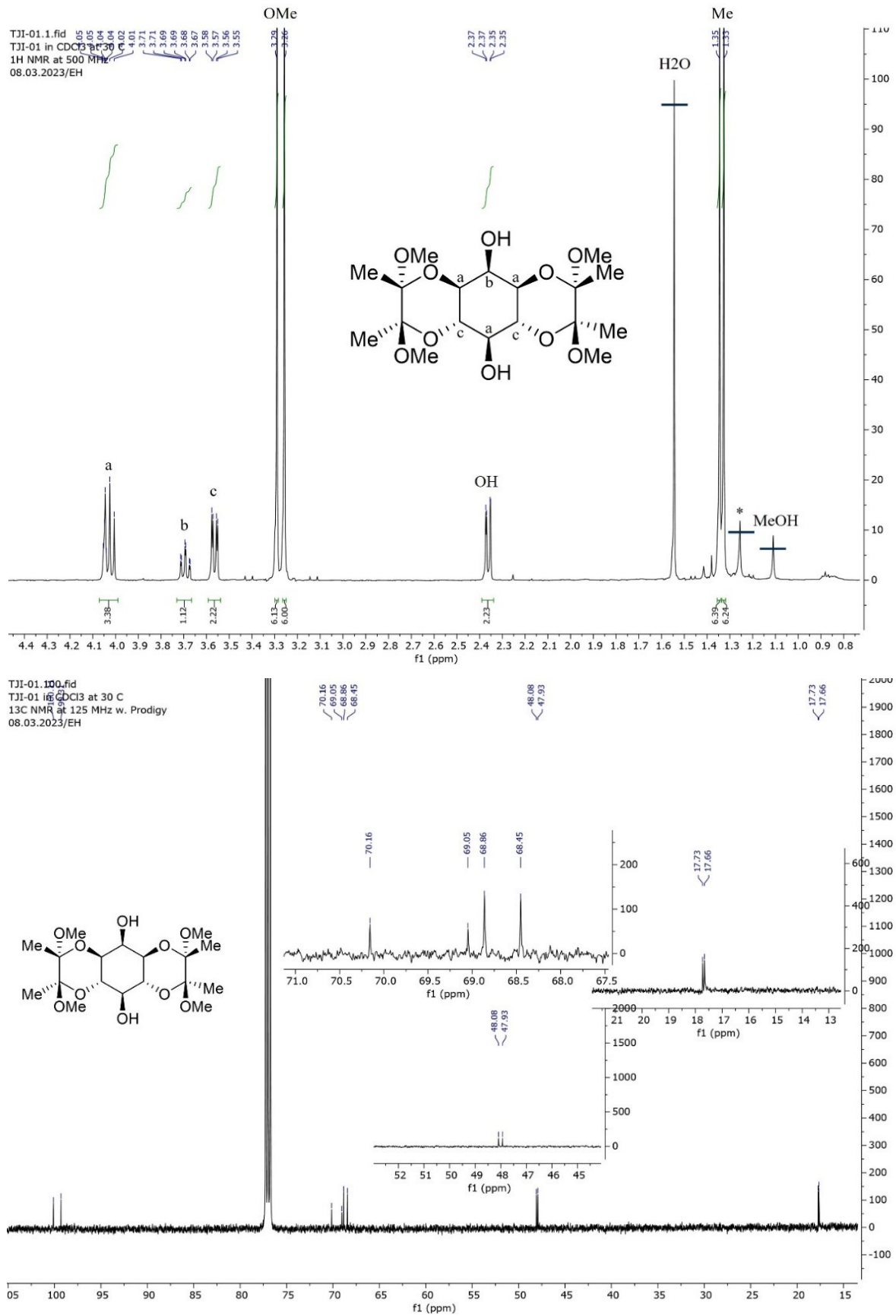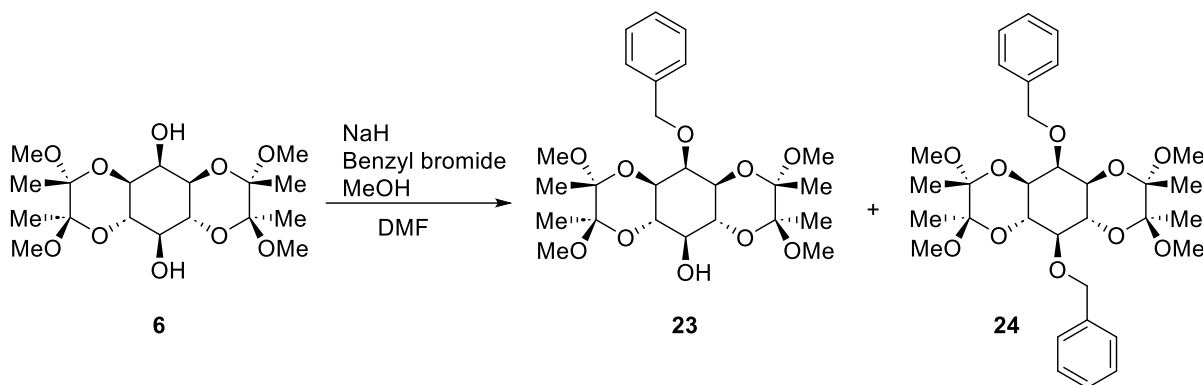
**FTIR** 924, 1033, 1106, 1123, 1380, 2932, 3492 cm⁻¹.

Figure 40. ¹H NMR spectrum (500 MHz, CDCl₃) (top) and ¹³C NMR spectrum (125 MHz, CDCl₃) (bottom) of 1,6:3,4-bis-[*O*-(2,3-dimethoxybutane-2,3-diyl)]-*myo*-inositol **6**.

## 11.2 2-*O*-benzyl-1,6:3,4-bis-[*O*-(2,3-dimethoxybutane-2,3-diyl)]-*myo*-inositol (23) and 2,5-di-*O*-benzyl-1,6:3,4-bis-[*O*-(2,3-dimethoxybutane-2,3-diyl)]-*myo*-inositol (24)



Scheme 7. Synthesis of 2-*O*-benzyl-1,6:3,4-bis-[*O*-(2,3-dimethoxybutane-2,3-diyl)]-*myo*-inositol **23** and 2,5-di-*O*-benzyl-1,6:3,4-bis-[*O*-(2,3-dimethoxybutane-2,3-diyl)]-*myo*-inositol **24**.

Vacuum-dried diol **6** (1000 mg, 2.45 mmol) was dissolved in anhydrous DMF (60 mL), and NaH (60 %, 120 mg, 5 mmol) was added portion-wise over 30 min under the $N_2$ atmosphere. The white suspension was stirred for 1 h, and the color changed to yellow. Benzyl bromide (0.32 mL, 2.69 mmol) was added dropwise over 30 min, and stirring was continued under the $N_2$ atmosphere at RT for 20 h. The progress of the reaction was monitored by TLC (Hex/EtOAc 1:1, Hanessian's stain). Two UV-active spots were seen, and the starting material was almost consumed. The reaction was stopped by adding methanol and stirred at RT for 15 min to deactivate the excess NaH. The solvents were removed under vacuum and co-evaporated once with toluene to remove DMF.

The brown residue was dissolved in DCM (100 mL) and washed with deionized water. The aqueous phase was back extracted with DCM, and the combined organic phases were washed with deionized water followed by saturated brine. The organic phase was dried ($MgSO_4$), and the solvent was evaporated under vacuum. The residue was purified by flash column chromatography (petroleum ether / ethyl acetate 4:1 to 1:1) to give mono- and di-benzylated protected *myo*-inositol **23** and **24**. The purified compounds were dried under vacuum for 24 h to give the mono-benzylated product **23** (white powder, 815 mg, 67 %) and di-benzylated

product **24** (white powder, 53.7 mg, 4 %). The $^1$H and $^{13}$C NMR spectra for products **23** and **24** are given in Figure 41 and Figure 42, respectively.

2-*O*-benzyl-1,6:3,4-bis-[*O*-(2,3-dimethoxybutane-2,3-diyl)]-*myo*-inositol **23**:

**M.p.** 211-214 °C

**$^1$H NMR (300 MHz, CDCl3):** δ 7.53 – 7.47 (m, Ar, 2H), 7.34 – 7.27 (m, Ar, 2H), 7.21 (d, J = 7.2 Hz, Ar, 1H), 4.85 (s, CH$_2$, 2H), 4.06 (t, J = 9.8 Hz, CH, 2H), 3.80 (t, J = 2.5 Hz, CH, 1H), 3.65 (td, J = 9.4, 2.0 Hz, CH,1H), 3.52 (dd, J = 10.3, 2.5 Hz, CH, 2H), 3.26 (s, OMe, 6H), 3.21 (s, OMe, 6H), 2.34 (d, J = 2.0 Hz, OH, 1H), 1.30 (s, Me, 12H)

**$^{13}$C NMR (125 MHz, CDCl3):** δ 139.64, 127.84, 127.61, 126.92 (Ar), 99.65 (C(Me)(OMe)), 99.14 (C(Me)(OMe)), 76.28 (CH, C2), 73.83 (CH$_2$), 70.67 (CH, C5), 69.37, 69.10 (CH, C1,3; C4, 6), 47.94 (OMe), 47.87 (OMe), 17.77 (Me), 17.68 (Me)

**HR-MS (ESI-TOF):** *m/z*: [M + K]$^+$ Calculated for [C$_{25}$H$_{38}$O$_{10}$K]$^+$ 537.2102; Found 537.2099; mass accuracy 0.3 mDa; FTIR 913, 1034, 1112, 1377, 1453, 2944, 3479 cm$^{-1}$.mp

2,5-di-*O*-benzyl-1,6:3,4-bis-[*O*-(2,3-dimethoxybutane-2,3-diyl)]-*myo*-inositol **24**:

**M.p.** 162-164 °C

**$^1$H NMR (500 MHz, CDCl3):** δ 7.50 (dd, J = 7.9, 1.4 Hz, Ar, 2H), 7.42 – 7.38 (m, Ar, 2H), 7.33 – 7.27 (m, Ar, 4H), 7.26 – 7.21 (m, Ar, 2H), 4.85 (d, J = 5.2 Hz, CH$_2$, 4H), 4.25 – 4.14 (m, CH, 2H), 3.80 (t, J = 2.5 Hz, CH, 1H), 3.60 – 3.50 (m, CH, 3H), 3.26 (s, OMe, 6H), 3.24 (s, OMe, 6H), 1.33 (d, J = 1.1 Hz, Me, 6H), 1.31 (d, J = 1.1 Hz, Me, 6H)

**$^{13}$C NMR (125 MHz, CDCl3):** δ 139.64, 128.04, 127.80, 127.65, 127.49, 127.16, 126.86 (Ar), 99.59 (C(OMe)Me)), 99.03 (C(OMe)Me)), 78.91 (CH, C5), 76.12 (CH, C2), 75.00 (CH$_2$-C5), 73.74 (CH$_2$-C2), 69.99, 69.35 (CH, C1,3; C4, 6), 47.91 (OMe), 47.80 (OMe), 17.91 (Me), 17.66 (Me)

**HR-MS (ESI-TOF):** *m/z*: [M + K]$^+$ Calculated for [C$_{32}$H$_{44}$O$_{10}$K]$^+$ 627.2572; Found 627.2555; mass accuracy 1.7 mDa; FTIR 884, 1035, 1111, 1139, 1380, 1453, 2895 cm$^{-1}$.
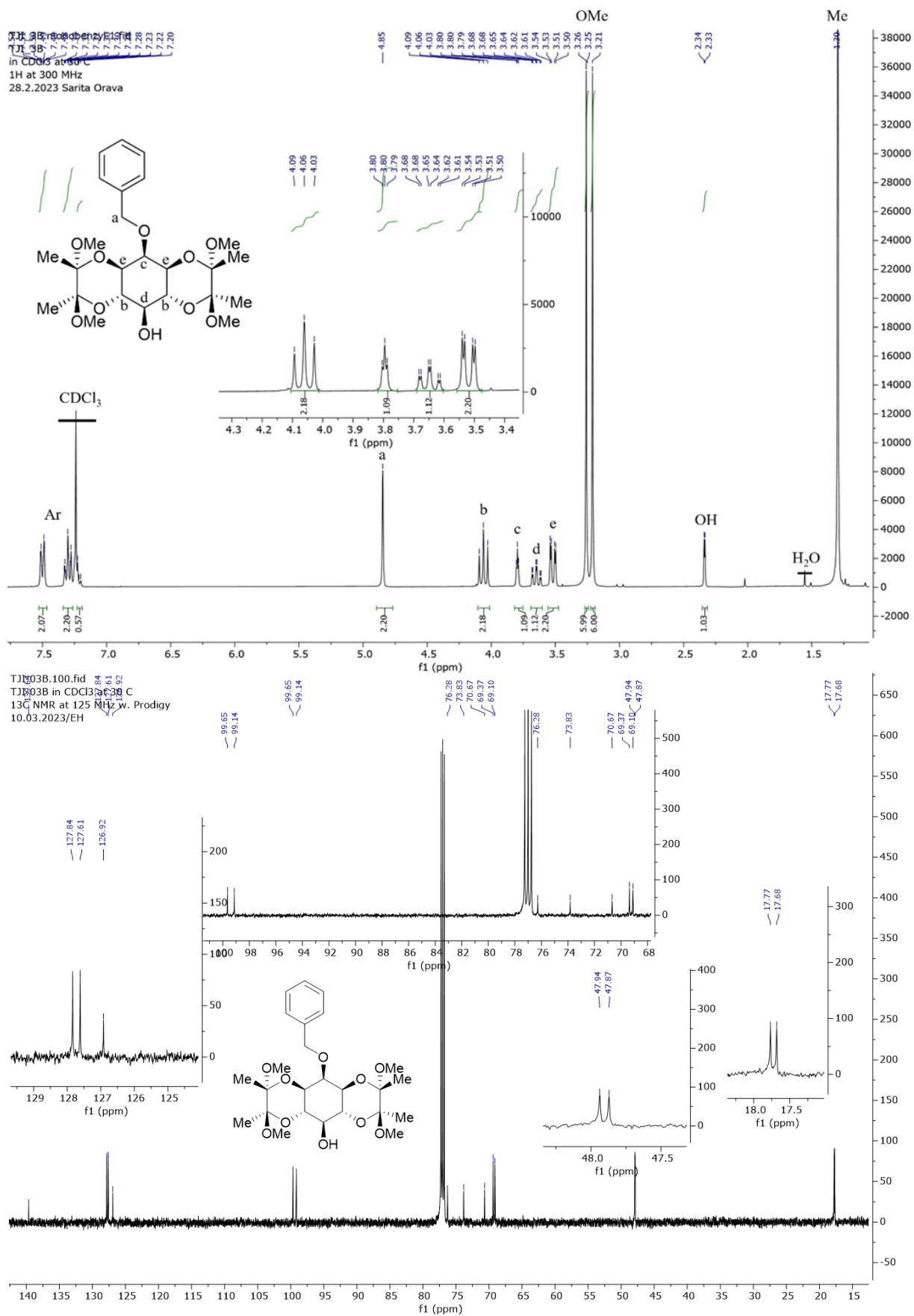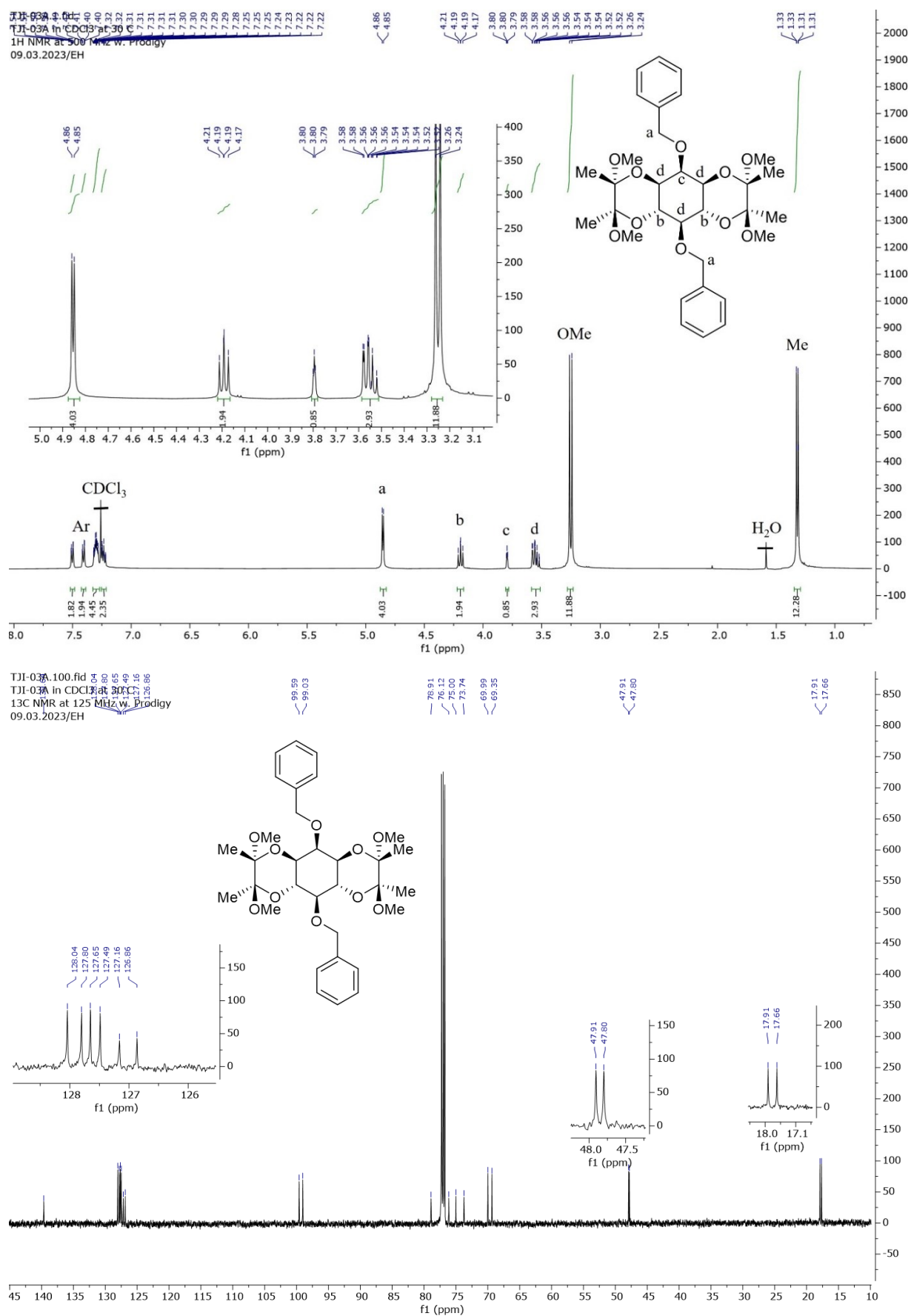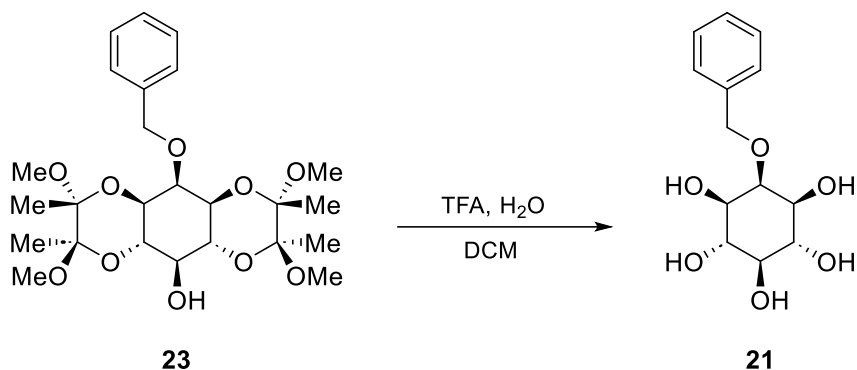
Figure 41. ¹H NMR spectrum (300 MHz, CDCl₃) (top) and
¹³C NMR spectrum (125 MHz, CDCl₃) (bottom) of 2-*O*-benzyl-1,6:3,4-bis-[*O*-(2,3-dimethoxybutane-2,3-diyl)]-*myo*-inositol **23**.

Figure 42. $^1$H NMR spectrum (500 MHz, CDCl$_3$) (top) and $^{13}$C NMR spectrum (125 MHz, CDCl$_3$) (bottom) of 2,5-di-*O*-benzyl-1,6:3,4-bis-[*O*-(2,3-dimethoxybutane-2,3-diyl)]-*myo*-inositol **24**.

## 11.3 2-*O*-benzyl-*myo*-inositol (21)



Scheme 8. Synthesis of 2-*O*-benzyl-*myo*-inositol **21**.

Mono-benzylated protected *myo*-inositol **23** (695.6 mg, 1.4 mmol) was dissolved in DCM (7 mL). Aqueous TFA (90 %, 7 mL) was slowly added to the stirred solution at RT. The color of the reaction mixture changed from white to yellow after the addition of TFA. Stirring was continued for 1 h at RT, and the reaction was monitored by TLC (Hex:EA 1:1, Hanessian's stain). The reaction was stopped after 1 h. After completion, the solvents were removed under vacuum and co-evaporated with methanol (x 6) to remove all butanedione, yielding the pure deprotected mono-benzylated *myo*-inositol **21** (white solid, 377.09 mg, stoichiometric yield). The $^1$H and $^{13}$C NMR spectra are given in Figure 43.

**M.p.** 241-244 °C

**$^1$H NMR (400 MHz, DMSO):** δ 7.39 (d, J = 7.1 Hz, Ar, 2H), 7.31 (t, J = 7.4 Hz, Ar, 2H), 7.24 (td, J = 7.4, 7.0, 3.2 Hz, Ar, 1H), 4.76 (s, CH$_2$, 2H), 3.71 (t, J = 2.6 Hz, C1-H, 1H), 3.41 (t, J = 9.3 Hz, C-4,6-OH, 2H), 3.26 (dd, J = 9.7, 2.6 Hz, C-1,3-OH, 2H), 2.93 (t, J = 8.9 Hz, C-5-OH, 1H)

**$^{13}$C NMR (100 MHz, DMSO):** δ 139.94, 127.83, 126.99, 126.80 (Ar), 81.89 (C2), 75.33 (C5), 74.15 (CH$_2$), 73.15(C4, 6), 72.12 (C1, 3)

**HR-MS (ESI-TOF):** *m/z*: [M + Na]$^+$ Calculated for [C$_{13}$H$_{18}$O$_6$Na]$^+$ 293.0996; Found 293.1000; mass accuracy – 0.4 mDa

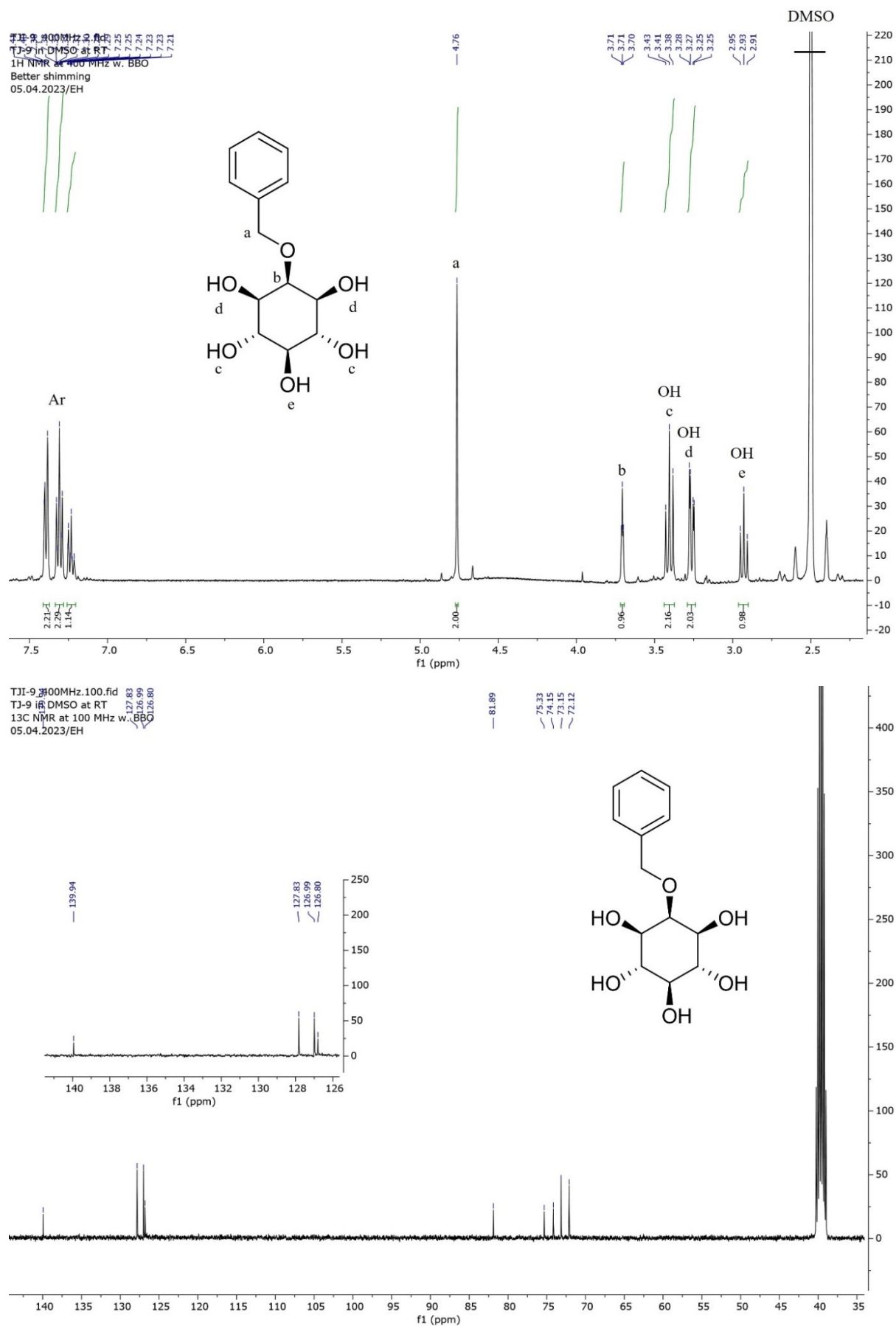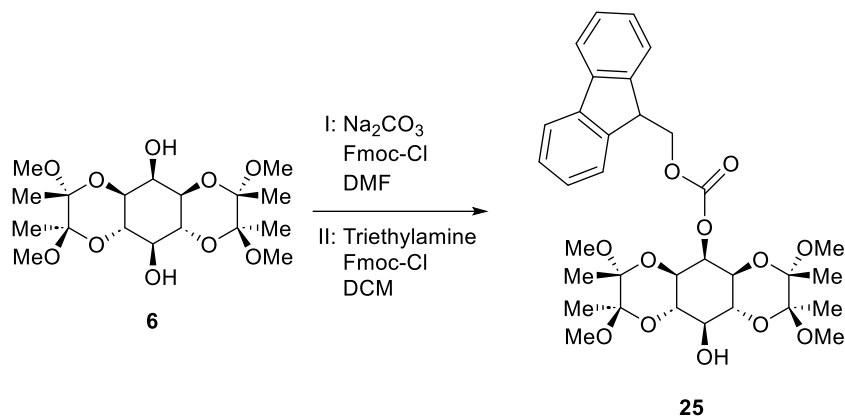**FTIR:** 715, 1033, 1119, 1368, 1451, 3231 cm$^{-1}$.

Figure 43. $^1$H NMR spectrum (400 MHz, DMSO) (top) and $^{13}$C NMR spectrum (100 MHz, DMSO) (bottom) of 2-*O*-benzyl-*myo*-inositol **21**.

## 11.4 2-*O*-Fmoc-1,6:3,4-bis-[*O*-(2,3-dimethoxybutane-2,3-diyl)]-*myo*-inositol (25)



Scheme 9. Two potential routes for the synthesis of 2-*O*-Fmoc-1,6:3,4-bis-[*O*-(2,3-dimethoxybutane-2,3-diyl)]-*myo*-inositol **25**.

In the first attempt to synthesize product **25**, $Na_2CO_3$ (129.7 mg, 1.2 mmol) was added to vacuum-dried diol **6** (200 mg, 0.49 mmol). Anhydrous DMF (8 mL) was added under the $N_2$ atmosphere. Fmoc-Cl (126.7 mg, 0.49 mmol) was dissolved in anhydrous DMF (2 mL) and added dropwise to the stirred solution at 0 °C. Stirring was continued under the $N_2$ atmosphere at RT for 22 h. The progress of the reaction was monitored by TLC (Hex/EtOAc 1:1 and EtOAc, Hanessian's stain).

Based on the TLCs, the workup was continued by removing the solvent under vacuum. The residue was dissolved in DCM (50 mL) and washed twice with deionized water. The aqueous phase was back extracted with DCM. The organic phase was dried ($MgSO_4$), and the solvent was evaporated under vacuum. The residue was dried under vacuum overnight, and the crude ^{1}H NMR spectrum (Figure 36) was measured. The residue was purified by flash column chromatography (petroleum ether/EtOAc 2:1 to 1:1). The fractions were collected and dried under vacuum, followed by ^{1}H NMR (Figure 37), which showed no reaction.

In the second attempt, the reaction conditions were changed. Vacuum-dried diol **6** (200 mg, 0.49 mmol) was dissolved in DCM (5 mL) and triethylamine (689 µL, 4.9 mmol) was added to the stirred solution at 0 °C. A catalytic amount of 4-dimethylaminopyridine was added to the solution. Fmoc-Cl (126.7 mg, 0.49 mmol) was dissolved in DCM (5 mL) and added dropwise to the stirred reaction mixture. Stirring was continued under the $N_2$ atmosphere at RT for 20 h. The progress of the reaction was monitored by TLC (Hex/EtOAc 1:1, Hanessian's stain). The result was qualitatively similar to the first attempt. Crude NMR was measured, which showed that no reaction occurred.

# 12 Conclusions

This thesis investigates *myo*-inositol, a naturally occurring polyol in eukaryotic cells and the most abundant form of inositol. *Myo*-inositol is a molecule of great biological importance: *myo*-inositol and its phosphorylated derivatives are involved in many metabolic and biochemical functions in organs and tissues. As part of cell membrane phospholipids, the phosphorylated derivatives act as secondary messengers in signaling pathways for cell growth, membrane development, and the transduction of hormones and neurotransmitters. They also play a key role in physiological processes such as reproduction, endocrine function, and metabolism.

Several mechanisms, such as endogenous synthesis from glucose, membrane transport, diet-dependent adsorption, the phosphoinositide cycle, and renal catabolism and excretion, influence the homeostasis of *myo*-inositol levels in cells and tissues. Given the broad role of *myo*-inositol in biological processes, it is not surprising that abnormalities in its metabolism are associated with a wide range of pathological conditions such as hypothyroidism, polycystic ovary syndrome, hormonal and metabolic imbalances such as weight gain, diabetes, and metabolic syndrome. In addition, *myo*-inositol deficiency may be associated with cancer, and neuropathologic and psychiatric diseases such as Parkinson's and Alzheimer's.

Considering the biological functions of *myo*-inositol, its incorporation into LMW gels is an interesting area of research, as these gels have several therapeutic applications due to their numerous beneficial properties. The aim of the experimental part was to prepare LMW gels by synthesizing *myo*-inositol based amphiphilic gelators. To support this, some examples of *myo*-inositol functionalization and reported *myo*-inositol based gels were presented in the literature part.

Working with *myo*-inositol is challenging due to its symmetry and multiple chemically corresponding hydroxyl groups, which presents challenges for the functionalization and synthesis of the desired derivatives. The use of protecting groups is a common method, but it increases the number of synthesis steps and reduces the overall efficiency. Therefore, direct functionalization methods are becoming increasingly popular in *myo*-inositol chemistry.

In this study, *myo*-inositol was attempted to functionalize with benzyl- and Fmoc-moieties and study the gelation properties of functionalized compounds towards biocompatible gels. Amphiphilicity was a basic requirement in this work to induce the gelation of *myo*-inositol derivatives. The functionalization was designed for the hydroxyl group in the axial position of the *myo*-inositol to reduce the steric barrier. To perform the functionalization, a three-step

retrosynthesis plan was designed: regioselective and stereoselective protection of *myo*-inositol, regioselective functionalization with the selected target molecule, and removal of the protecting groups.

The *myo*-inositol protection reaction yielded a symmetrical diol with two free hydroxyl groups, at positions 2 (axial) and 5 (equatorial). The protection reaction was time-consuming due to more than 40 hours of reflux time and the need to purify the desired product by flash column chromatography. The recovery rate in this reaction is relatively low, only just over 20 %. However, it was possible to carry out the screening reaction on a relatively large scale, which meant that only two reactions yielded sufficient products for all subsequent steps. The purity and structure of the products obtained in all reactions were determined by measuring NMR, FTIR and HR-MS spectra and melting points.

The functionalization of protected *myo*-inositol was attempted by attaching benzyl- and Fmoc-moieties. The benzyl derivative was obtained from the reaction with benzyl bromide, resulting in both mono- and di-benzylated protected *myo*-inositol. The mono-benzylated product was the main target towards which the reaction was optimized. It is believed that mono-benzylated *myo*-inositol would act as a gelator better than di-benzylated *myo*-inositol.

The Fmoc derivative was attempted to synthesize with Fmoc-Cl. The reaction was performed under two different reaction conditions, but the desired Fmoc derivative could not be synthesized. This is thought to be due to the large size of the Fmoc group and the steric barrier. The Fmoc group is so large that even in a successful reaction, it is not believed to attach to the equatorial hydroxyl group. In the future, the reaction could be done in the presence of NaH, resulting in a more reactive alkoxide from the protected *myo*-inositol before adding Fmoc-Cl.

The removal of the protection group is a reversible reaction for the protection reaction in which water is cleaved. To succeed, the deprotection reaction needs water. Using 99.5 % TFA acid was unsuccessful, but when the acid was changed to 90 % TFA, the deprotection was successful. The final reaction of this three-step synthetic pathway gave the unprotected mono-benzylated *myo*-inositol to proceed with gelation experiments. As benzylation had been optimized towards the mono-benzylated product, there was not enough di-benzylated *myo*-inositol derivative for the deprotection step and consequent gelation experiments.

We hypothesized that the benzyl- and Fmoc-moieties of *myo*-inositol derivatives offer the required amphiphilicity and that π-π stacking and ionic interactions may be the driving forces of self-assembly toward gelation. Gelation tests were performed on mono-benzylated *myo*-inositol. 10 mg of mono-benzylated *myo*-inositol derivative in 1 mL of PBS produced flakes,

while lower amounts yielded clear solutions and higher amounts (20-30 mg/1mL of PBS or deionized water) produced partial gels. Based on this result, some of the amphiphilic derivatives of *myo*-inositol could act as a gelator in biocompatible gels.

In the future, gelation could also be tested for di-benzylated unprotected *myo*-inositol to observe the similarities and differences in the gelation behaviour of mono- and di-benzylated *myo*-inositols. Based on our hypothesis and gelation results, the functionalization of *myo*-inositol could be tested by incorporating cinnamoyl-, coumaroyl- and caffeoyl-moieties into *myo*-inositol (Figure 44).
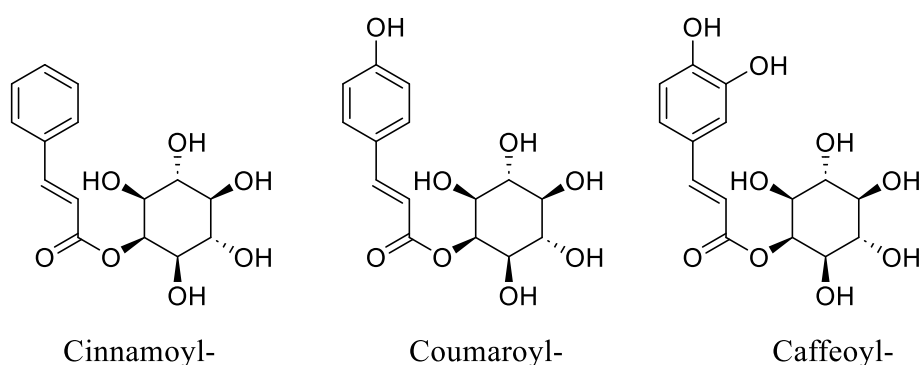


Figure 44. Alternative derivatives of amphiphilic *myo*-inositol derivatives.

Working with *myo*-inositol is quite challenging as the symmetrical shape (meso form) of the molecule makes the interpretation of spectra difficult. Based on this study, amphiphilic derivatives of *myo*-inositol could have the potential to act as gelators towards biocompatible gels. However, further research is needed to confirm the role of amphiphilic *myo*-inositol derivatives as gelators before the hypothesis can be confirmed.

# References

1. Derkaczew, M.; Martyniuk, P.; Osowski, A. and Wojtkiewicz, J., Cyclitols: from basic understanding to their association with neurodegeneration, *Nutrients*, **2023**, *15*, 2029.

2. Irvine, R. F., A short history of inositol lipids, *J. Lipid Res.*, **2016**, *57*, 1987–1994.

3. Sureshan, K. M.; Shashidhar, M. S.; Praveen, T. and Das, T., Regioselective protection and deprotection of inositol hydroxyl groups, *Chem. Rev.*, **2003**, *103*, 4477–4504.

4. Su, X. B.; Ko, A.-L. A. and Saiardi, A., Regulations of myo-inositol homeostasis: Mechanisms, implications, and perspectives, *Adv. Biol. Regul.*, **2023**, *87*, 100921.

5. Croze, M. L. and Soulage, C. O., Potential role and therapeutic interests of myo-inositol in metabolic diseases, *Biochimie*, **2013**, *95*, 1811–1827.

6. Cao, H.; Guo, T.; Deng, X.; Huo, X.; Tang, S.; Liu, J. and Wang, X., Site-selective C–H alkylation of myo-inositol via organic photoredox catalysis, *Chem. Commun.*, **2022**, *58*, 9934–9937.

7. Li, Y.; Han, P.; Wang, J.; Shi, T. and You, C., Production of myo-inositol: Recent advance and prospective, *Biotechnol. Appl. Bioc*, **2022**, *69*, 1101–1111.

8. Basu, N.; Chakraborty, A. and Ghosh, R., Carbohydrate derived organogelators and the corresponding functional gels developed in recent time, *Gels*, **2018**, *4*, 52.

9. Tripathy, D.; Gadtya, A. S. and Moharana, S., Supramolecular gel, its classification, preparation, properties, and applications: A review, *Polym.-Plast. Tech. Mat.*, **2023**, *62*, 306–326.

10. Draper, E. R. and Adams, D. J., Low-molecular-weight Gels: The state of the art, *Chem.*, **2017**, *3*, 390–410.

11. Sureshan, K. M.; Yamaguchi, K.; Sei, Y. and Watanabe, Y., Probing gelation at the molecular level: Head-to-tail hydrogen-bonded self-assembly of an inositol-based organogelator, *Eur. J. Org. Chem.*, **2004**, *2004*, 4703–4709.

12. Vidyasagar, A. and Sureshan, K. M., Stoichiometric sensing to opt between gelation and crystallization, *Angew.Chem. Int. Ed.*, **2015**, *54*, 12078–12082.

13. Joshi, S. A. and Kulkarni, N. D., A new trinuclear Cu(II) complex of inositol as a hydrogelator, *Chem. Commun.*, **2009**, 2341–2343.

14. Siracusa, L.; Napoli, E. and Ruberto, G., Novel chemical and biological insights of inositol derivatives in mediterranean plants, *Molecules*, **2022**, *27*, 1525.

15. Deng, F.; Zheng, X.; Sharma, I.; Dai, Y.; Wang, Y. and Kanwar, Y. S., Regulated cell death in cisplatin-induced AKI: relevance of myo-inositol metabolism, *Am. J. Physiol. Renal Physiol.*, **2021**, *320*, F578–F595.

16. Best, M. D.; Zhang, H. and Prestwich, G. D., Inositol polyphosphates, diphosphoinositol polyphosphates and phosphatidylinositol polyphosphate lipids: Structure, synthesis, and development of probes for studying biological activity, *Nat. Prod. Rep.*, **2010**, *27*, 1403–1430.

17. Balla, T., Phosphoinositides: Tiny lipids with giant impact on cell regulation, *Physiol. Rev.*, **2013**, *93*, 1019–1137.

18. Turner, B. L.; Papházy, M. J.; Haygarth, P. M. and McKelvie, I. D., Inositol phosphates in the environment., *Philos. Trans. R. Soc. Lond. B Biol. Sci.*, **2002**, *357*, 449–469.

19. Best, M. D.; Zhang, H. and Prestwich, G. D., Inositol polyphosphates, diphosphoinositol polyphosphates and phosphatidylinositol polyphosphate lipids: Structure, synthesis, and development of probes for studying biological activity, *Nat. Prod. Rep.*, **2010**, *27*, 1403–1430.

20. Posor, Y.; Jang, W. and Haucke, V., Phosphoinositides as membrane organizers, *Nat. Rev. Mol. Cell. Biol.*, **2022**, *23*, 797–816.

21. Chen, M.; Wen, T.; Horn, H. T.; Chandrahas, V. K.; Thapa, N.; Choi, S.; Cryns, V. L. and Anderson, R. A., The nuclear phosphoinositide response to stress, *Cell Cycle*, **2020**, *19*, 268–289.

22. Gardocki, M. E.; Jani, N. and Lopes, J. M., Phosphatidylinositol biosynthesis: Biochemistry and regulation, *Biochim. Biophys. Acta - Mol.Cell Biol. Lipids*, **2005**, *1735*, 89–100.

23. Falkenburger, B. H.; Jensen, J. B.; Dickson, E. J.; Suh, B.-C. and Hille, B., Phosphoinositides: lipid regulators of membrane proteins, *J. Physiol.*, **2010**, *588*, 3179–3185.

24. Dinicola, S.; Minini, M.; Unfer, V.; Verna, R.; Cucina, A. and Bizzarri, M., Nutritional and Acquired Deficiencies in Inositol Bioavailability. Correlations with Metabolic Disorders, *Int. J. Mol. Sci.*, **2017**, *18*, 2187.

25. Derkaczew, M.; Martyniuk, P.; Osowski, A. and Wojtkiewicz, J., Cyclitols: From Basic Understanding to their association with neurodegeneration, *Nutrients*, **2023**, *15*, 2029.

26. Owczarczyk-Saczonek, A.; Lahuta, L. B.; Ligor, M.; Placek, W.; Górecki, R. J. and Buszewski, B., The healing-promoting properties of selected cyclitols—A Review, *Nutrients*, **2018**, *10*, 1891.

27. Carlomagno, G. and Unfer, V., Inositol safety: clinical evidences, *Eur. Rev. Med. Pharmacol. Sci.*, **2011**, *15*, 931–936.

28. Chen, Q.; Shen, L. and Li, S., Emerging role of inositol monophosphatase in cancer, *Biomed. Pharmacother.* **2023**, *161*, 114442.

29. Gonzalez-Uarquin, F.; Rodehutscord, M. and Huber, K., Myo-inositol: its metabolism and potential implications for poultry nutrition—a review, *Poultry Science*, **2020**, *99*, 893–905.

30. Beemster, P.; Groenen, P. and Steegers-Theunissen, R., Involvement of Inositol in Reproduction, *Nutrition Rev.*, **2002**, *60*, 80–87.

31. Lepore, E.; Lauretta, R.; Bianchini, M.; Mormando, M.; Di Lorenzo, C. and Unfer, V., Inositols depletion and resistance: principal mechanisms and therapeutic strategies, *Int. J. Mol. Sci.*, **2021**, *22*, 6796.

32. Fu, H.; Li, B.; Hertz, L. and Peng, L., Contributions in astrocytes of SMIT1/2 and HMIT to myo-inositol uptake at different concentrations and pH, *Neurochem. Int.*, **2012**, *61*, 187–194.

33. Schneider, S., Inositol transport proteins, *FEBS Lett.*, **2015**, *589*, 1049–1058.

34. Kiani, A. K.; Paolacci, S.; Calogero, A. E.; Cannarella, R.; Renzo, G. C. D.; Gerli, S.; Berardinis, E. D.; Giudice, F. D.; Stuppia, L.; Facchinetti, F.; Dinicola, S. and Bertelli, M., From myo-inositol to D-chiro-inositol molecular pathways, *Eur. Rev. Med. Pharmacol Sci.*, **2021**, *25*, 2390–2402.

35. Watanabe, Y.; Uemura, T.; Yamauchi, S.; Tomita, K.; Saeki, T.; Ishida, R. and Hayashi, M., Regioselective functionalization of unprotected myo-inositol by electrophilic substitution, *Tetrahedron*, **2013**, *69*, 4657–4664.

36. Mills, S. J.; Riley, A. M.; Liu, C.; Mahon, M. F. and Potter, B. V. L., A definitive synthesis of D-myo-inositol 1,4,5,6-tetrakisphosphate and its enantiomer D-myo-inositol 3,4,5,6-tetrakisphosphate from a novel butane-2,3-diacetal-protected inositol, *Chem. Eur. J.*, **2003**, *9*, 6207–6214.

37. Montchamp, J.-L.; Tian, F.; Hart, M. E. and Frost, J. W., Butane 2,3-bisacetal protection of vicinal diequatorial diols, *J. Org. Chem.*, **1996**, *61*, 3897–3899.

38. Shashidhar, M. S., Regioselective protection of myo-inositol orthoesters – recent developments, *Arkivoc.*, **2002**, *2002*, 63–75.

39. Lloyd, D. J., The problem of gel structure. In: Alexander, J., (ed.), *Colloid Chemistry*, New York: The Chemical Catalog Co., **1926**, pp. 767–782.

40. Lan, Y.; G. Corradini, M.; G. Weiss, R.; R. Raghavan, S. and A. Rogers, M., To gel or not to gel: correlating molecular gelation with solvent parameters, *Chem. Soc. Rev.*, **2015**, *44*, 6035–6058.

41. Adams, D. J., Personal perspective on understanding low molecular weight gels, *J. Am. Chem. Soc.*, **2022**, *144*, 11047–11053.

42. Raghavan, S. R. and Cipriano, B. H., Gel formation: phase diagrams using tabletop rheology and calorimetry. In: Weiss, R. G. and Terech, P. (eds.), *Molecular Gels*,, Springer, Dordrecht, **2006**, pp. 241–252.

43. Zurcher, D. M. and McNeil, A. J., Tools for identifying gelator scaffolds and solvents, *J. Org. Chem.*, **2015**, *80*, 2473–2478.

44. Luboradzki, R.; Gronwald, O.; Ikeda, M.; Shinkai, S. and Reinhoudt, D. N., An attempt to predict the gelation ability of hydrogen-bond-based gelators utilizing a glycoside library, *Tetrahedron*, **2000**, *56*, 9595–9599.

45. Vatankhah-Varnoosfaderani, M.; GhavamiNejad, A.; Hashmi, S. and J. Stadler, F., Mussel-inspired pH-triggered reversible foamed multi-responsive gel – the surprising effect of water, *Chem. Commun.*, **2013**, *49*, 4685–4687.

46. Zhang, T.; Wu, Y.; Gao, L.; Song, Z.; Zhao, L.; Zhang, Y. and Tao, J., A novel Na + coordination mediated supramolecular organogel based on isosteviol: water-assisted self-assembly, in situ forming and selective gelation abilities, *Soft Matter*, **2013**, *9*, 638–642.

47. Gronwald, O. and Shinkai, S., Sugar-integrated gelators of organic solvents, *Chemis. Eur. J.*, **2001**, *7*, 4328–4334.

48. Riley, A. M.; Jenkins, D. J. and Potter, B. V. L., A concise synthesis of neo-inositol, *Carbohydrate Res.*, **1998**, *314*, 277–281.

49. Hesek, D.; Lee, M.; Noll, B. C.; Fisher, J. F. and Mobashery, S., Complications from dual roles of sodium hydride as a base and as a reducing agent, *J. Org. Chem.*, **2009**, *74*, 2567–2570.

50. Wang, H.; Godage, H. Y.; Riley, A. M.; Weaver, J. D.; Shears, S. B. and Potter, B. V. L., Synthetic inositol phosphate analogs reveal that PPIP5K2 has a surface-mounted substrate capture site that is a target for drug discovery, *Chem. Biol.*, **2014**, *21*, 689–699.
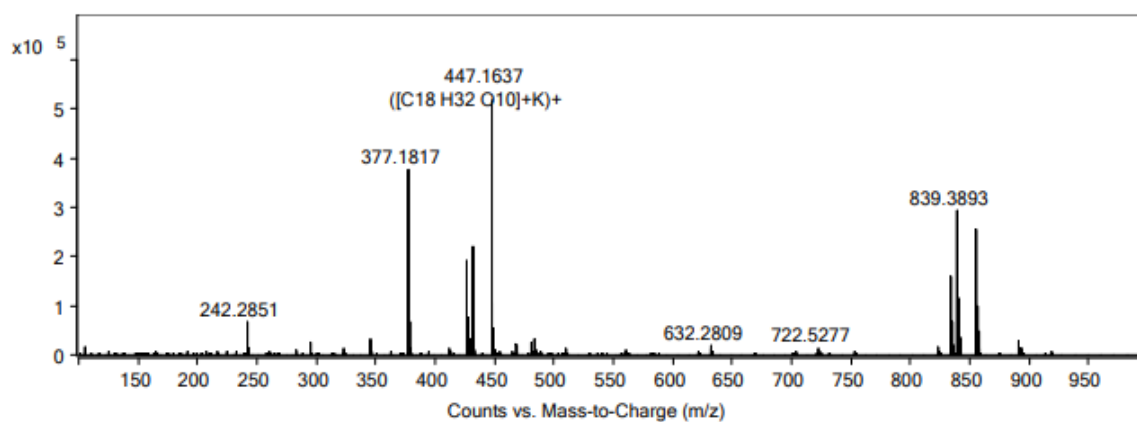
# Appendices
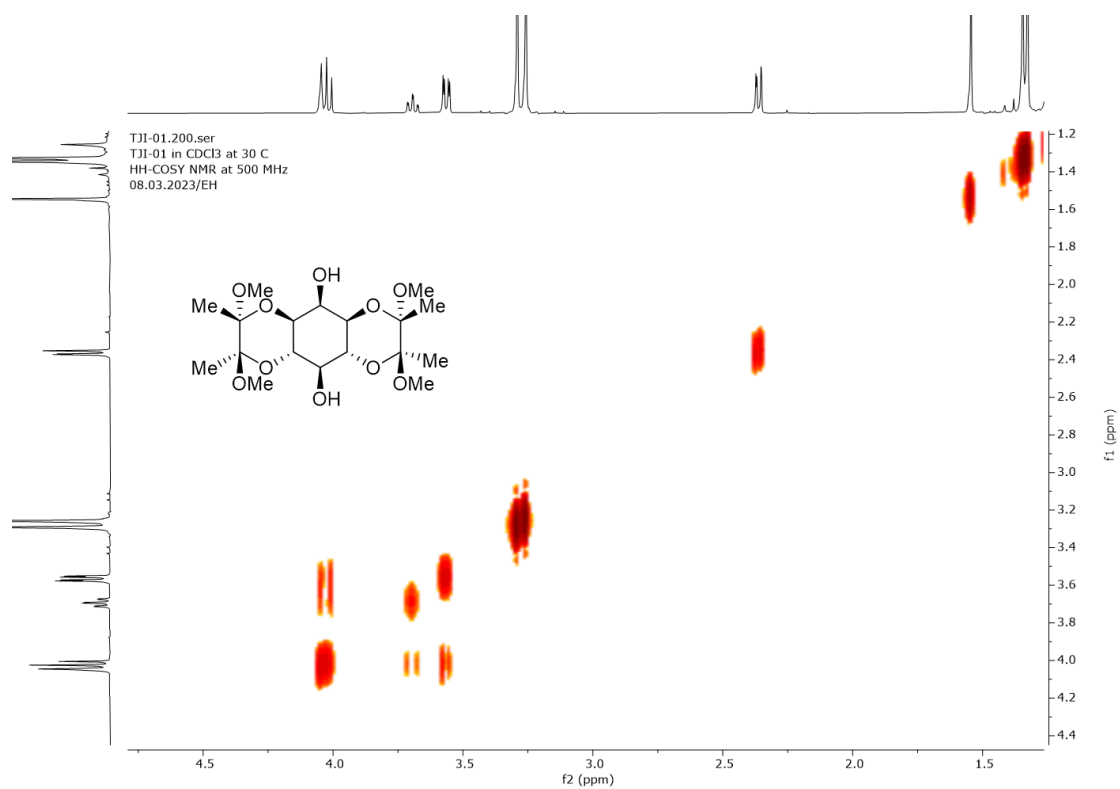
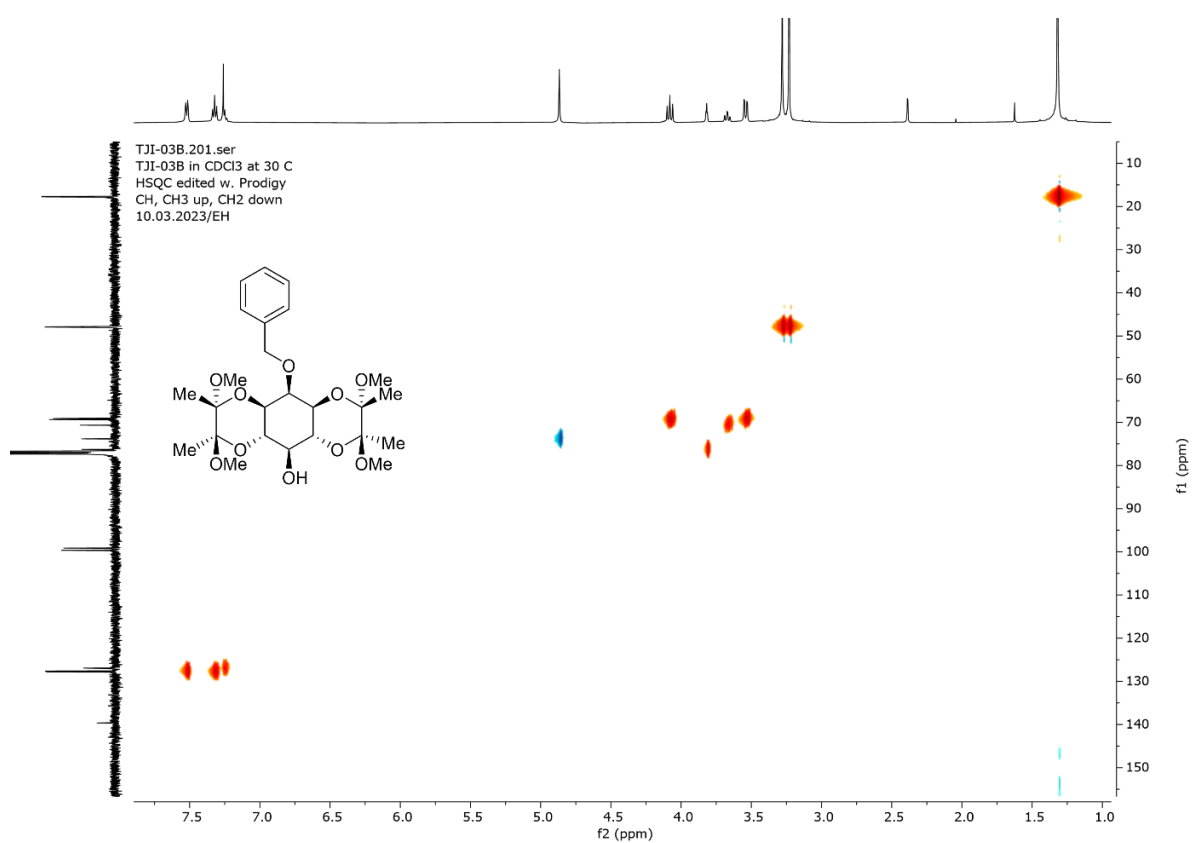Figure A1. HH-COSY NMR (500 MHz, CDCl$_3$) spectrum of *myo*-inositol derivative **6**.
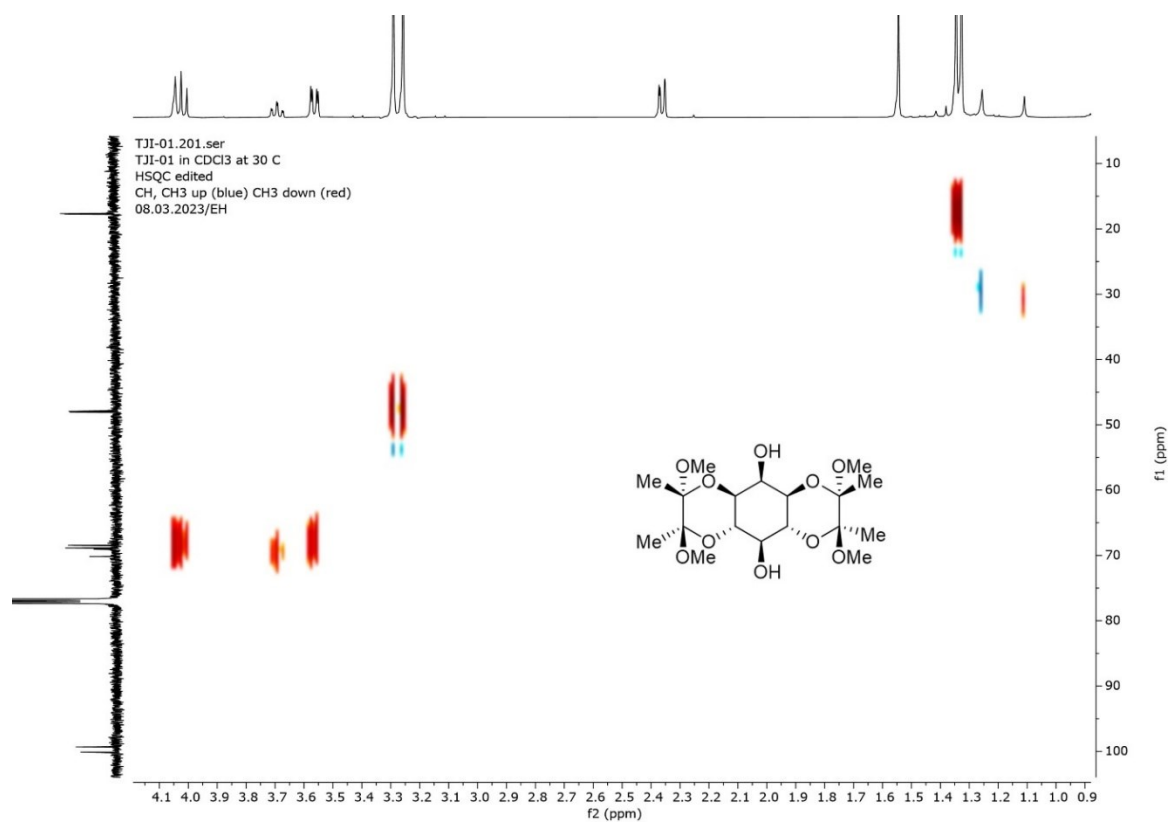


Figure A2. HSQC NMR (500 MHz, CDCl$_3$) spectrum of *myo*-inositol derivative **6**.
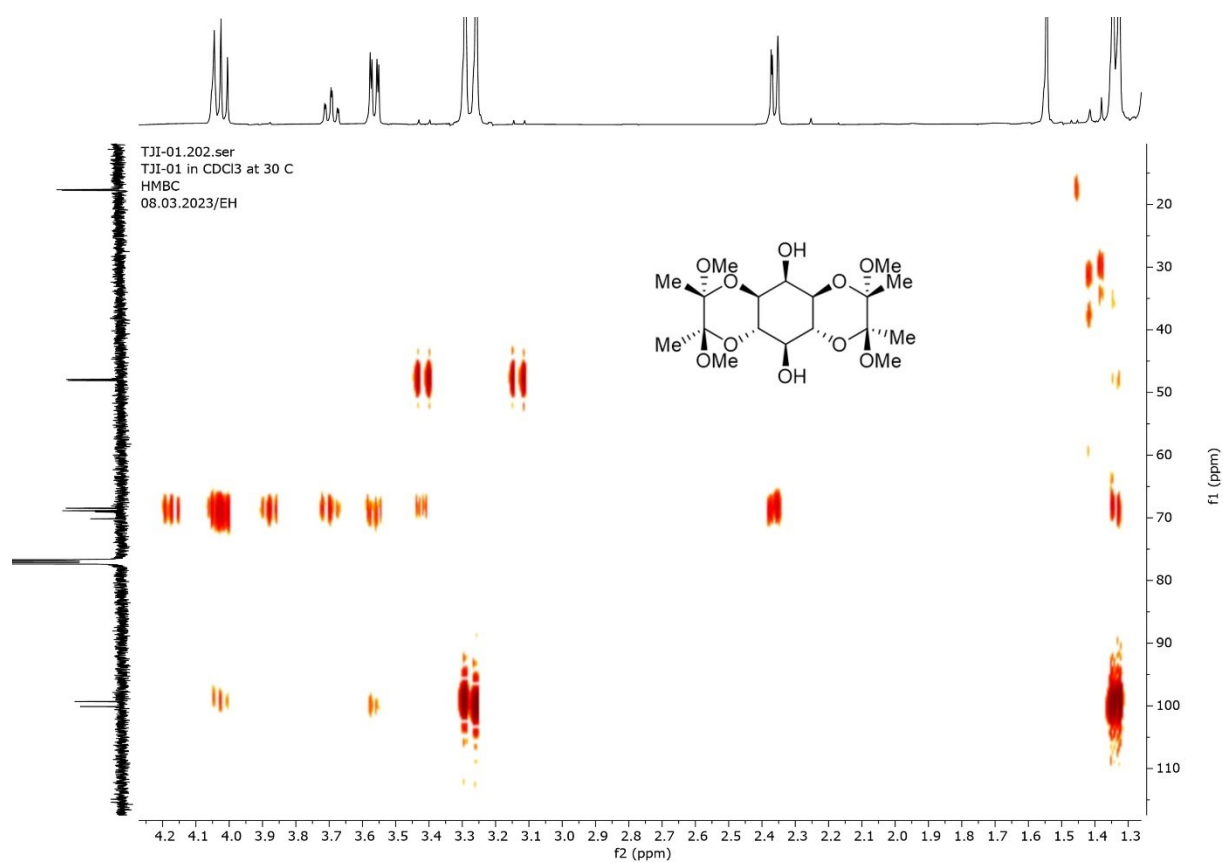
Figure A3. HMBC NMR (500 MHz, CDCl$_3$) spectrum of *myo*-inositol derivative **6**.

| Fragmentor Voltage | Collision Energy | Ionization Mode |
|---|---|---|
| 350 | 0 | ESI |



**Peak List**

| m/z | z | Abund | Formula | Ion |
|---|---|---|---|---|
| 377.1817 | 1 | 378503.02 | | |
| 447.1637 | 1 | 517490.84 | C18 H32 O10 | (M+K)+ |
| 839.3893 | 1 | 293111.04 | | |

**Formula Calculator Element Limits**

| Element | Min | Max |
|---|---|---|
| C | 18 | 18 |
| H | 32 | 32 |
| O | 10 | 10 |
| N | 0 | 2 |

**Formula Calculator Results**

| Formula | Best | Mass | Tgt Mass | Diff (ppm) | Ion Species | Score |
|---|---|---|---|---|---|---|
| C18 H32 O10 | True | 408.2003 | 408.1995 | -1.73 | C18 H32 Na O10 | 98.38 |
| C18 H32 O10 | True | 408.2004 | 408.1995 | -2.2 | C18 H32 K O10 | 97.57 |

Figure A4. HR-MS spectrum and mass accuracies of *myo*-inositol derivative **6**.
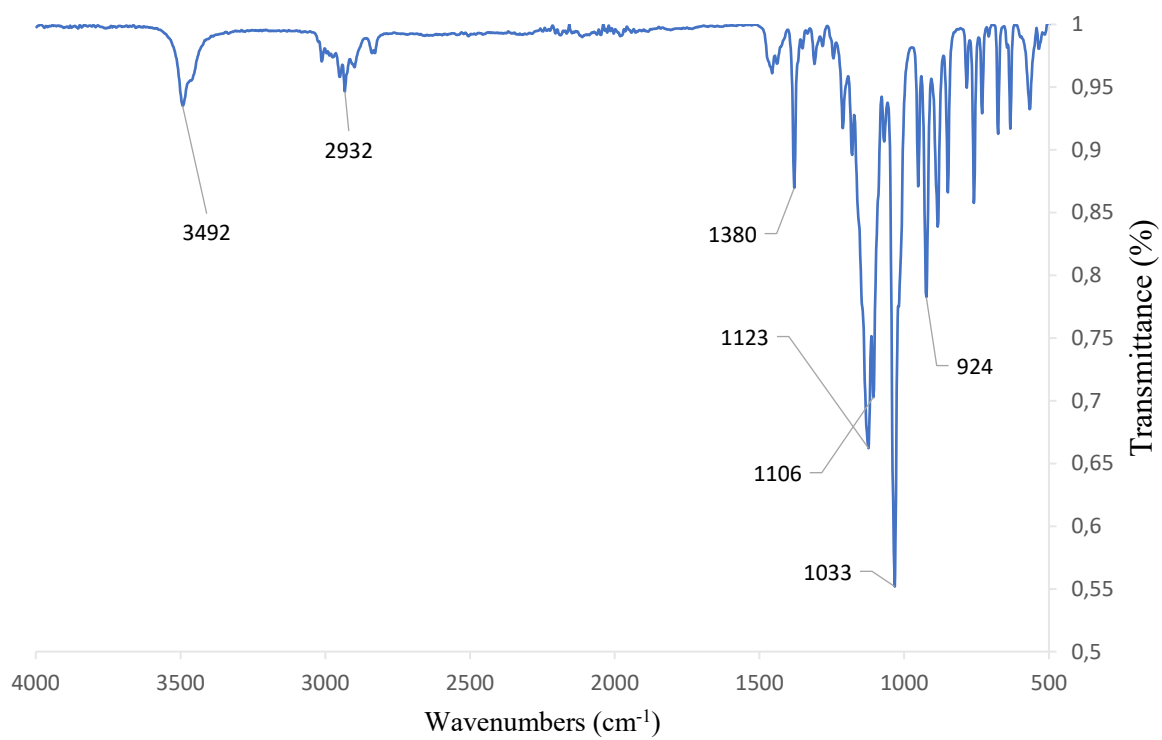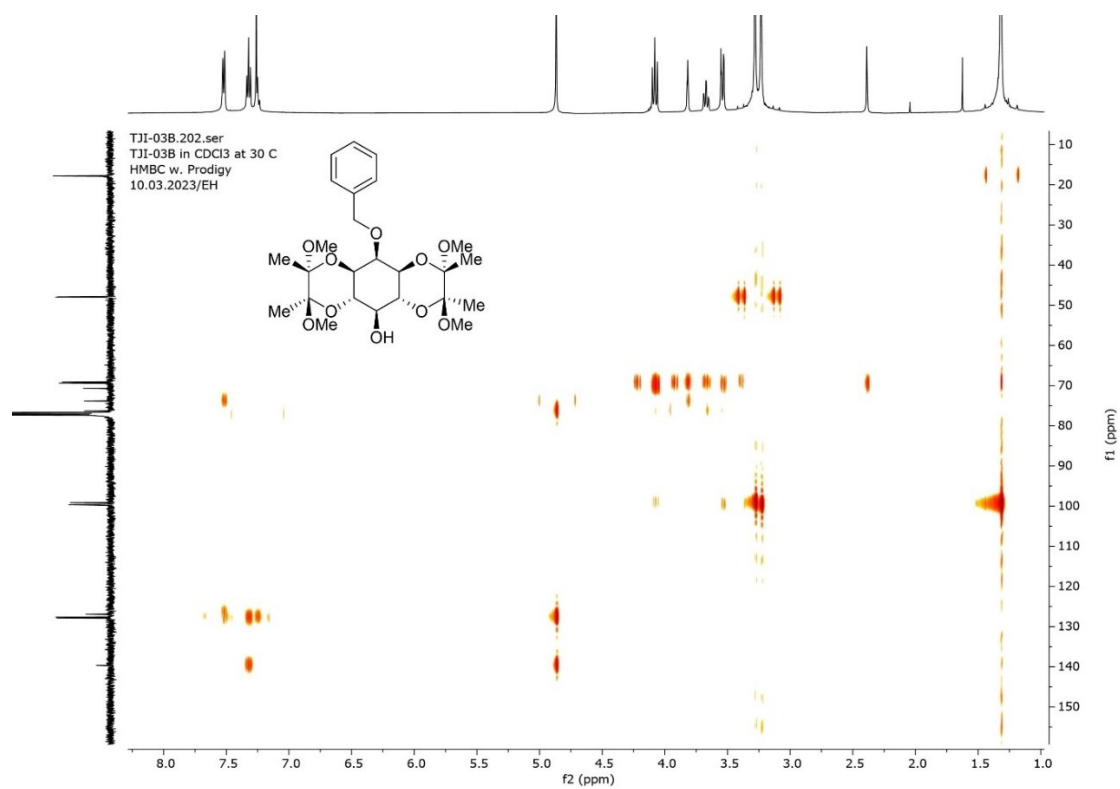
Figure A5. FTIR spectrum of *myo*-inositol derivative **6**.

TJI-03B.101.fid
TJI-03B in CDCl3 at 30 C
135DEPT NMR at 125 MHz w. Prodigy
10.03.2023/EH

TJI-03B.100.fid
TJI-03B in CDCl3 at 30 C
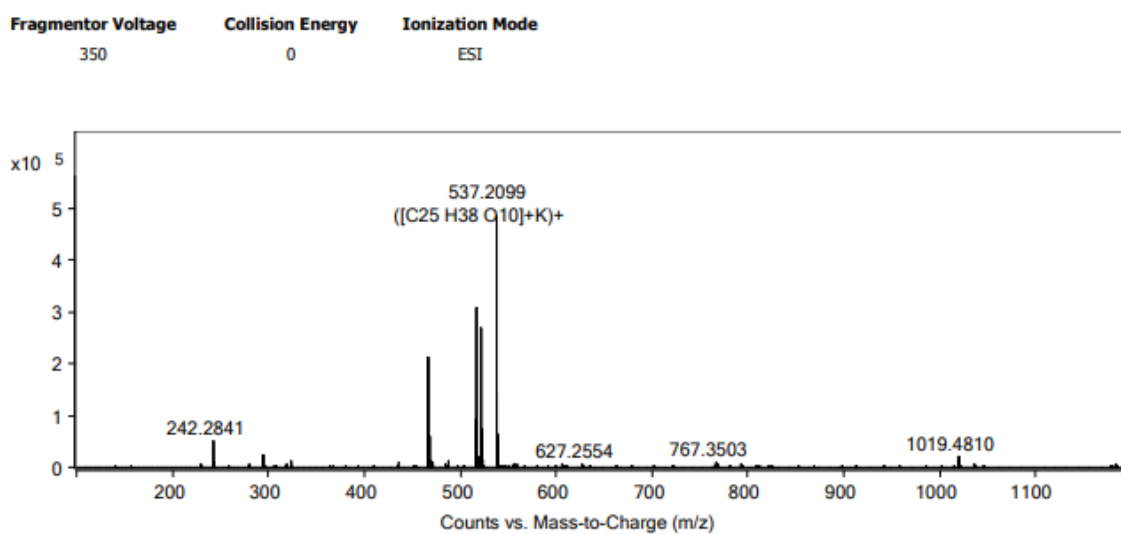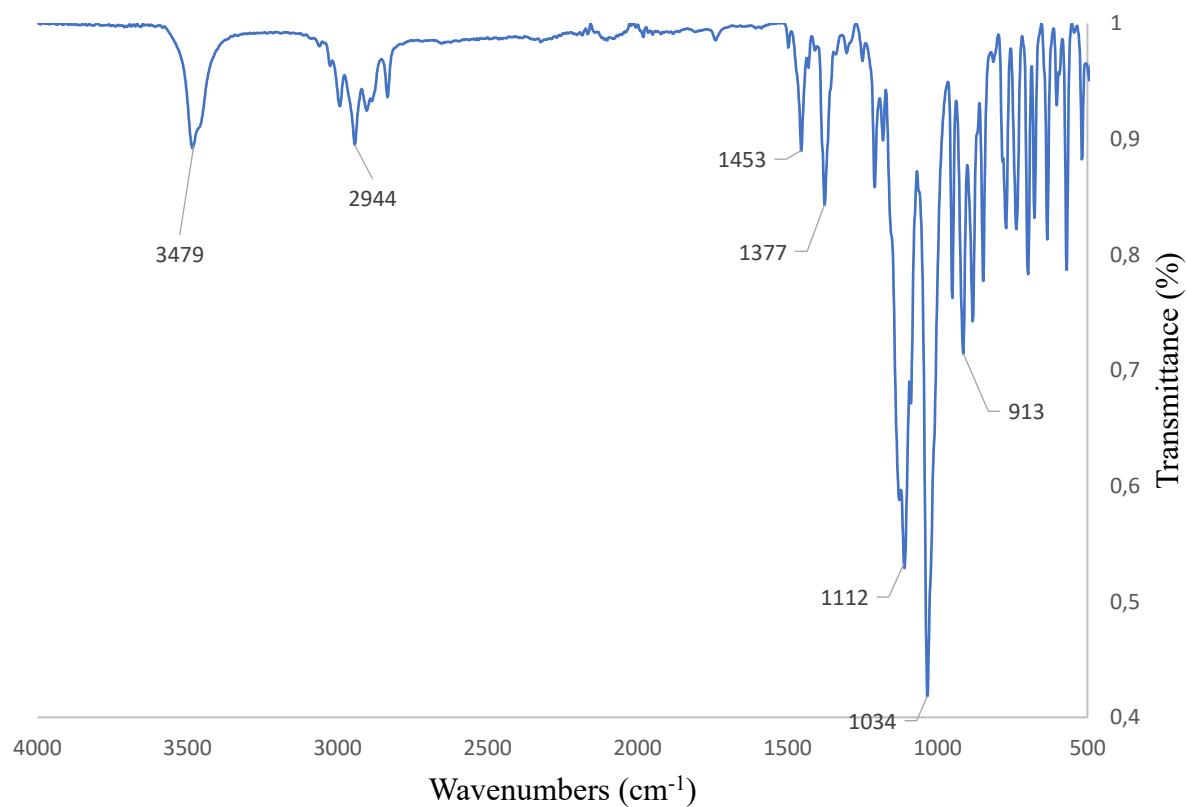13C NMR at 125 MHz w. Prodigy
10.03.2023/EH
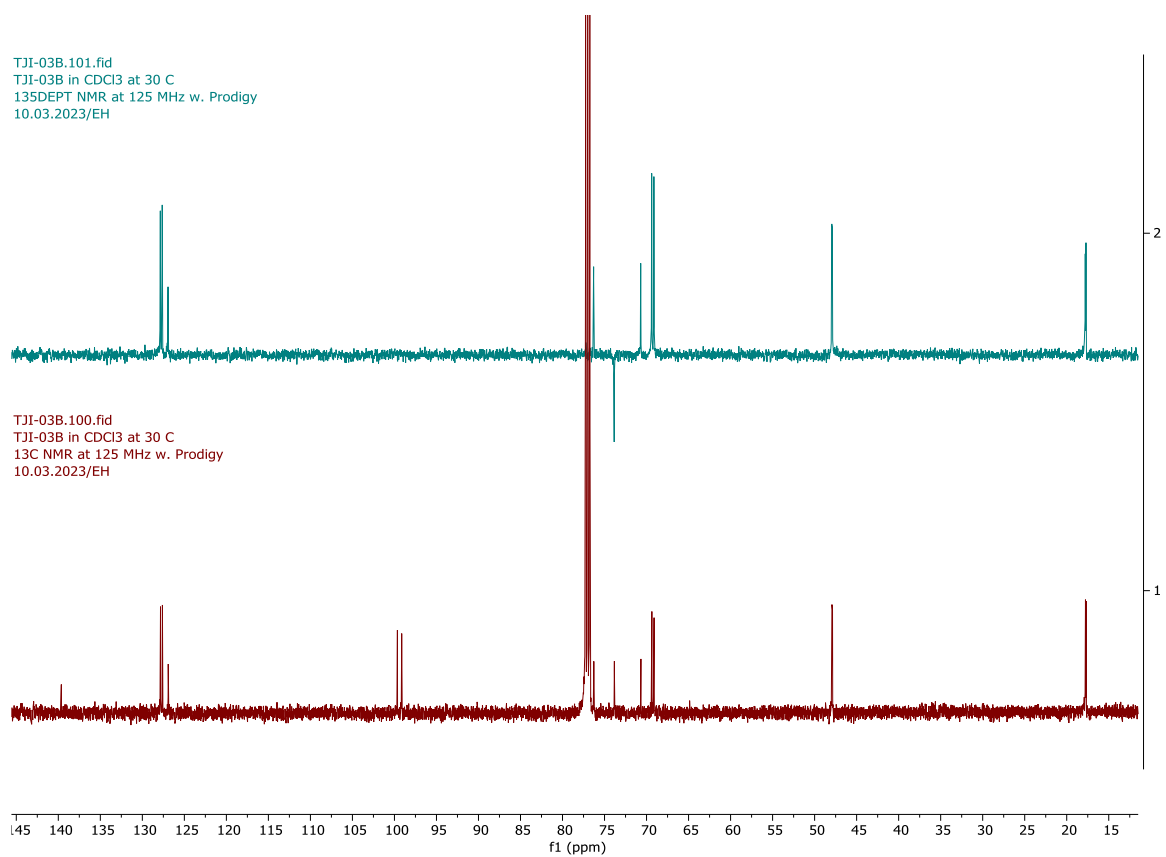
Figure A6. DEPT NMR (125 MHz, CDCl$_3$) spectrum of *myo*-inositol derivative **23**.

Figure A7. HSQC NMR (500 MHz, CDCl$_3$) spectrum of *myo*-inositol derivative **23**.



Figure A8. HMBC NMR (500 MHz, CDCl$_3$) spectrum of *myo*-inositol derivative **23**.

| Fragmentor Voltage | Collision Energy | Ionization Mode |
|:---:|:---:|:---:|
| 350 | 0 | ESI |



**Peak List**

| m/z | z | Abund | Formula | Ion |
|---|---|---|---|---|
| 516.28 | 1 | 317834.67 | | |
| 521.2354 | 1 | 272373.07 | C25 H38 O10 | (M+Na)+ |
| 537.2099 | 1 | 493751.35 | C25 H38 O10 | (M+K)+ |

**Formula Calculator Element Limits**

| Element | Min | Max |
|---|---|---|
| C | 25 | 25 |
| H | 38 | 38 |
| O | 10 | 10 |
| N | 0 | 0 |

**Formula Calculator Results**

| Formula | Best | Mass | Tgt Mass | Diff (ppm) | Ion Species | Score |
|---|---|---|---|---|---|---|
| C25 H38 O10 | True | 498.246 | 498.2465 | 0.93 | C25 H38 Na O10 | 98.65 |
| C25 H38 O10 | True | 498.2465 | 498.2465 | -0.06 | C25 H38 K O10 | 96.48 |

Figure A9. HR-MS spectrum and mass accuracies of *myo*-inositol derivative **23**.

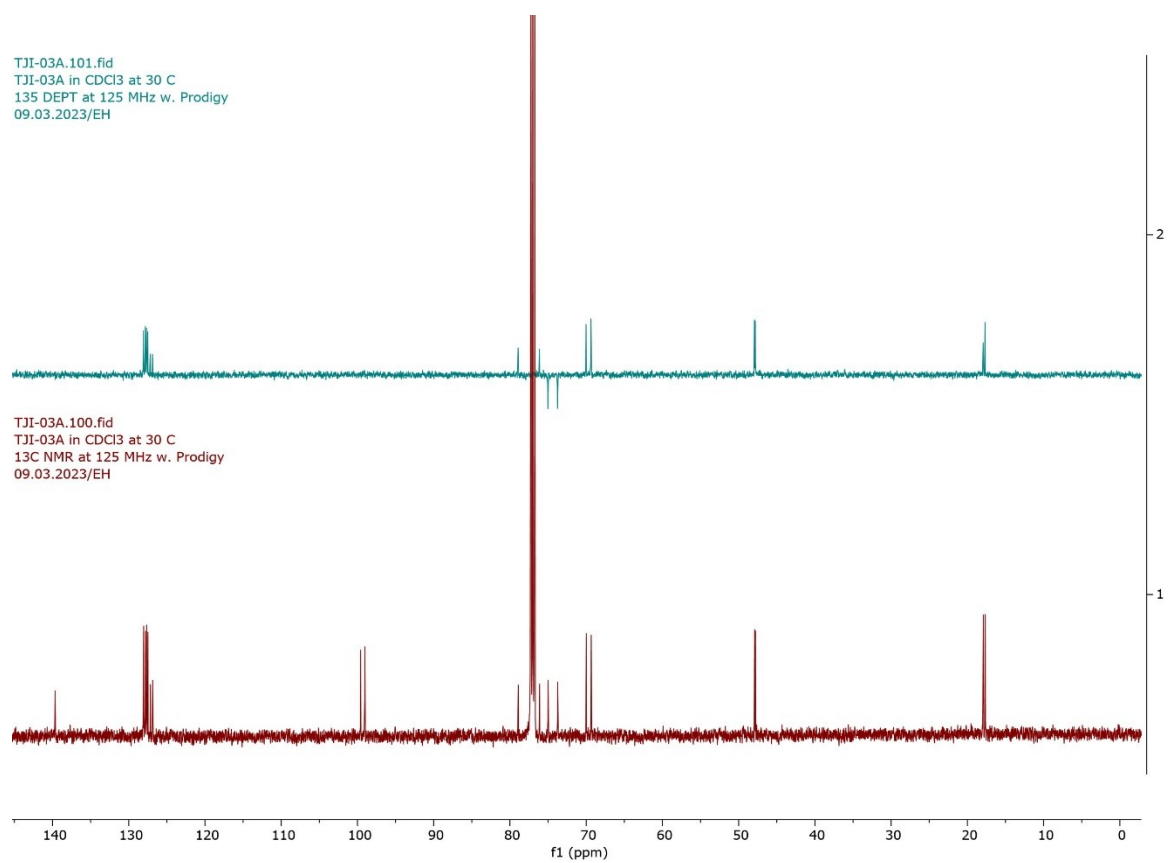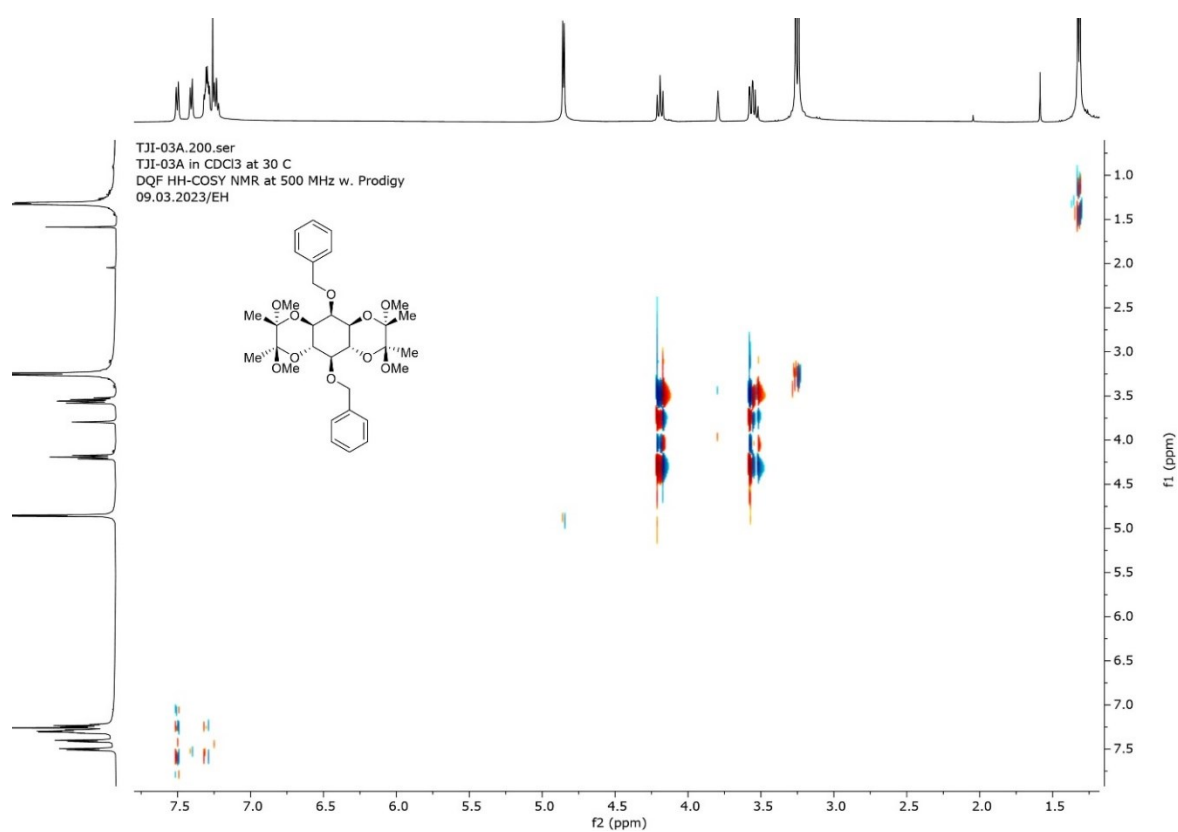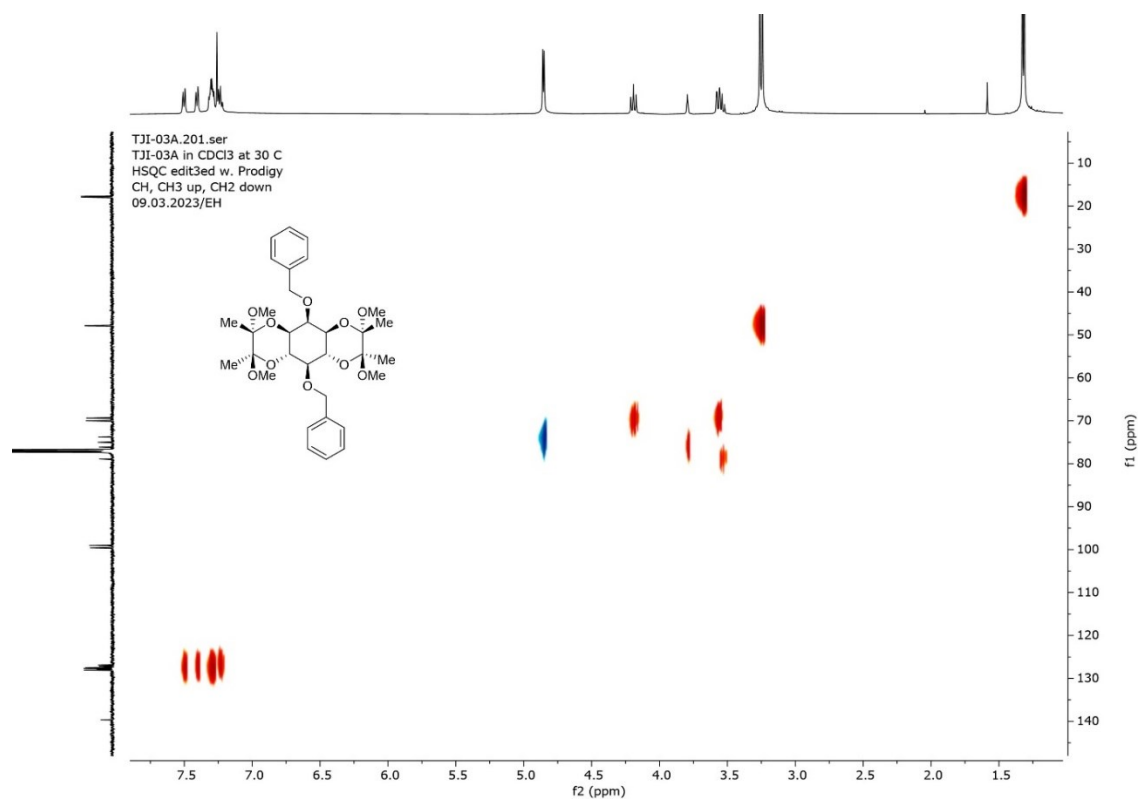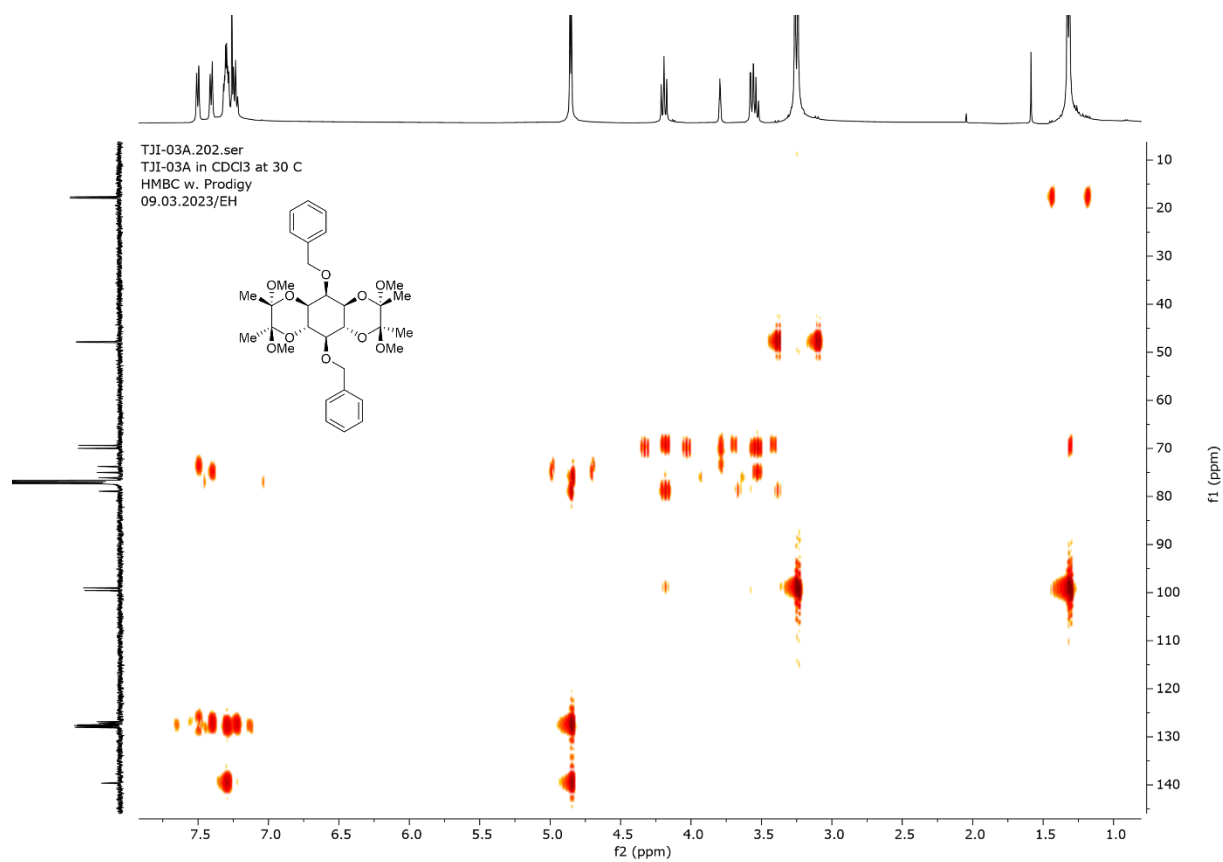Figure A10. FTIR spectrum of *myo*-inositol derivative **23**.

TJI-03A.101.fid
TJI-03A in CDCl3 at 30 C
135 DEPT at 125 MHz w. Prodigy
09.03.2023/EH

TJI-03A.100.fid
TJI-03A in CDCl3 at 30 C
13C NMR at 125 MHz w. Prodigy
09.03.2023/EH

f1 (ppm)

Figure A11. DEPT NMR spectrum (125 MHz, CDCl$_3$) of *myo*-inositol derivative **24**.

TJI-03A.200.ser
TJI-03A in CDCl3 at 30 C
DQF HH-COSY NMR at 500 MHz w. Prodigy
09.03.2023/EH

Figure A12. HH-COSY NMR spectrum (500 MHz, CDCl₃) of *myo*-inositol derivative **24**.



TJI-03A.201.ser
TJI-03A in CDCl3 at 30 C
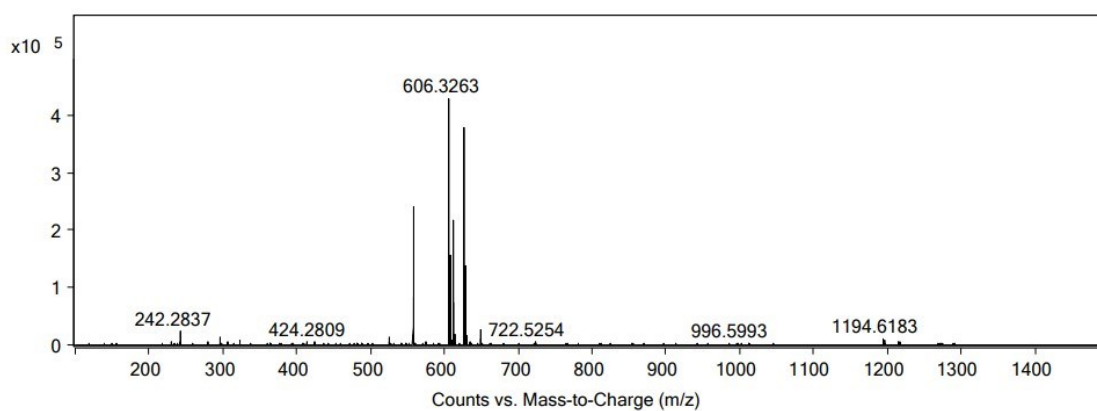HSQC edit3ed w. Prodigy
CH, CH3 up, CH2 down
09.03.2023/EH

Figure A13. HSQC NMR spectrum (500 MHz, CDCl₃) of *myo*-inositol derivative **24**.

Figure A14. HMBC NMR spectrum (500 MHz, CDCl₃) of *myo*-inositol derivative **24**.

| Fragmentor Voltage | Collision Energy | Ionization Mode |
|---|---|---|
| 350 | 0 | ESI |
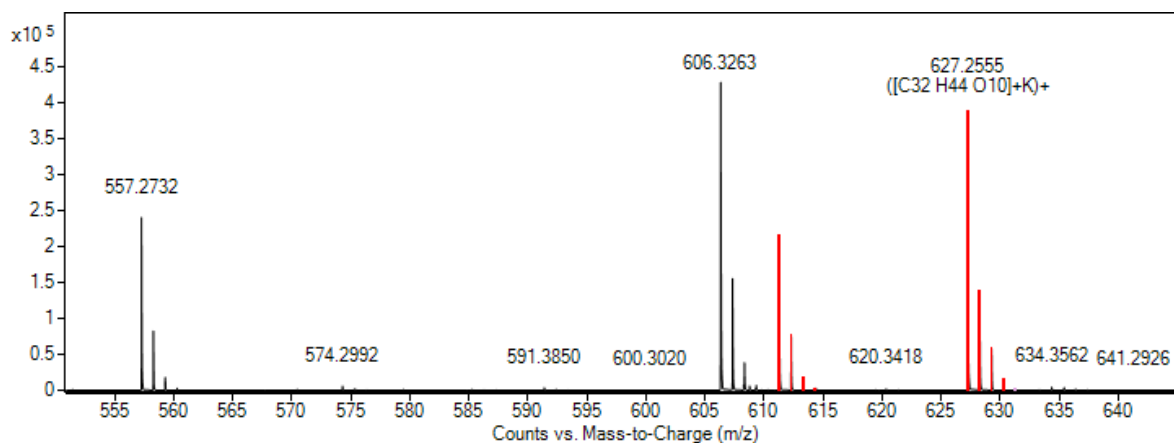




**Peak List**

| m/z | z | Abund | Formula | Ion |
|---|---|---|---|---|
| 557.2732 | 1 | 242872.64 | | |
| 606.3263 | 1 | 446290.64 | | |
| 627.2555 | 1 | 386426.72 | C32 H44 O10 | (M+K)+ |

**Formula Calculator Element Limits**

| Element | Min | Max |
|---|---|---|
| C | 32 | 32 |
| H | 44 | 44 |
| O | 10 | 10 |
| N | 0 | 0 |

**Formula Calculator Results**

| Formula | Best | Mass | Tgt Mass | Diff (ppm) | Ion Species | Score |
|---|---|---|---|---|---|---|
| C32 H44 O10 | True | 588.2919 | 588.2934 | 2.63 | C32 H44 Na O10 | 96.06 |
| C32 H44 O10 | True | 588.2922 | 588.2934 | 2.12 | C32 H44 K O10 | 96.86 |

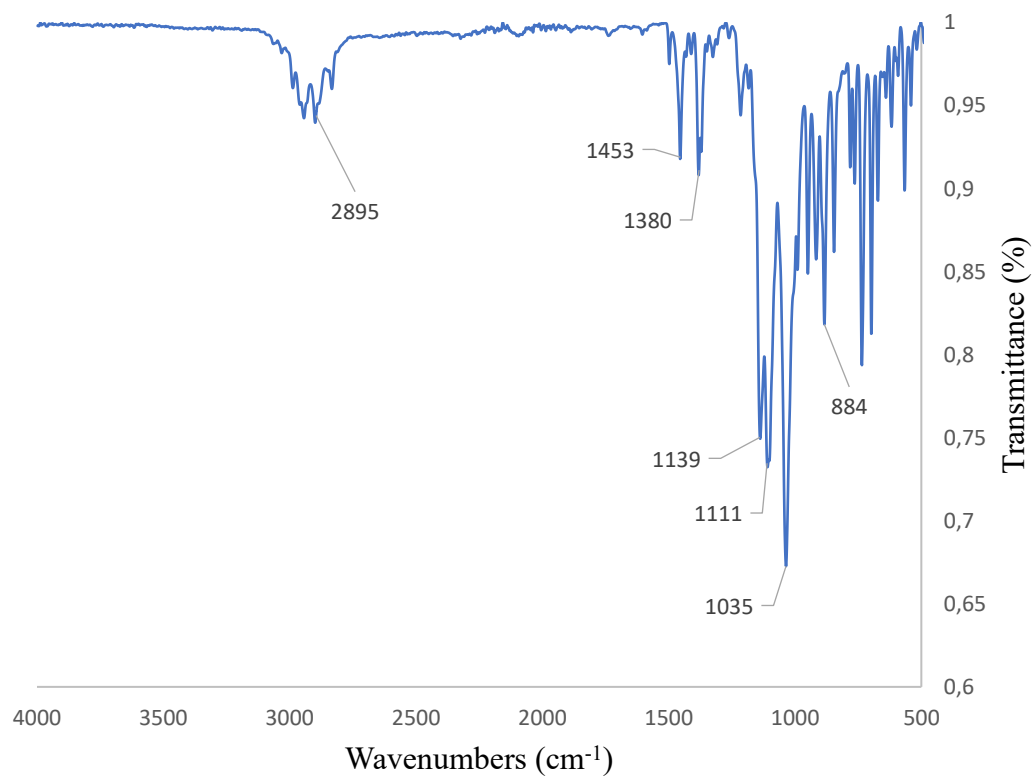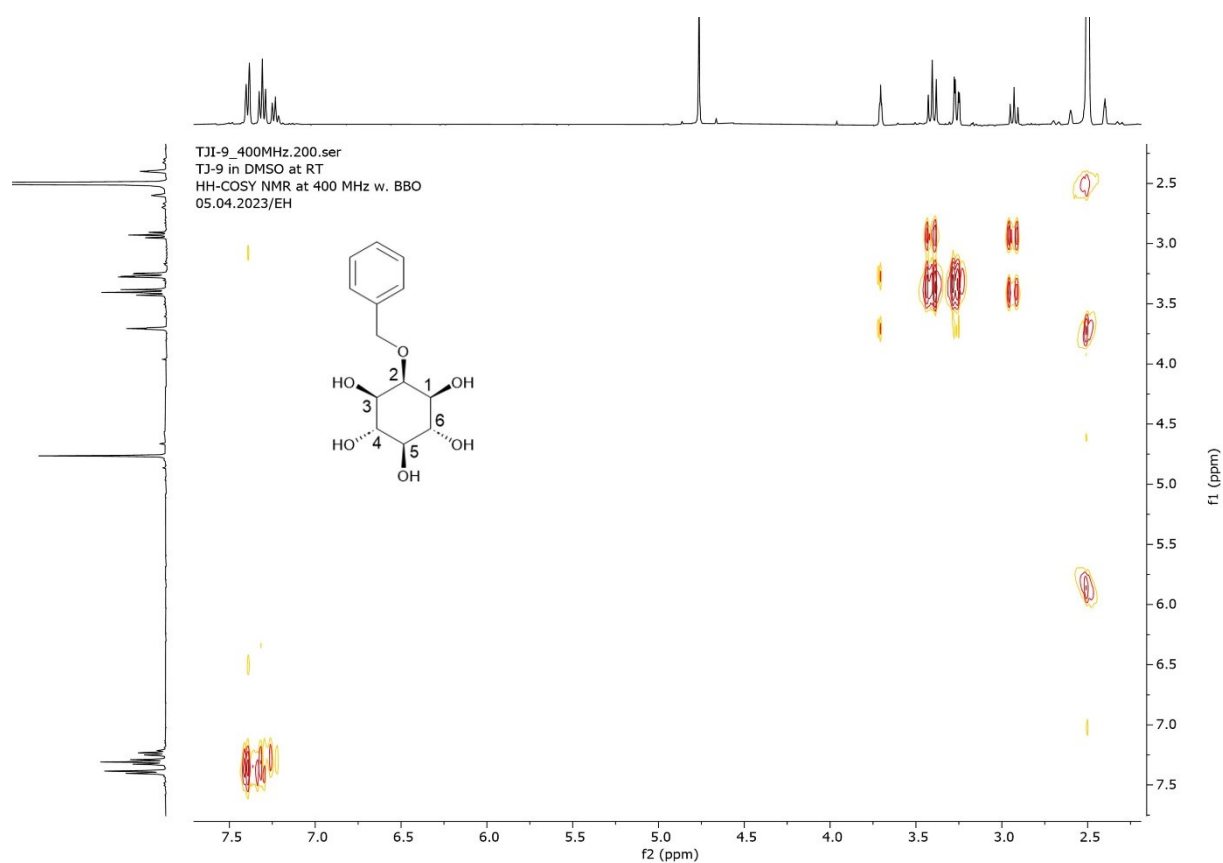Figure A15. HR-MS spectrum and mass accuracies of *myo*-inositol derivative **24**.
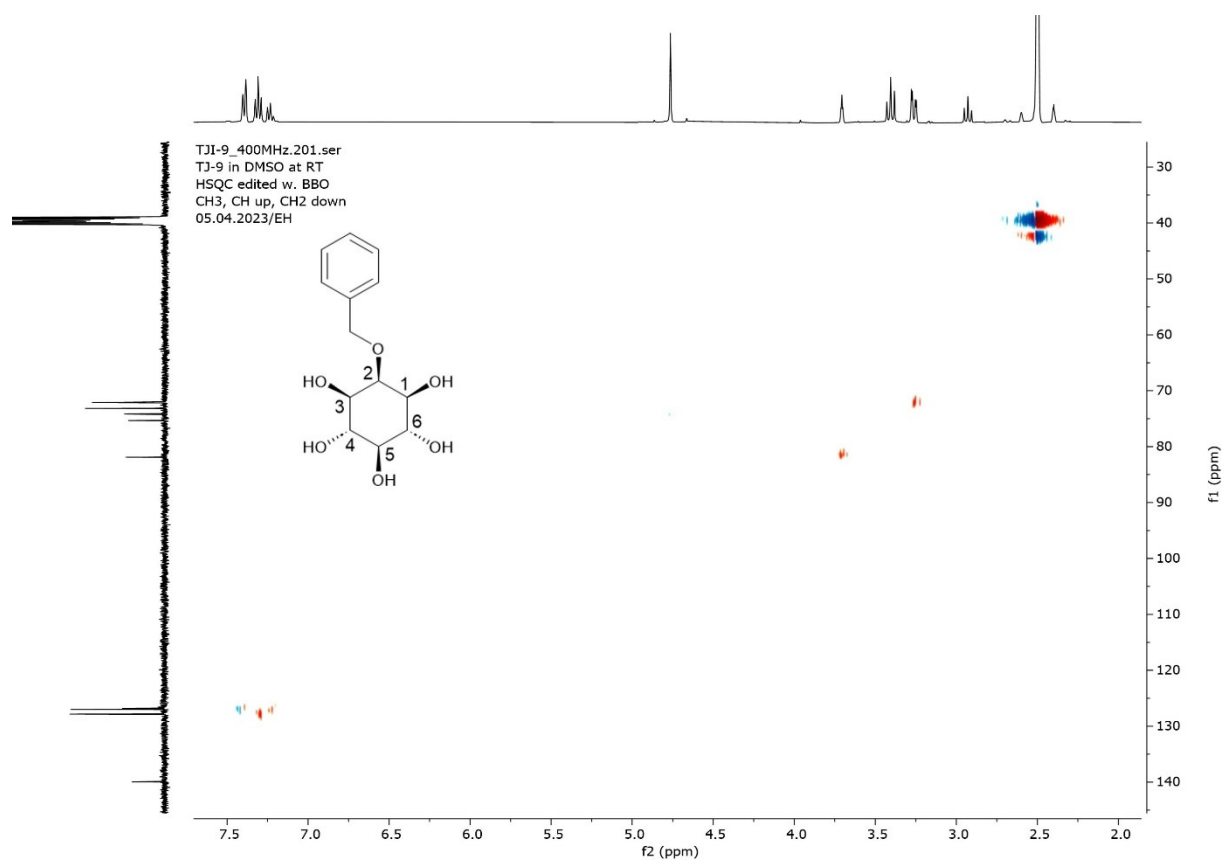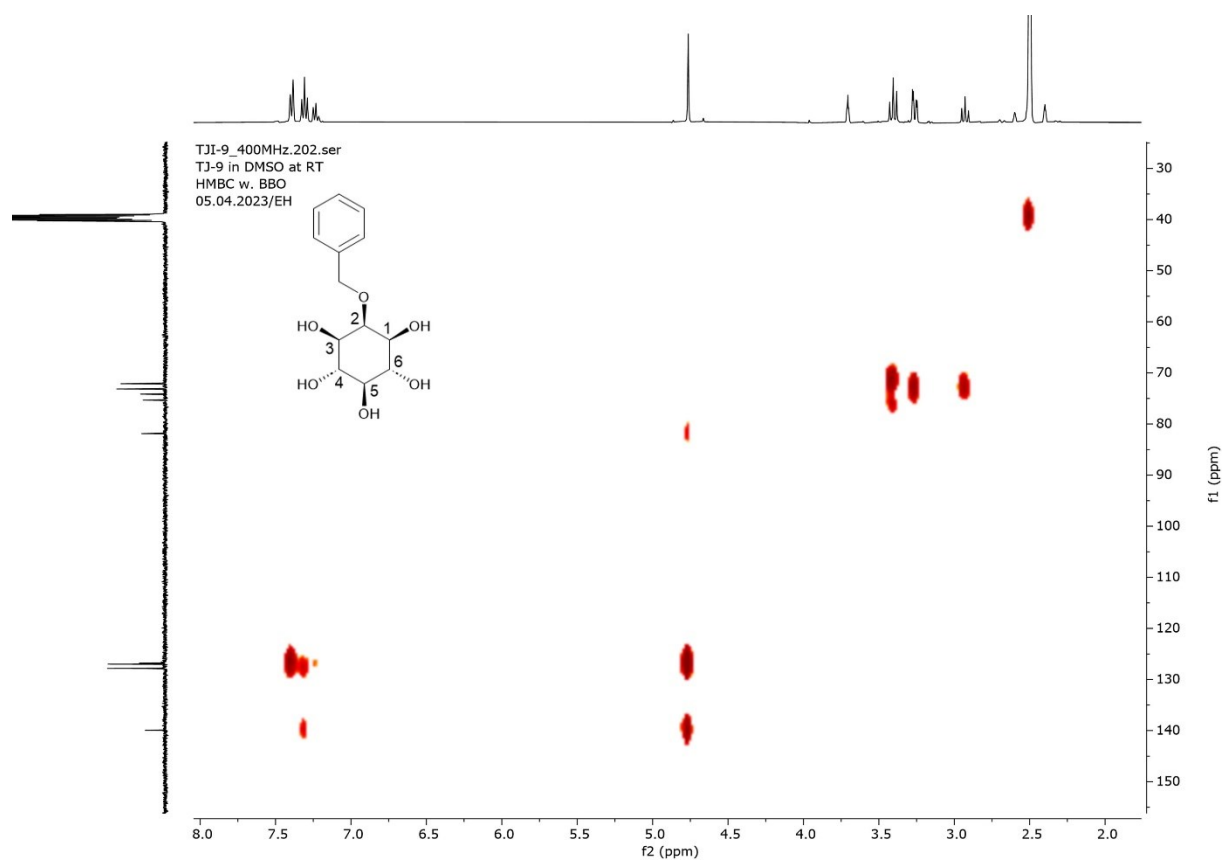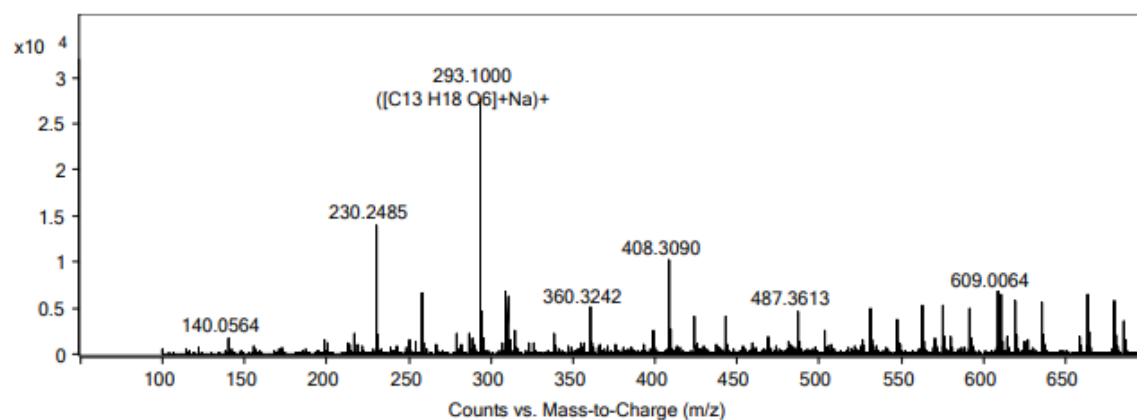
Figure A16. FTIR spectrum of *myo*-inositol derivative **24**.

Figure A17.  HH-COSY NMR (400 MHz, DMSO) spectrum of *myo*-inositol derivative **21**.



Figure A18. HSQC NMR (400 MHz, DMSO) spectrum of *myo*-inositol derivative **21**.

Figure A19. HMBC NMR (400 MHz, DMSO) spectrum of *myo*-inositol derivative **21**.

| Fragmentor Voltage | Collision Energy | Ionization Mode |
|---|---|---|
| 350 | 0 | ESI |



**Peak List**

| m/z | z | Abund | Formula | Ion |
|---|---|---|---|---|
| 230.2485 | 1 | 14353.79 | | |
| 293.1 | 1 | 28267.97 | C13 H18 O6 | (M+Na)+ |
| 408.309 | 1 | 10281.79 | | |

**Formula Calculator Element Limits**

| Element | Min | Max |
|---|---|---|
| C | 13 | 13 |
| H | 18 | 18 |
| O | 6 | 6 |
| N | 0 | 0 |

**Formula Calculator Results**

| Formula | Best | Mass | Tgt Mass | Diff (ppm) | Ion Species | Score |
|---|---|---|---|---|---|---|
| C13 H18 O6 | True | 270.1108 | 270.1103 | -1.76 | C13 H18 Na O6 | 98.14 |
| C13 H18 O6 | True | 270.1105 | 270.1103 | -0.77 | C13 H18 K O6 | 95.33 |

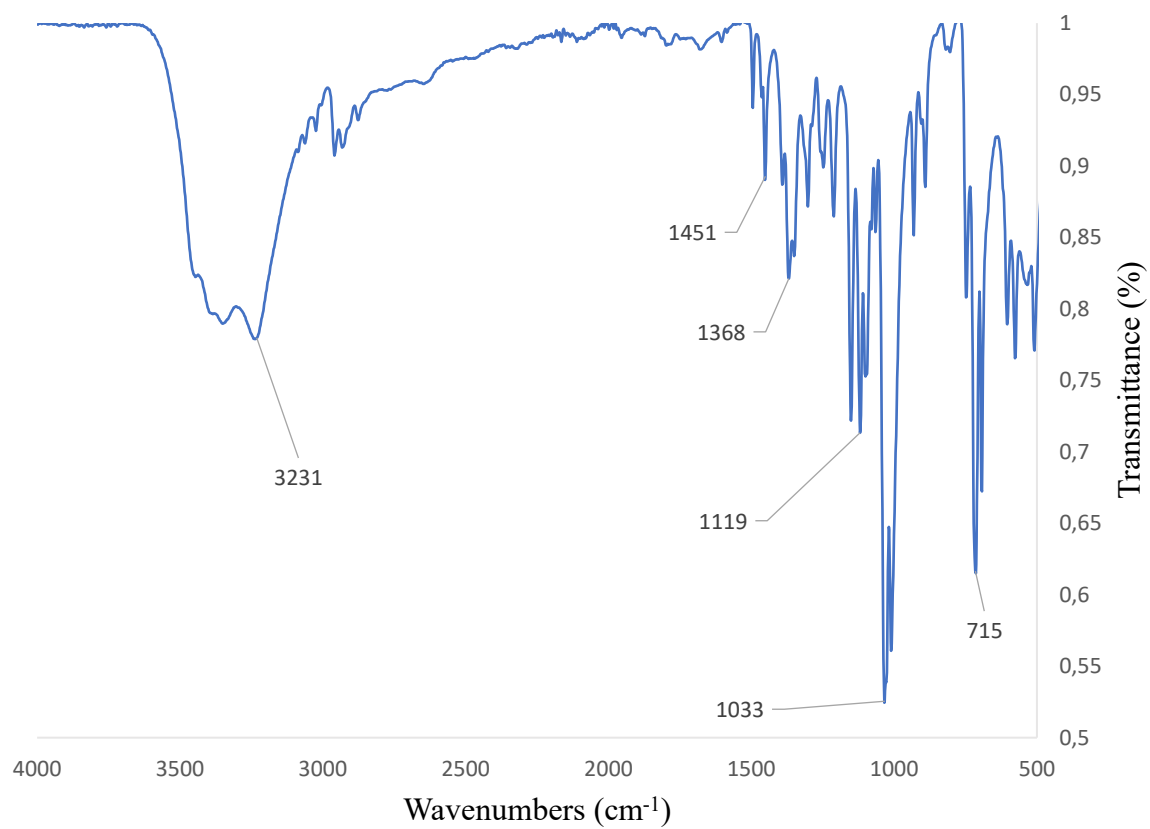Figure A20. HR-MS spectrum and mass accuracies of *myo*-inositol derivative **21**.

Figure A21. FTIR spectrum of *myo*-inositol derivative **21**.